Electronic muscles and skins: a review of soft sensors and actuators

Dustin Chen and Qibing Pei*

Department of Materials Science and Engineering, Henry Samueli School of Engineering and Applied Science, University of California, Los Angeles, California, 90095

KEYWORDS: Compliant electrodes, actuators, electronic skins, wearable electronics, sensors, artificial muscles

ABSTRACT: This article reviews several classes of compliant materials that can be utilized to fabricate electronic muscles and skins. Different classes of materials range from compliant conductors, semiconductors, to dielectrics, all of which play a vital and cohesive role in the development of next generation electronics. This Review covers recent advances in the development of new materials, as well as the engineering of well-characterized materials for the repurposing in applications of flexible and stretchable electronics. In addition to compliant materials, this Review further discusses the use of these materials for integrated systems to develop soft sensors and actuators. These new materials and new devices pave the way for a new generation of electronics that will change the way we see and interact with our devices for the decades to come.

1. Introduction

As a species, we collectively as mankind have always been simultaneously fascinated and terrified of the unknown. In particular, the idea of either the absence or presence of a higher power, other sentient beings, or creatures of higher intelligence than us can elicit emotions ranging from euphoria, to confusion, to terror. Perhaps in part to mitigate this fear of the unknown, or perhaps to elevate the stature of humankind, work steadily progressed in developing forms of artificial intelligence (AI) due to, as writer Pamela McCorduck wrote, "an ancient wish to forge the gods.[1]" The integration of this abstract concept of artificial thinking to functioning autonomous machines manifested physically in the development of humanoid machines. In 1928, this intersection of artificial thinking and autonomous machinery culminated in the development of one of the first humanoid robots, Eric Robot, who was capable of head and hand movements through remote or voice control.[2] Navigating chronologically through the years, our fascination with these artificial beings never waned, with increasingly sophisticated and complex systems portrayed in science fiction, from the beloved duo C-3PO and R2D2, to Terminator, to the all-mighty Optimus Prime.

However, the transition from the reality posited by writers of science fiction to a functional reality poses several technological challenges. Though the 'artificial' in these artificial beings inherently implies a deviation from realism, the increasingly sophisticated and complex systems being developed in real life mandate increasingly sophisticated and complex capabilities approaching the organic equivalent. Key amongst the organic equivalents that researchers strive for are the sensory perceptions afforded by human skin, and the range and type of motion made possible by living muscle.

To emulate the properties of human skin, electronic skins have been developed and heavily researched with the advent of wearable electronics. In an attempt to mimic the sensory functions of their organic counterparts, significant work has been reported in developing electronics skins with capabilities conducive to this end such as pressure[3–8] and temperature sensors.[9–12] As the future of electronic devices continued to trend towards mobile and wearable electronics, these artificial skins were augmented with progressively complex attributes such as touch sensing,[13,14] gas sensing,[15–17] and bio-sensing.[18–20] By combining these additional sensing modalities in conjunction with the properties inherently associated with skin such as flexibility,[21–23] stretchability,[24–26] and self-healing,[27,28] the world of electronics is positioned to experience a paradigm shift in coming decades.

In line with asymptotically approaching behavior representative of the human body, technological advances

have come about in recent years to mimic the movement of human muscles. Salient properties to emulate to enable the functionality of real muscle include maintaining the energy density of muscle, the capability of withstanding high strains, ability to store and recuperate energy, high power-to-weight ratio, and the ability to perform natural motion patterns.[29–32] Electroactive polymers pose one such possibility in approaching the properties of real muscles, and due to their inherent material characteristics, have garnered the title "artificial muscle."[32] These electronic muscles respond to electric fields by generating mechanical motion, and are inherently lightweight, inexpensive, and compliant.[32–34]

Continual progress into these electronic skins and muscles has the potential to bring about radical changes and unprecedented new applications to a myriad of different industries. The development of self-aware, autonomous robots with human-like movement and sensing capabilities has unparalleled significance in fields of medicine and diagnostics, law enforcement, and manufacturing, to name a few. Even minor advancements towards this end have the capability of improving diagnostics,[35,36] enabling continuous real-time health care monitoring,[21,35,37,38] and developing humanoid robots to accomplish simple tasks.[39,40] A timeline of important events in the history of robotics is illustrated in **Figure 1**.

To realize these potential applications and open up the realm of possibilities, these flexible and stretchable electronic devices have been fabricated through several various methods. These methods can be generally grouped into two categories: engineered structures such as nanoscale ribbons[41,42] or amalgamating discrete rigid components with an elastomeric junction[43–45] designed to synthetically introduce a certain degree of stretchability, or; the use of intrinsically stretchable materials to form integrated systems.[46–48] The former leverages well established materials such as silicon and metals to induce small-strain deformability through thin or wavy structures to withstand with the large-strain deformation in the elastomeric junctions, while the latter involves synthesizing new materials that are inherently compliant and can retain critical electronic properties while undergoing large-strain elongations. Within the category of intrinsically stretchable materials, a distinction is further made between materials who by themselves possess an innate capacity to be stretched while possessing any required additional properties such as conductivity or semiconductivity, and composite stretchable materials which leverage unique properties from individual materials to form useful stretchable electronic materials. Though in the strictest of definitions these composites are not fully 'intrinsically' stretchable on

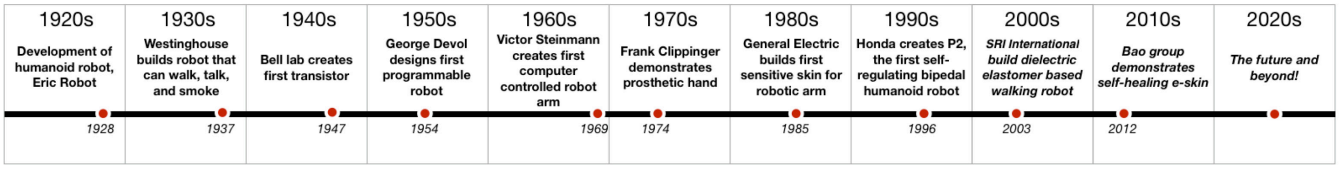

Figure 1: A timeline of important events in the history of robotics, leading to the modern day development of electronic skins and actuators.

the molecular level, they are, on a macroscopic scale, "uniformly "stretchable, and for this Review, are grouped together with intrinsically stretchable materials. The scope of this Review will be limited to these two classes of intrinsically stretchable materials. In the first portion of this review, different classes of intrinsically compliant materials used to fabricate electronic devices will be discussed at length, including conductors, dielectrics, semiconductors, and electroactive polymers. The second portion of the Review will focus on the integration of these various classes of materials for electronic skins and muscles.

2. Materials

The development of wearable electronics has pushed researchers to develop new materials that can accommodate the additional dimensionality of flexibility and stretchability. In some cases, previously studied materials were applied or studied more in depth to serve as components for these new electronic devices. In other cases, composite systems were developed to meet the ever-changing needs and requirements of these new systems. This section of the Review analyzes these different materials and their ability to meet the performance requirements mandated by electronic skins and muscles. Though flexible materials will be introduced, the bulk of this section will focus on stretchable materials and composites.

2.1. Compliant conductors

In contrast to the relatively new field of stretchable electronics, stretchable, and by default, flexible conductors have been explored for a more extensive period of time.[49] Though stretchable conductors can trace their origins to nanostructures engineered to be able to withstand strains,[49,50] intrinsically compliant conductors have been researched and developed in more recent years.

Optoelectronic applications have been a driving force for the development of not only mechanically compliant electrodes, but transparent compliant electrodes to replace the commonly used indium tin oxide (ITO). Applications of optoelectronic devices for electronic skin purposes include the use of organic light emitting diodes (OLEDs) for instantaneous readouts and displays,[51,52] and organic photovoltaics (OPVs) for lightweight and mechanically resilient power sources.[53,54] One approach widely used is the fabrication of composite hybrid materials comprising conductive materials and a soft matrix. For the simplest compliant electrodes a conductive medium can be deposited on a substrate with the desired mechanical

properties. With this method, Yu *et al.* fabricated carbon nanotube (CNT) flexible electrodes by transferring a film of CNTs from a porous alumina filter paper onto a polyethylene terephthalate (PET) substrate.[55,56] The resulting transparent conductive electrode (TCE) exhibited performance metrics verifying its efficacy as a flexible electrode: a sheet resistance of 500 ohm/sq. was observed with a transparency of 85% in the visible spectrum;[55] and bending the TCE to a 12.5 mm radius was observed to negligibly change the sheet resistance.[56]

However, while these compliant electrodes may serve as a proof-of-concept of the efficacy of depositing a composite medium on a flexible substrate, several limitations persist, specifically for OLED applications. CNT networks inherently have a high resistance, which, when considering the 10 ohm/sq. sheet resistance at 85% transparency commonly used for OLED applications, serves to be a large barrier for adaptation of this technology. From a morphological point of view, the thickness of the CNT network on a polymer substrate may be on the same order of magnitude of thickness as the total active material for the OLED. As a result, significant shorting between the anode and cathode often arises, physically manifesting in a lower luminance and reduced current efficacy.

Silver nanowires (AgNW) may be an attractive alternative to CNTs using the same technology, and in recent years, have risen to the forefront as one of the more promising alternatives to replace ITO.[57,58] The high conductivity of these nanowire networks in conjunction with the large open area between individual nanowires for high transparency allows these electrodes to function well as transparent conductors. With regards to mechanical properties, the choice of the underlying substrate and fabrication processes can tailor the properties of the electrode for the desired application. To address the issue of high surface roughness when depositing nanowires on a polymer substrate, the Pei group explored embedding the nanowires within a polymer matrix.[59–62] Briefly, the silver nanowires are coated from solution onto a release substrate. Due to the porous nature of the resulting network formed, a bifunctional monomer with photoinitiator or soluble polymer overcoated on top of the AgNW network can infiltrate the network and come in contact with the underlying substrate.[59,62] After UV irradiation or drying of the electrode to drive off solvent, a freestanding film with the AgNW network embedded within a polymer matrix can be peeled off. Because the monomer or polymer ink is able to contact the underlying release substrate, the freestanding electrode inherits the surface topography of the release substrate, resulting in the formation of surfaces with a surface roughness (R_{RMS}) < 1 nm, a value lower than that observed in ITO. Atomic force microscopy (AFM) images of ITO, AgNWs coated directly on a polymer substrate, and AgNWs embedded within a polymer matrix are illustrated in **Figure 2a**, **Figure 2b**, and **Figure 2c**.[63] This reduction in the surface roughness of electrodes mitigates the issue of shorting between electrodes in OLEDs to enable the fabrication of high

efficiency devices.

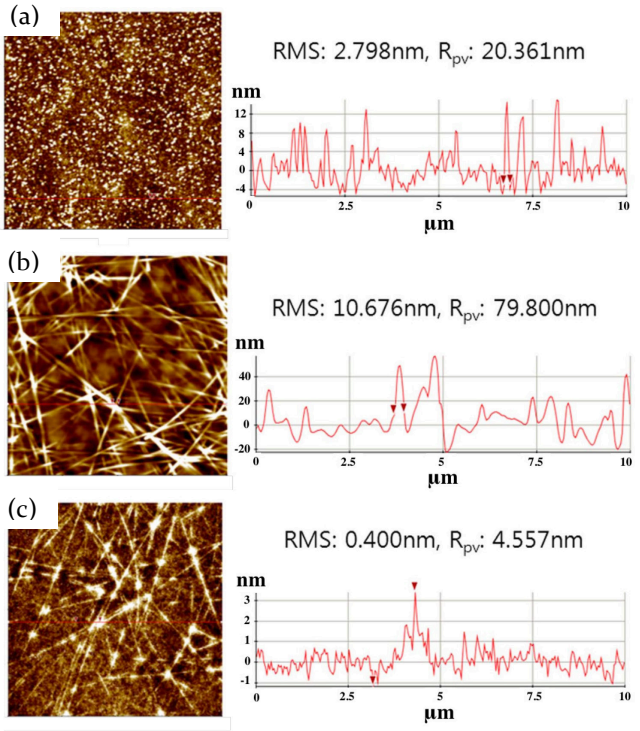

Figure 2: (a) AFM image of ITO sputtered on a polymer substrate. (b) AFM image of AgNWs coated on a polymer substrate, highlighting the roughness of non-embedded AgNWs. (c) AFM image of AgNWs embedded within a polymer matrix, demonstrating the low roughness that can be achieved with embedded AgNWs, necessary for certain applications. Adapted and reproduced with permission from ref.[63], licensed under https://creativecommons.org/licenses/by/3.0/.

A variety of different polymer matrices can be utilized for various functionalities. Using a blend of acrylates, ethoxylated (3) trimethylolpropane triacrylate, ethoxylated (6) bisphenol A dimethacrylate, and Tris (2-hydroxy ethyl) isocyanurate triacrylate to impart both mechanical flexibility and thermal resistance up to 200 °C, Li *et al.* demonstrated an transparent AgNW conductor capable of withstanding bending at a 4 mm radius for 1000 cycles while maintaining a sheet resistance of 25 ohm/sq. at 87% transparency.[64] Chen *et al.* further increased the temperature the electrode could withstand to 300 °C for six hours by embedding ZnO-coated (deposited with atomic layer deposition (ALD) AgNWs nanowires within a colorless, transparent polyimide,[62] with a similar work completed by Spechler *et al.* using sol-gel processed metal oxides on AgNWs to achieve the same goal.[65]

Several other capabilities can be endowed upon the AgNW conductors besides high transparency and conductivity, flexibility, and thermal resistance. To impart stretchability upon the electrodes, Hu *et al.* used an elastomeric polyurethane (PU) matrix to transfer the silver nanowires.[66] A schematic of the fabrication of such a stretchable electrode is provided in **Figure 3**. The use of the elastomeric matrix was not observed to degrade the optoelectronic properties, with the freestanding electrode having performance metrics of 8 ohm/sq. at 75% transparency, while allowing the electrode to reversibly stretch up to 170% strain.[66]

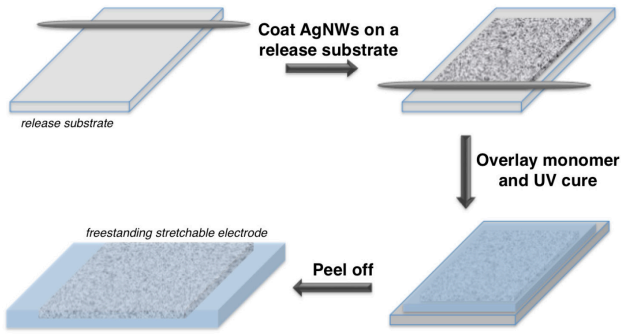

Figure 3: Schematic of the fabrication of one type of freestanding, composite stretchable electrode.

To make stretchable AgNW conductors with shape memory characteristics, Yun *et al.* embedded the nanowires within a copolymer of tert-butyl acrylate (TBA) and acrylic acid (AA).[67] The use of TBA enabled the shape-memory characteristics of the electrode as it is a bistable

electroactive polymer (BSEP), which combines the properties of shape memory polymers and dielectric elastomers. Further discussion of electroactive polymers will proceed in later sections. However, as the embedded nanowire conductors are hybrid materials, the electrically conductive component and mechanically compliant component require compatibility with each other; TBA, while exhibiting shape memory characteristics, has poor interfacial bonding with the nanowires due to its hydrophobicity, leading to incomplete transfer of the silver nanowires. The addition of the hydrophilic AA was found to increase bonding between the conductive component and polymer matrix via the carboxylic acid group, minimizing the rate of increase of resistance when stretched. The optical concentration of AA was determined through a balance between strengthening bonding between the two components, and increasing the glass transition temperature (T_g) with increasing values of AA.[67] The high T_g with increasing AA increases the actuation temperature of the BSEP, leading to high power consumption when used for shape memory applications. **Figure 4** illustrates the effect of AA concentration on the sheet resistance of the AgNW electrodes when subjected to uniaxial strain (**Figure 4a**) and cyclical loadings (**Figure 4b**).[67] It was observed that the addition of 5% AA was optimal in limiting the increase in sheet resistance upon both uniaxial and cyclical stretching. At this concentration, the nanowire electrode was able to recover 98% of sheet resistance change upon removal of the external load at 30% strain, 95% at 70% strain, and 90% and 90% strain.[67]

Self-healing AgNW conductors[14,27,68] have also been developed as healable electronics have becoming more intensely researched.[69–73] Before discussing these nanowire conductors however, it is pertinent to first discuss the self-healing mechanism. The self-healing

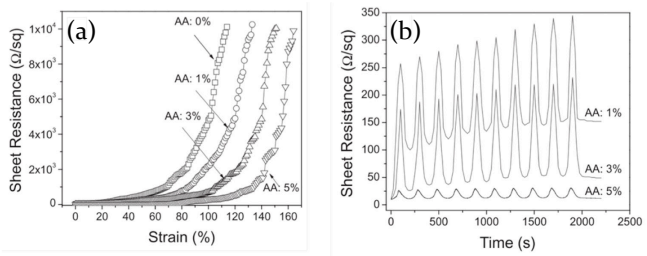

Figure 4: (a) Sheet resistance as a function of strain for a stretchable AgNW-TBA/AA composite electrode for various concentrations of AA. (b) Sheet resistance as a function of time for a stretchable AgNW composite during 10 cycles of loading of 0-50% strain at a constant strain rate of 0.005 /s. Reprinted with permission from ref.[67]. Copyright {2012} Wiley-VCH.

ability of polymeric composites can be segregated into two categories: (1) extrinsic self-healing achieved through intentionally embedded healing agents;[28,72] and (2) intrinsic self-healing accomplished through polymers containing dynamic bonds.[28,73–75] Regarding the latter, dynamic bonds can be defined as bonds capable of undergoing reversible breaking and reformation, and can also be broken down into two categories: supramolecular interactions; and dynamic covalent bonds.[74] Looking at the latter, dynamic covalent bonds can break and reform with irreversible side reactions, with access to these dynamic characteristics quickly occurring only upon exposure to specific external factors.[74,75] For the former, the relatively weak dynamic process exists in continuous equilibrium,

and as a result, are susceptible to various external conditions, allowing them to form dynamic materials responsive to a variety of stimuli.[74]

Williams *et al.* reported one of the first conductive thermal-healing composite using dynamic covalent bonds.[28,76] As seen in **Figure 5a**, a conductive polymer composite with reversible bonds was synthesized by bonding N-hetero-cyclic carbenes (NHCs) with transition metals, both conductive and structurally dynamic components.[76] **Figure 5b** demonstrates a schematic of the operation of the self-healing material; a film with an externally applied crack to disrupt the electrical network can be healed at 200 °C as a result of the dynamic feature of the complex at elevated tempreatures.[76]

However, the aforementioned self-healing conductor suffered from an intrinsically low conductivity and the necessity of high temperatures. To ameliorate these shortcomings, the Bao group reported the first room-temperature self-healing composite exhibiting conductivities as high as 40 S/cm, sufficient for self-healing electrodes and tactile sensors.[69] The self-healing conductor was synthesized using a supramolecular polymeric hydrogen-bonding network with T_g below room temperature, with micro-nickel particles providing the conductivity, as illustrated in the schematic in **Figure 6**.[69] These hydrogen bonds preferentially break during mechanical disruption, and due to the large number of these bonds, the polymer can dynamically associate to self-heal at the surface at room temperatures.[69,77–79] Due to the tendency for nickel particles to form a thin oxide layer on the surface, the conductive fillers can form hydrogen bonding with the polymer network. The resulting self-healing composite demonstrated a reversion to 90% of its original electrical performance 15 seconds after being mechanically damaged.[69]

For optoelectronic applications, Li *et al.* reported the first self-healing, elastomeric transparent conductor using a Diels-Alder (DA) cycloaddition polymer in conjunction with AgNWs and poly(3,4-ethylenedioxythiophene) polystyrene sulfonate (PEDOT:PSS).[27] The transparent elastomeric polymer was synthesized through a reversible DA cycloaddition reaction of a monomer with four furan groups (FGEEDR)[68] with two maleimides,[80,81] as shown in **Figure 7a**. To form the composite conductor, AgNWs were deposited on a release glass substrate, followed by spin-coating a solution of PEDOT:PSS and a flurosurfactant, with the resulting film transferred into the surface of the DA polymer

The use of PEDOT:PSS allows the sheet resistance to remain low for optimal optoelectronic performance. While the AgNW network remains 'locked' on the release glass substrate, when transferred with the DA pre-polymer, the nanowires may redistribute in the low viscosity ink during the six-hour time frame required for polymerization. The use of PEDOT confines the nanowires to the surface of the DA polymer, resulting in a sheet resistance of 15 ohm/sq. With the nanowires locked in the top surface of the DA polymer, the composite conductor was able to recover a significant portion of the electrical performance after razor-blade cutting the electrical surface. **Figure 7b**

illustrates the evolution of resistance as a function of time after cutting the AgNW free-standing film and allowing it to self-heal through thermal treatment.[27] It was observed that the healing temperature of 100 °C enabled the originally 15 ohm/sq electrode to recover to 18 ohm/sq after 3 minutes, while annealing at 85 °C and 70 °C recovered to 19 ohm/sq. after 5 min and 20 ohm/sq. after 8 min, respectively. **Figure 7c** illustrates the mechanical robustness of the composite film after self-healing. When a composite film originally at 15 ohm/sq. was allowed to recover its resistance to 18 ohm/sq., the resulting electrical performance was comparable to a composite film not mechanically damaged at all. Though the razor-blade damaged film exhibited higher resistances than the fresh film at high strains, the difference between the two films were comparable up to around 50% strain. This proof-of-concept of elastomeric transparent self-healing electrodes could help pave the way for mechanically robust, self-healing electronic skins.

While the aforementioned discussion focused largely in part on the use of composite conductors based on AgNWs for optoelectronic applications, the field of intrinsically compliant conductors has a significantly broader scope. In some cases, previously characterized materials were repurposed for new applications. One such material is what is colloquially known today as liquid, or amorphous metal. The initiation of liquid metal research began with the reports of the vitrification of a liquid gold-silicon alloy,[82] and since its initial conception, have been developed primarily for structural applications due to intrinsic properties such as higher tensile and elastic strains in contrast to their polycrystalline metal alloy counterparts.[83,84] In recent years, another facet has been introduced to this technology, with the amorphous metal being used in its liquid state to provide an intrinsically stretchable conductor. The Dickey group has demonstrated several examples of using a eutectic gallium indium (EGaIn) in a microfluidic channel as stretchable conductors for various applications.[85–88]

The fabrication of these liquid metal conductors consists typically of injection of the liquid metal into an elastomeric microchannel. As an illustration, Kim et al. fabricated a polydimethylsiloxane (PDMS) microchannel, as illustrated in **Figure 8a**.[89] Briefly, a PDMS base layer was defined from standard lithography procedures on a silicon wafer. After deposition of a gold wetting layer for the subsequent liquid metal insertion, and removal of the gold from select regions of the mold, a second PDMS layer with both inlet and outlet holes for tubing is attached to the base PDMS layer. The base layer with a gold wetting buffer is then filled with room-temperature EGaIn (gallium:indium = 75.5:24.5) before introduction of a top capping PDMS layer. Optical images of the microchannel at various stages of the fabrication process are illustrated in **Figure 8b**.[89]

Using a similar method, Park *et al.* injected EGaIn in interconnected channels of plasma-treated 3D porous PDMS.[90] The observed conductivity of the intrinsically stretchable conductor was 24,100 S/cm, on par with the

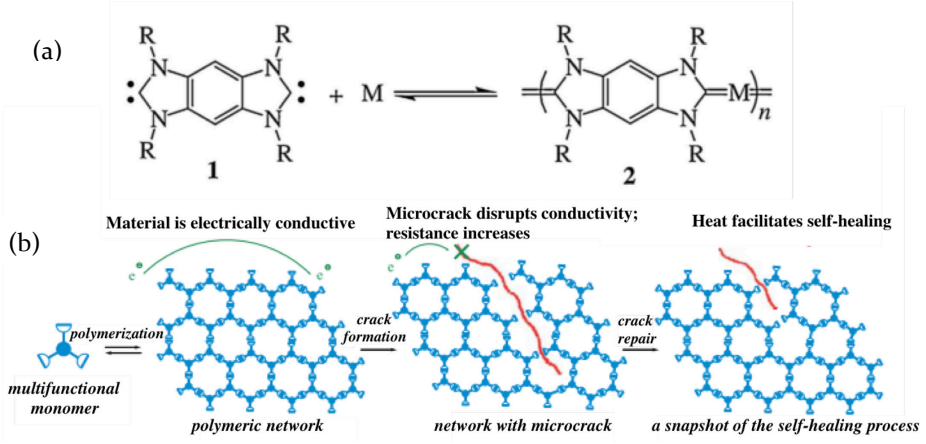

Figure 5: (a) Dynamic equilibrium between a monomer (left) and organometallic polymer (right). (b) Operation of a self-healing material controlled through an external stimulus such as heat. Adapted and reproduced with permission from ref.[76]. Copyright {2007} The Royal Society.

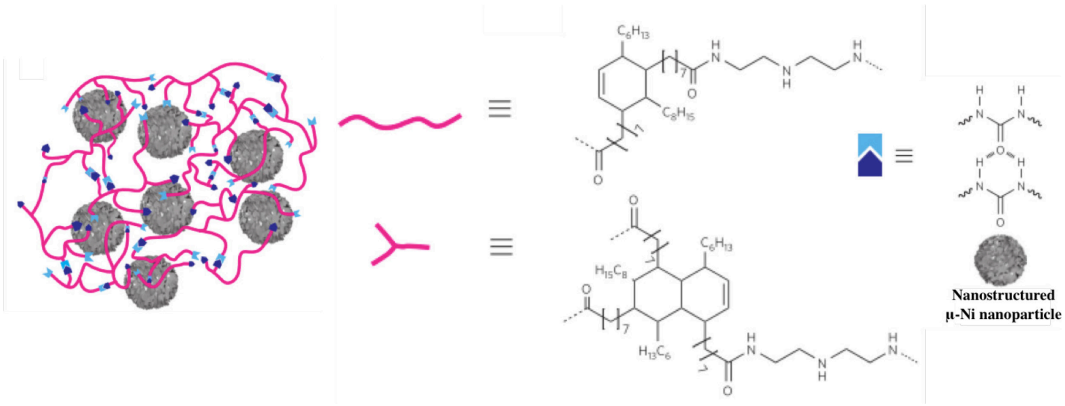

Figure 6: Illustration of the self-healing composite. Pink lines denote the linear and branched polymers forming the randomly branched network, while blue and purple shapes represent urea groups at the end of the branched polymers responsible for the primary hydrogen bonds between polymer chains. Adapted and reproduced with permission from ref.[69]. Copyright {2012} Nature Publishing Group.

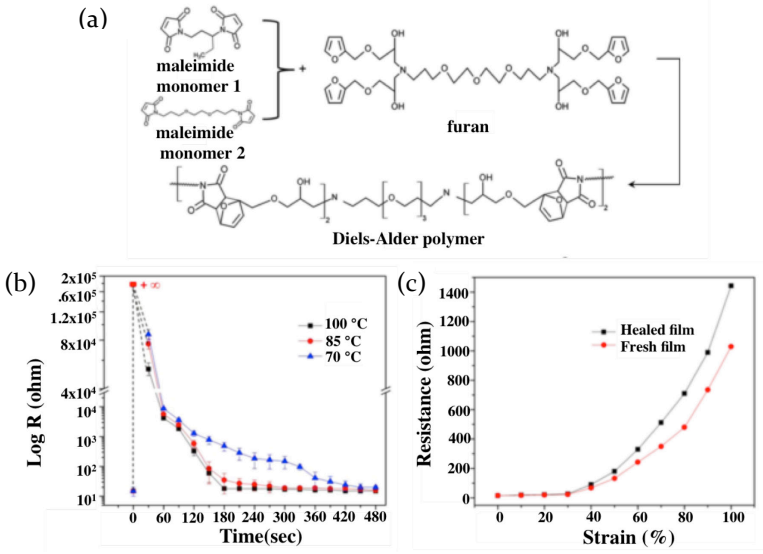

Figure 7: (a) Synthesis of the DA copolymer elastomer. (b) Resistance as a function of time for the composite electrodes during the healing process at 100, 85, and 70 °C. (c) Resistance as a function of strain of a fresh and healed electrode. Adapted and reproduced with permission from ref.[27]. Copyright {2015} American Chemical Society.

intrinsic conductivity of the liquid metal itself. Furthermore, no degradation in conductivity was observed upon application of uniaxial stress, due to the ability of the liquid phase EGaIn to conform to the form factor of the PDMS, as seen in **Figure 9a**. The stretchable conductor also performed well under cyclical testing,

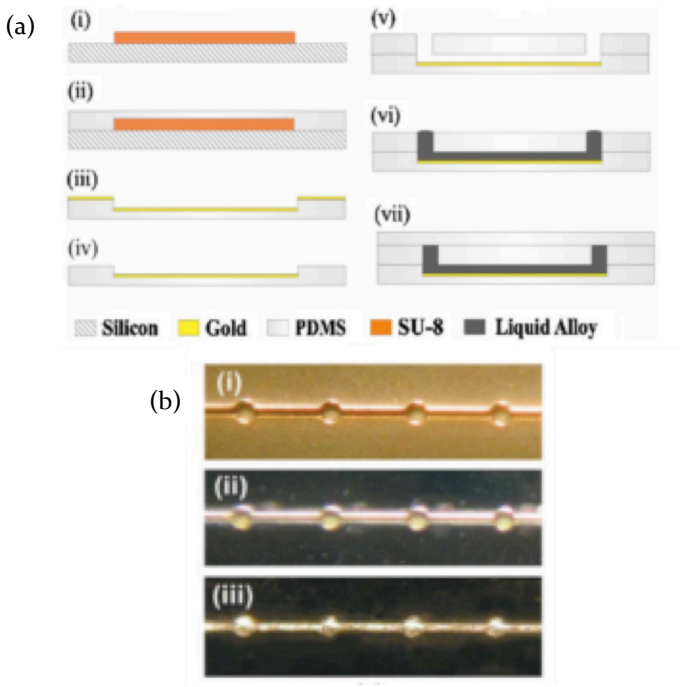

Figure 8: (a) Fabrication sequence of a linear stretchable interconnect. (b) Optical images of (i) gold-coated base layer; (ii) substrate after removal of gold film from regions of the top surface; (iii) microchannel filled with EGaIn. Reprinted with permission from ref.[89]. Copyright {2008} American Institute of Physics.

maintaining its conductivity over 10,000 cycles of 90% strain (**Figure 9b**). PEDOT:PSS represents another well-characterized material that has found applications in stretchable electronics. Previously, the use of PEDOT:PSS as a binding agent to prevent the migration of nanowires was discussed for self-healing, elastomeric AgNW conductors.[27] However, PEDOT:PSS has also been demonstrated to function itself as the conducting medium in stretchable conductors, as opposed to a serving in an auxiliary capacity.[91–95] This conducting polymer has been widely used in a variety of applications including OLEDs[96–98] and OPVs[99–101] due to its high conductivity in its doped state and its stability. In its most common form, PEDOT is doped with poly(styrenesulfonic acid) (PSS), which allows the conductive polymer to be dispersed in an aqueous solution, and modulates of the resulting conductivity of PEDOT:PSS. One of the most widely used forms of PEDOT, Clevios PH 1000 has a reported conductivity of 850 S/cm with the addition of dimethylsulfoxide (DMSO), which is able to increase the conductivity by 2-3 orders of magnitude.[91,102] Xia *et al*. also demonstrated significant increases in conductivity for PEDOT:PSS by preferential solvation of PEDOT:PSS with a cosolvent.[103]

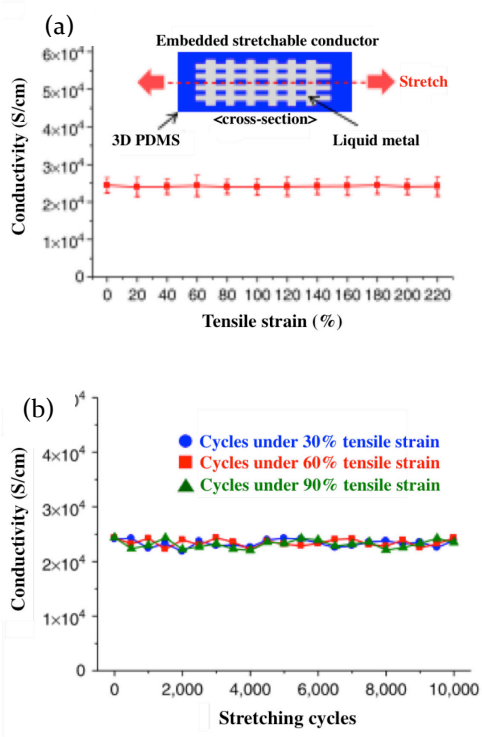

Figure 9: (a) Conductivity of the stretchable conductor as a function of strain, demonstrating the mechanical

compliancy of the conductor. (b) Conductivity of the stretchable conductor as a function of stretching cycles, indicating its stability to repeated deformation. Adapted and reproduced with permission from ref.[90]. Copyright {2012} Nature Publishing Group.

However the intrinsic conductivity of PEDOT:PSS is prohibitively low for certain applications, and though PEDOT:PSS posses better mechanical properties than traditional conductors due to its polymeric nature, dried films are still readily broken during mechanical stressing due to its hard segments.[94,104] To fabricate a highly elastic conductive polymer, Hansen *et al*. blended a polyurethane (PU) elastomer with PEDOT to form an composite with an initial high conductivity of 100 S/cm.[95] The PEDOT/PU film increased in resistance by a factor of 2 at an initial 50% strain, but negligible further increases in resistance in following cycles. Vosgueritchian *et al*. enhanced the conductivity while maintaining the elastomeric properties by adding a fluorosurfactant, Zonyl-FS300 to PEDOT:PSS/DMSO.[91] In addition to the 35% increase in conductivity, the addition of the fluorosurfactant allowed the conductive polymer to wet the surfaces of hydrophobic films. Furthermore, aside from merely the high conductivity with the addition of Zonyl, Savagatrup *et al.* demonstrated the addition of the fluorosurfactant was simultaneously able to improve the mechanical compliance of the PEDOT:PSS film.[105] For optoelectronic properties, Kim *et al*. reported that the addition of N,N-dimethylacetamide (DMAc) maintained the electrical performance of the PEDOT films while increasing light transmittance.[106] Typically, these PEDOT based elastomeric conductors can be subjected to 50% strain with negligible decrease of conductivity, and approach 200% strain before fracture.[28,91,95]

The stretchability of graphene has also been investigated by several groups[107–109] due to its well characterized electrical and mechanical properties.[110,111] Kim *et al*. used chemical vapor deposition (CVD) to grow graphene on a nickel substrate, and transferred the film to a PDMS substrate.[112] With this method, a sheet resistance of 280 ohm/sq. was achieved, and recoverable conductivity at tensile strains up to 6% was observed. However, further stretching resulted in catastrophic mechanical failure of the stretchable conductor. While this work served as a proof of concept of the efficacy of graphene to serve as a compliant conductor, it also highlighted some intrinsic limitations of the use of graphene. Though the theoretical sheet resistance of pristine graphene has been estimated to be as low as 30 ohm/sq.,[113] the difficulty in pristine graphene has resulted in high experimental sheet resistances on the order of 1 kohm/sq.[108,114] Furthermore, while graphene exhibits remarkable mechanical properties, the high elastic modulus[113,115] inherently limits the strain the film can be subjected to without degradation of its electrical properties.

To overcome these shortcomings, hybrid composites based on graphene have been developed for electronic skin applications.[108,116,117] Xu *et al*. chemically reduced silver nanoparticles on continuous graphene fibers to increase the conductivity by 330% compared to non-doped graphene fibers.[116] Chen *et al.* fabricated a

graphene foam (GF) by growing graphene on a nickel foam, depositing a layer of poly(methyl methacrylate) (PMMA) on the surface of graphene to provide mechanical support, etching away the nickel skeleton, dissolving the PMMA layer, and infiltrating the graphene skeleton with PDMS. The schematic of the fabrication procedure is illustrated in **Figure 10**.[117] With this process, the electrical conductivity was enhanced 6 orders of magnitude when compared to chemically derived graphene-based composites, and increased only 30% in resistance under 50% stretching.

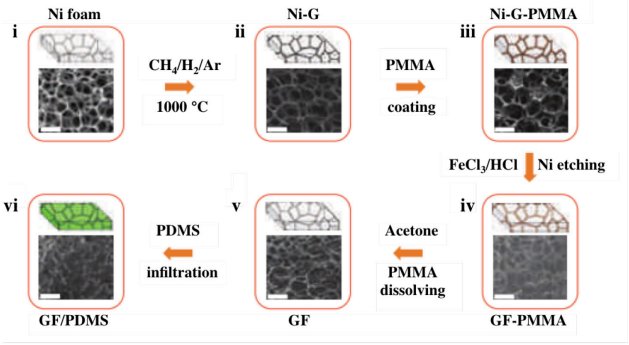

Figure 10: Fabrication of GF (i) Nickel foam (ii) CVD growth of graphene on Ni foam (iii) PMMA coated on graphene film (iv) GF coated with PMMA after etching Ni foam with $FeCl_3$/HCl solution (v) freestanding GF after dissolving PMMA with acetone (vi) Infiltration of GF with PDMS for elastomeric conductor. Adapted and reproduced with permission from ref.[117]. Copyright {2011} Nature Publishing Group.

Lee *et al*. reported graphene and silver nanowire hybrid conductors for high conductivity, transparent, stretchable electrodes.[108] By comparing the resistance of the hybrid conductor, it was observed that the sheet resistance of the hybrid was lower than the sheet resistance of the two individual components in parallel, complimentarily improving their own conductances. The cohabitation of these two conducting materials serve to mitigate each others' limitations; the AgNWs can bridge the defects of the polycrystalline graphene, while graphene can occupy the void spaces of the AgNW network. When transferred on to a PDMS elastomeric substrate, negligible resistance change was observed up to 100% tensile strain,[108] a significant improvement to the 6% strain achievable with pristine graphene on PDMS.[112]

For more niche applications, Keplinger *et al*. developed stretchable, transparent ionic conductors for high voltage, high frequency, and stretchable applications.[118] The design of the ionic conductor is based on two electrodes, and ionic conductor, and a dielectric, with the electrode/electrolyte interface forming an electrical double layer. This electrical double layer in conjunction with the dielectric act as two capacitors in series, allowing the control of electrochemical reaction and electromechanical transduction.[118] The stretchable ionic conductor was fabricated in a transparent loudspeaker as a proof of concept, and demonstrated large strains and production of sound over the entire audible range. Furthermore though higher resistivities are observed when compared to electronic conductors, a lower sheet resistance than all existing electronic conductors was demonstrated under large strains.[118] More applications using ionic gels will be elucidated upon in the following section.

The aforementioned materials represent different intrinsically compliant conductors. In some cases, the inherent properties of individual materials enable their use in flexible or stretchable electronics. Others require

integration within composite materials to endow the properties required for their desired application. With the large variety of materials to choose from, compliant conductors can be tailored for specific use in a multitude of different electronic muscle and skin applications.

2.2. Compliant semiconductors

Since the advent of what is regarded as the first transistor in 1947,[119] semiconductors have been ubiquitous in all electronic devices. Similarly, organic semiconductors have been the building blocks of organic electronics. Though these organic semiconductors are generally flexible,[120–127] their intrinsic stretchability is limited, due in part to the difficulty of retaining the high mobility in the π-π stacking charge transport network under strain.[28] Few reports, however, have indeed been conducted. Lipomi *et al*. reported the ability of poly(3-hexylthiophene) (P3HT) to stretch 2% when blended with (6,6)-phenyl C_{63} butyric acid methyl ester (PCBPM).[128] Savagatrup *et al*. built on this work by demonstrating that when the length of the side chain of P3HT was increased from six to seven carbon atoms (poly(3-heptylthiophene) (P3HpT), and blended with PCBM in a 1:1 ratio, the mechanical properties were enhanced while the electrical performance approached that of neat P3HT.[129] Graphene was previously discussed as a conductor capable of withstand a 6% tensile strain when used as a conductor.[112] Lee *et al*. reported a similar strain when graphene was used as the semiconducting channel in a stretchable transistor.[107] Liang *et al*. reported the use of a yellow light emitting polymer (SuperYellow) in an elastomeric polymer light emitting electrochemical cell (PLEC), citing the high molecular weight of SuperYellow to aid in large-strain stretchability.[130] However, though the device remained lit at a strain of 120%, the luminance was observed to decrease by over 80%.

Due to the relatively low strains achievable with individual semiconducting materials, a more prudent approach is to develop hybrid materials comprising semiconductors and elastic matrices. As an example of the efficacy of this method, the relatively unstretchable P3HT discussed previously were assembled in nanowires and blended in a PDMS matrix.[131] Unstretched, the resulting composite semiconductor exhibited comparable electrical performance to a homo-P3HT (unblended) nanowire organic channel when fabricated in a thin film transistor (TFT) with a bottom-contact configuration. To verify the semiconducting properties of the blended P3HT under strain, the active material was stretched, and contacted with SiO_2/Si substrates with pre-patterned source drain electrodes.[131] With this method, illustrated in **Figure 11a**, the mecho-electrical properties of the P3HT could be selectively analyzed without external influence from stretching either the electrode or dielectric layers.[131,132] The bottom-gate devices (**Figure 11b**) were characterized at strains from 0-100%, with the resulting average mobility plotted as a function of strain (**Figure 11c**).[131] While both homo- and blended-P3HT showed a significant initial drop in mobility up to 20% strain, the blended-P3HT based TFTs

exhibited stable mobilities at higher strains up to 100%, whereas most homo-P3HT based TFTs were non-functioning at the same strain. Similar characteristics were observed under cyclical strain testing, with the mobility relatively unchanged for the blended-P3HT devices after 5000 stretching cycles at 100%, but non-functioning for the homo-P3HT devices. AFM phase images were taken to examine morphological differences between the two P3HT behaviors under strain. The significant drop in mobility observed in both samples up to 20% was attributed to the rigidity of the P3HT homopolymer, fracturing the nanowires at low strains.[131,133,134] However, though the breaking of the P3HT nanowires in both systems along the stretching direction caused an initial drop in conductivity, a majority of the nanowires remained in a network in the PDMS blend under strain, whereas irreparable cracks formed in the homo-P3HT blend.

Similar to the P3HT / PDMS semiconductor blend, CNTs used in conjunction with an elastomeric matrix exhibit good mechanical[135,136] and current modulating properties,[137,138] and are amongst the leading materials used for stretchable semiconductors.[139–142] However, though individual semiconducting CNTs can have mobilities exceeding those of silicon, devices based on these nanotubes suffer from poor performance due in part to poor uniformity of the nanotubes.[143–145] Instead, random networks and films of nanotubes have resulted in more reliable performance and higher yields due to facile processing and their applications in deformable electronics.[145–147] Chortos *et al*. sprayed a network of CNTs as the active layer in a bottom gate, top contact device with resulting mobility of 0.18 ± 0.03 $cm^2V^{-1}s^{-1}$.[148] When the nanotube based TFT was stretched by 100%, the on current was observed to decrease by 50%.[148]

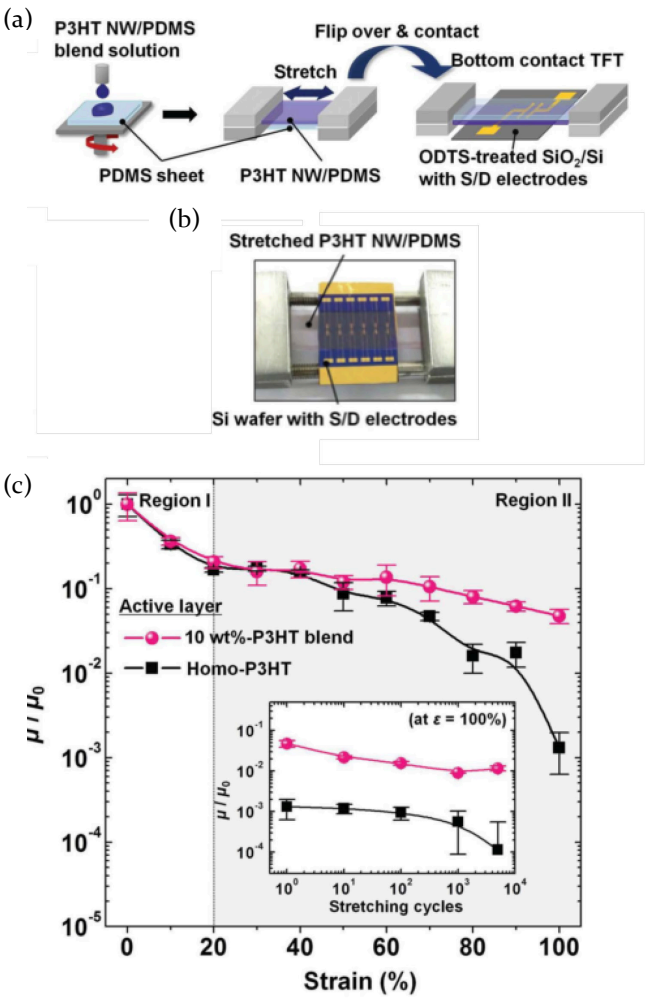

Figure 11: P3HT blends under strain (a) Schematic illustration of the process used to measure electrical properties of the organic TFTs (b) Optical image of the bottom-contact TFTs (c) Strain dependence of the homo-P3HT and 10 wt% P3HT-blend TFT. Inset shows the electrical characteristics of the device with repeated stretching cycles at 100% strain. Adapted and reproduced with permission from ref.[131]. Copyright {2012} Wiley-VCH.

Son *et al*. functionalized the surface of a substrate with poyl-L-lysine to form an amine-terminated surface, and formed random networks of SWCNTs by dip-coating

them into a solution of 99.9% semiconductive single walled carbon nanotubes (SWCNTs).[142] With these nanotubes, a mobility of ~5 $cm^2V^{-1}s^{=1}$ was realized in the fabrication of charge-trap floating-gate memory units and logic gates.[142] Using the same SWCNTs, Liang *et al.* used the 99+% (SWCNT) ink mixed with a fluorosurfactant and propylene glycol as an active channel deposited on pre-patterned AgNW source drain electrodes embedded in a polyurethane substrate.[46] The mobility of resulting devices was ~30 $cm^2V^{-1}s^{-1}$, could be stretched to 50% strain without significant loss in electrical property, and yielded a high enough output current to drive an OLED.[46]

In a work recently published by the Bao group, important strides were made in developing not only intrinsically stretchable, but healable semiconductor polymers as well.[149] In this work, chemical moieties were introduced to promote dynamic, non-covalent crosslinking of the conjugated polymers, which can achieve high stretchability by allowing the dynamic bonds to be easily broken to allow for energy dissipation upon strain. Hydrogen bonds were incorporated with the addition of 2,6-pyridine dicarboxamide (PDCA), which allow for the recovery of mechanical property. The resulting polymer was able to recover its high mobility after 100% strain during bending and unbending for 100 cycles.[149] As a proof of concept, TFTs were fabricated, tested, with the mobility of damaged devices after stretching being almost fully recovered after solvent and thermal healing treatment which were observed to greatly reduce the size and density of nanocracks.[149]

Though the development of these intrinsically stretchable semiconducting materials has not progressed as far as the field of stretchable conductors, stretchable semiconductors are the building blocks for wearable electronics. For intrinsically compliant electronic devices to not only become commercially viable, but to compete with stretchable electronics fabricated through the engineering and manufacturing of stretchable structures, significant work must still be done on development high performing, mechanically robust, compliant semiconductors.

2.3. Compliant dielectrics

In contrast to semiconductors, a wider range of compliant dielectrics exist due to the natural tendency of several polymers to have some degree of insulating properties. Poly(vinyl cinnamate) (PVCi) is one such dielectric commonly used in organic TFTs (OTFTs).[150–153] Jang *et al.* demonstrated the use of PVCi in a flexible organic TFT by dip coating a substrate in a solution of PVCi in chloroform, followed by photocuring the polymer at 255 nm through the chemical reaction illustrated in **Figure 12**.[154,155] When a metal insulator metal (MIM) capacitor was fabricated, the capacitance of the resulting structure was calculated to be ~6 nF/cm^2 when the dielectric layer was 500 nm thick.[155] In another study, Jang *et al.* showed the lack of hydroxyl groups in the crosslinked polymer resulted in hysteresis free OTFTs when PVCi was used as the gate dielectric.[154] Bae *et al.*

found that anisotropic photocrosslinking occurred when PVCi was exposed to linearly polarizing ultraviolet light.[156] This anisotropy arises from the breaking of the C=C bonds of the cinnamate side chains parallel to the direction of the polarized light, which cause [2+2] cycloaddition in the broken sidechains adjacent to the main chains and anisotropic distribution of cross-linked molecules perpendicular to the polarized light.[156,157] A subsequently deposited layer of pentacene was able to directionally align with PVCi, enhancing the mobility.[156]

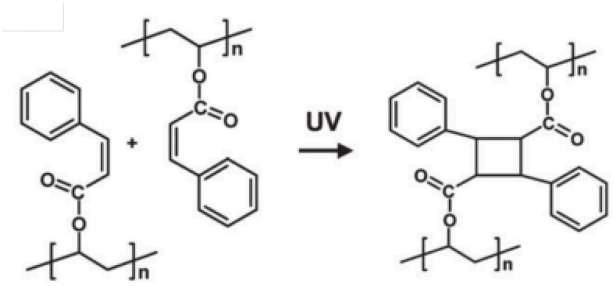

Figure 12: The chemical structure of PVCi (left), and photocrosslinked PVCi (right). Reprinted with permission from ref.[154]. Copyright {2008} American Institute of Physics.

The use of PVCi has been limited to, for the most part, flexible electronics. For applications requiring more stringent mechanical performance, the oft-mentioned elastomeric PDMS, previously only mentioned as a substrate material, has also been utilized as a dielectric.[158–162] Though the capacitance of the elastomeric dielectric is lower than the previously mentioned PVCi, the mechanical properties may enable its use for other applications. Ling *et al*. reported the use of PDMS with a capacitance of 2.9 nF/cm² that was used as the gate dielectric for a pentacene based TFT.[160] With the same dielectric, Cao *et al*. operated SWCNT TFTs successfully at tensile strains of 3.5%, demonstrating the use of PDMS as a dielectric for electronic applications. Continual improvements in material properties may facilitate the development of fully stretchable electronics. As an example, the Skov group prepared grafted cross-linkers by reacting 1-ethynyl-4-nitrobenzene and 3-4-((4-nitrophenyl) diazenyl)phenoxy)-prop-1-yn-1-ylium to prepare well-distributed dipole-functionalized PDMS networks in an effort to enhance the dielectric properties.[163] With 0.46 wt% of dipole-functional cross-linker, the dielectric constant was observed to increase by ~20% with low dielectric loss.[163] The Opris group synthesized polysiloxanes *via* anionic polymerization of 1,3,5-tris(3,3,3-trifluoropropyl)-1,3,5-trimethylcyclosiloxane with octamethylcyclotetrasiloxane to introduce CF_3 groups, which was able to increase the dielectric constant to 6.2 while still allowing the material to withstand up to 400% strain.[164]

However, because of the relatively low dielectric constant of PDMS, various other materials are often selected in its stead for use as stretchable dielectrics. Ionic gels, a polymer network swollen with an ionic liquid, represent another category of dielectrics used in stretchable electronics. For OTFT applications, ionic gels have been actively researched due to their high ionic conductivity, printability, and mechanical properties.[165–169] The operation of TFTs based on this class of dielectric is based

on the formation of a high capacitance electric double layer (EDL) at the dielectric/semiconductor and dielectric/gate interfaces under an electric field. Lee *et al*. utilized a UV cross-linked ion gel ink of poly(ethyleneglycol) diacrylate, 2-hydroxy-2-methylpropiophenone initiator, and 1-ethyl-3-methylimidazolium bis(trifluoromethylsulfonyl)imide ([EMIM][TFSI]) for a photo-patternable dielectric which could simultaneously serve as a negative photoresist to pattern the underlying graphene channel.[170] The use of the high capacitance (7.29 μF cm^{-2} at 10 Hz), patternable ion gel dielectric resulted in low voltage operation of the TFT, high on/off ratio, and a hole mobility of 852 ±124 cm^2 V^{-1} s^{-1}.[170] The Frisbie group reduced the polarization response time for applications requiring higher switching speeds by gelling ionic liquids with a self-assembled triblock copolymer (poly(styrene-*block*-ethylene oxide-*block*-styrene).[168] The high ionic conductivity (> 10^{-3} S cm^{-1}) enabled by the minimal amount of polymer required for gelling resulted in ion gel-gated OTFTs capable of operating at frequencies up to 1 kHz, an order of magnitude improvement over their previous report on ion-gel gated TFTs.[168,171] As a proof of concept of these materials for stretchable applications, Lee *et al*. fabricated a stretchable transistor using a printed poly(stryrene-methyl methacrylate-styrene) triblock copolymer and ([EMIM][TFSI]) ionic liquid.[107]

However, the intrinsic properties of individual materials may not always be sufficient. As in previously discussed classes of materials, composite materials combining the high-*k* nature of dielectric fillers and the mechanical compliancy of polymer matrices may lead to enhanced performance. Oh *et al*. demonstrated a stretchable dielectric comprising SWCNT embedded in PDMS, with the mechanical and dielectric properties enhanced with the addition of an ionic liquid (1-butyl-3-methyl-imidazolium bis(trifluoromethanesulfonyl)imide ([BMIM][TFSI]).[172] Kohlmeyer reduced the dielectric loss (and ehnahced the dielectric constant) of the CNT / PDMS dielectric by substituting the SWCNT for multi-walled CNTs (MWCNTs), with the outer graphene layer covalently functionalized to become nonconducting, while inner layers remain unfunctionalized and electrically conducting.[173] It was observed that the dielectric constant increased from ~3.3 (pure PDMS) to ~1249 with the incorporation of 9% hydroxylated MWCNTs.[173] Furthermore, the efficacy of the hydroxylated MWCNTs was demonstrated with a significant lower dielectric loss (~0.80) in contrast to the dielectric loss of the CNT / PDMS dielectric incorporating non-functionalized MWCNTs (~2.31).[173]

These composite dielectrics have been used to realize higher performing organic devices. Shi *et al*. formed a composite of PDMS with organic-capped titanium dioxide (TiO_2) nanoparticles as the dielectric layer in OTFTs. The integration of TiO_2 eliminates the requirement of an excessively thin PDMS film to obtain a sufficiently high capacitance to avoid short channel effects (SCE) in the transistors. With a 4:1 ratio of nanoparticles to PDMS, the dielectric constant increased

approximately three-fold, and yielded organic transistors with a mobility of 0.038 $cm^2V^{-1}s^{-1}$ and on off ratio of 10^4 – 10^5 when poly(3,3'''-didodecylquaterthiophene) (PQT-12) was used as the active material.[174] Zirkl *et al*. used a composite of PVCi and zirconium dioxide (ZrO_2) with a pentacene active material to record even higher values of the on/off ratio (~10^6) and mobility (0.9 – 1.2 $cm^2V^{-1}s^{-1}$).[175] Tien *et al*. combined highly crystalline piezoelectric poly(vinylidene fluoride-trifluoroethylene) (P(VDF-TrFE)) and barium titante (BT) nanoparticles to achieve a large-electro-physical coupling effect for physically responsive field-effect transistors.[176]

The aforementioned materials are by no means an exhaustive list of dielectrics utilized in compliant electronic devices. More materials, and the re-purposing of common materials for dielectric applications are continuously being researched and developed. As an example, in a deviation from the most commonly used solid state dielectrics, liquid dielectrics such as the ionic gels previously discussed, and vacuum and air dielectrics have also been explored.[177–180] This continual development of materials and techniques broaden the available resources for researchers to select to, allowing the development of new dielectrics to be used for a variety of different applications. Dielectric elastomers described in a following section are another important class of compliant dielectrics. While these are primarily treated for electromechanical transduction, their high mechanical compliancy and dielectric strength bode well for stretchable electronic applications.

2.4 Compliant electromechanically transducing materials

The development of materials and devices capable of mimicking muscle functions has long been sought after. One salient performance metric to emulate in the development of these materials and devices is mechanical energy density. Natural muscle has a mechanical density on the order of 150 J/kg and can peak at around 300 J/kg.[181] By this measure alone, electromagnetic (EM) motors and combustion engines should theoretically be able to match or exceed the performance of natural muscle.[182] However, as made evident by current cutting-edge robots (e.g. Boston Dynamics's Big Dog)[183] the applicability of conventional-actuator-based robotics to real-world applications is heavily limited. As an example, EM motors necessitate heavy battery packs and capacitor banks that require frequent recharging. By increasing the overall mass of the robotic device, the effective energy density as well as range and mobility are simultaneously adversely affected. Scaling down these bulky components to mitigate these issues similarly reduces the power efficiency while increasing the difficulty of fabrication. Furthermore, EM motors and gears generate significant noise, making them environmentally disruptive. Pneumatic systems have also been utilized due to their linear operation approaching the movement natural muscle. McKibben artificial muscles in particular are intrinsically compliant, and have been investigated for robotic applications.[184,185]

However, these systems require air compressors that are also bulky, and are further limited in response speed due to the pumping of air into and out of the actuators.

Several "smart materials" have been proposed as alternatives to natural muscle. Amongst these alternative muscles that have been suggested are shape memory alloys (SMA), magnetostrictive alloys (MSA), and piezoelectrics.[30,186] However though SMAs are capable of producing relatively large linear displacements, they are limited by the time required to cool the alloy and return to the rest position. With regards to the latter two, magnetostrictive alloys and piezoelectric ceramics both intrinsically suffer from small strains and high stiffness, rendering this trio of materials all unfit to serve in the stead of natural muscle.

Electroactive polymers (EAPs) are an emerging actuator technology wherein a lightweight polymer responds to an electric field by generating mechanical motion.[187] Due to their ability to mimic the properties of natural muscle so accurately, the moniker "artificial muscle" has been coined to describe EAPs. The concept of these materials can be traced back to 1880 in a paper published by Roentgen.[188] In his experiments, he observed that a film of natural rubber could alter its form factor through the application of a large electric field, the first observation of actuation of a dielectric elastomer material. Since 1880, the number of electroactive polymers and technologies based on these materials has grown substantially. For a more comprehensive overview of the field, readers of this Review may refer to the proceedings of the annual SPIE's Smart Structures and Materials Symposium on Electroactive Polymer Actuators and Devices,[187,189,190]

EAPs can be broadly divided into ionic and field-activated EAPs based on their actuation mechanism. Ionic polymer-metal composites, ionic gels, carbon nanotubes, and conductive polymers fall under the former classification, while ferroelectric polymers, polymer electrets, electrostrictive polymers, and dielectric elastomers fall under the latter. In addition to these classifications, there are also a variety of responsive polymers such as shape memory polymers, nylon 6,6 monofilament sewing thread, and polymers whose deformations are triggered by chemical reactions, including responsiveness to pH and temperature change.[191] In this section of the Review, several important EAP materials will be highlighted, with a specific focus on dielectric elastomers. Table 1 summarizes the actuation properties for several of these materials, alongside other actuation technologies including mammalian muscle. It is important to note

Table 1: A comparison of actuation properties of important EAP materials.

Type	Maximum Strain (%)	Maximum Pressure (MPa)	Specific Elastic Energy Density (J/g)	Relative Speed (full cycle)	Ref.

Dielectric Elastomer (Acrylic with prestrain)	380	7.2	3.4	Medium	[192]
Dielectric Elastomer (Silicone with prestrain)	63	3	0.75	Fast	[192]
Dielectric Elastomer (Silicone - nominal prestrain)	32	1.36	0.22	Fast	[193]
Dielectric Elastomer (Polyurethane - nominal prestrain)	11	1.6	0.087	Fast	[193]
Electrostrictor polymer (P(VDF-TrFE-CFE))	4.5		1.1	Fast	[194]
Electrostatic devices (integrated force array)	50	0.03	0.0015	Fast	[195]
Electromagnetic (Voice Coil)	50	0.1	0.003	Fast	[193]
Piezoelectric Ceramic (PZT)	0.2	110	0.013	Fast	[196]
Piezoelectric Single Crystal (PZT-PT)	1.7	131	0.13	Fast	[193]
Piezoelectric Polymer (PVDF)	0.1	4.8	0.0013	Fast	[193]
Relaxor ferroelectric polymer (PVDF-TrFE-CFE)	7	21	0.73	Fast	[197]
Shape memory alloy (TiNi)	> 5	> 200	> 15	Slow	[198]
Shape memory polymer (Polyurethane)	100	4	2	Slow	[199]
Thermomechanical twisted polymer fiber (nylon 6,6 monofilament)	35	16		Slow	[191]
Thermal (Expansion - Al dT=500 K)	1	78	0.15	Slow	[193]
Conducting Polymer (PANI)	0.85	100	0.32	Slow	[200]

IPMC	3	30			[201,202]
Carbon naotubes (CNT paper)	1	27	0.04	Slow-fast	[30]
Magnetostrictive (Terfenol-D)	0.2	70	0.025	Fast	[203]
Natural Muscle (Peaks in nature)	100	0.8	0.04	Slow-Fast	[204]

that these data were recorded for different materials under different conditions; as a result, information provided in **Table 1** should be used only for qualitative comparison

2.4.1 Ionic EAPs

Actuators based on conductive polymers were first proposed by Baughman *et al.* in 1990.[205] Following the development of this work, Pei and Inganas explored the uptake of counter-ions during the electrochemical redox of polypyrrole, and designed bilayer beam actuators to obtain large bending deformations.[206–208] Otero *et al.*, amongst others, extensively investigated the underlying electrochemical mechanisms.[209,210] As shown in **Figure 13**, for polypyrrole doped with small counter anions (such as perchlorate), the oxidized state causes the polymer chains to expand due to the presence of the counter anions; in the reduced state, the ions migrate away and the polymer chains relax. In polymers doped with bulky counter anions (such as dodecylbenzene sulfonate), the reduction involves uptake of cations into the polymer, resulting in the reduced polymer being in the expanded state.[207,208,211] Because both the oxidized and reduced states are stable, these actuators are considered bistable. The most commonly used of these conducting polymers for actuation purposes are polypyrrole, polyaniline, and poly(3,4-ethylenedioxythiophene) (PEDOT).[212–217] Actuators based on these materials typically have low actuation voltages (1-2 V),[217] with strains varying from 1 to ~40%,[30,218,219] and force densities up to 100 MPa.[200] However, these conductive polymers suffer from a very low operating efficiency and electromechanical coupling, both ~1%.[30] Furthermore, actuation speeds are limited as the mechanism relies on the migration of ions,[220] in

addition to the internal resistance between the electrolyte and polymer.[30] Research efforts into this aspect focuses more on the ionic migration and actuator design for important application, rather than molecular designs of the polymer chains.

PPy (A^-) when the dopant is small

Reduction: $PPy^+(A^-) + e^- \rightarrow PPy^o + A^-$

Oxidation: $PPy^o - e^- + A^- \rightarrow PPy^+(A^-)$

PPy (A^-) when the dopant is large

Reduction: $PPy^+(A^-) + e^- + M^+ \rightarrow PPy^o(A^-M^+)$

Oxidation: $PPy^o(A^-M^+) - e^- \rightarrow PPy^+(A^-) + M^+$

Figure 13: Counterion insertion and repulsion during the electrochemical redox of polypyrrole.

Molecular actuators are organic compounds or polymers that undergo giant shape change upon charge transfer. The Nobel Prize in Chemistry in 2016 was awarded jointly to Jean-Pierre Sauvage, Sir J. Fraser Stoddart and Bernard L. Feringa for the design and synthesis of such molecular machines based on catenane and rotaxane.[221] Poly(calixarene-hinged thiophene) was synthesized by Anquetil *et al.* to produce large macroscopic strains, as illustrated in **Figure 14**.[222] This copolymer comprises a calix[4]arene scaffold that could be driven between the cone and 1,3-alternate conformation, and a quaterthiophene unit that is redox active. A T space-filling model suggests that one dimensional changes of as large as a factor of 5 are possible, driven by π-stacking between the thiophene oligomers.[223] Molecular simulation indicates that a single molecule of calix[4]arene-quaterthiophene could produce at most 92 pN of average active force. The proportion of energy converted to work (electromechanical coupling efficiency) of the copolymer acting as a molecular actuator is estimated to potentially be as high as 66.7%, which would fare better than conducting polymer actuators on a macroscopic scale. However, the macroscopic actuation performance of the molecular actuators has not been reported. Reported works thus far include Erbas-Cakmak *et al.*, who have extensively surveyed the molecular architectures for nanomachines and attempted to use ratchet mechanisms to create motor-mechanisms.[224]

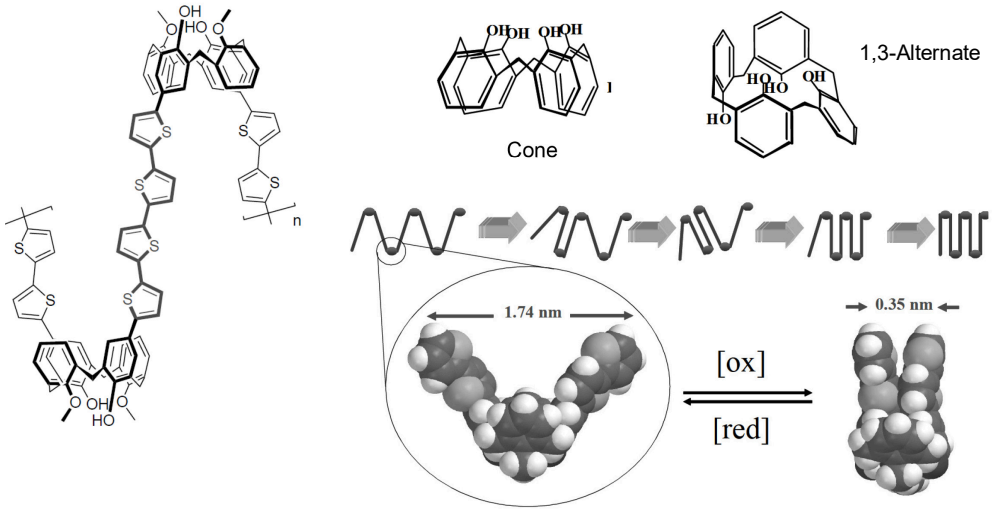

Figure 14: A molecular machine based on a molecular rotaxane copolymer.[222] Reprinted with permission from ref[225]. Copyright {2002} SPIE.

Ionic polymer-metal composites (IPMCs) consist of a solvent swollen ion-exchange polymer membrane laminated between two thin flexible metals (typically percolated Pt nanoparticles or Au).[226,227] Application of a bias voltage to the device results in the migration of mobile ions within the film to the oppositely charged electrode causing one side of the membrane to swell and the other to contract, resulting in a bending motion.[228] Over time the actuator slightly relaxes due to the built-up pressure gradient. Typical membrane materials include Nafion and Flemion[220] with anionic side groups or polystyrene ionomers with anionic-substituted phenyl rings.[30,181,226] Driving voltages are typically on the order of a few volts, and actuation strains and stresses of >3%[202] and 30 MPa[229] have been reported. Several studies have demonstrated that IPMCs are well suited for use as soft actuators for bending and sensing.[230]

Individual carbon nanotubes (CNTs) possess a high tensile modulus approaching that of diamond (640 GPa), and their tensile strength is estimated to be 20-40 GPa, an order of magnitude larger than any other continuous fiber.[231] However, the mechanical properties of CNT bundles typically used in actuator tests tend to be significantly lower as they are held together by relatively weak van der Waals forces.[232] These bundles of CNTs suspended in an electrolyte are capable of expanding in length due to double-layer charge injection.[30] The resulting actuation is due to these effects, in addition to Coulombic forces.[30,233] When actuated, CNTs possess low actuation voltages (~1 V), high operating loads (26 MPa), high effective power to mass ratios of 270 W/Kg, strains < 2%,[30] and a response speed in the millisecond range.[234] Like conducting polymers and IPMCs, CNTs also suffer from very poor electromechanical coupling. Aliev *et al.* reported on novel giant-stroke, superelastic CNT aerogel muscles fabricated from highly ordered CNT forests which are capable of anisotropic linear elongations of 220%.[235] Foroughi *at al.* recently reported that an electrolyte-filled twist-spun CNT yarn much thinner than a human hair can function as a torsional electrochemical artificial muscle.[236] This yarn was actuated to a reversible 15,000° rotation and 590 revolutions per minute through hydrostatic mechanisms. This mechanism mimics muscular hydrostats observed in nature, and leads to simultaneous occurrence of lengthwise contraction and torsional rotation during the yarn volume increase caused by the electrochemical double-layer charge injection.[236]

2.4.2 Field activated EAPs

Ferroelectric polymer poly(vinylidene fluoride trifluoroethylene), P(VDF-TrFE), exhibits piezoelectric responses after appropriate poling.[237] Their piezoelectric actuation properties are typically worse than ceramic piezoelectric crystals; however, they offer the advantages of being lightweight, flexible, easily formed, and are not brittle. The actuation strain of P(VDF-TrFE)s can be

increased by breaking down the size of the nanocrystalline domain, thus transforming the polymer into a relaxor ferroelectric. The resulting polymers are termed electrostrictive polymers, and have a spontaneous electric polarization. Zhang *et al.* demonstrated that irradiation with high-energy electrons or protons is an effective technique to increase this actuation strain, and reported a P(VDF-TrFE) with actuation strain as high as 7%.[197,238] Other mechanisms include adding a bulky side group by introducing co-monomers such as cholorofluoroethylene (CFE), chlorotrifluoroethylene (CTFE), or hexafluoropropylene (HFP), which produces similar results while avoiding radiation treatment which tends to make the copolymer more brittle.[239,240] Electrostriction has also been obtained from graft copolymers wherein polar crystallites are grafted to flexible polymer backbones. Electrostriction has also been obtained from graft copolymers wherein polar crystallites are grafted to flexible polymer backbones.[241]

Liquid crystal elastomers (LCEs) combine the orientational ordering properties of liquid crystals with the elastic properties of elastomer networks.[242] These elastomers were first used as artificial muscles by de Gennes in the late 1990s.[243] In their first iteration in this capacity, the activated LCEs displayed strains on the order of 35-45%, but were limited in response speed due to the requirement for heat diffusion.[243–245] Electrically activated LCEs exhibit significantly faster response speeds (10 ms)[246] than their thermally activated counterparts, and the required fields (1.5-25 MV/m) required for actuation are lower than most other field activated EAP technologies. The tradeoff, however, is the relatively small actuation strains (<10%) and low work density.[246,247] It was recently reported that cholesteric liquid crystal elastomers swollen by low-molecular-mass liquid crystals could be electrically actuated up to 30% strain along the electric field axis.[248]

Dielectric elastomers (DE) denote a class of dielectric materials capable of deformation upon application of an electric field. The detailed operations of a DE transducer can be found in literature from Pelrine *et al*. and Carpi *et al*.,[249,250] and is illustrated in **Figure 15**.[251] Briefly, a DE transducer consists of a polymer film sandwiched between two compliant electrodes. For substantial actuation, the electrodes must be composed a softer material than the DE film.[252] Upon application of a voltage difference between the two electrodes, actuation occurs due to Maxwell pressure, given by:[40,253]

$$\sigma_{Maxwell} = \varepsilon_0 \varepsilon_r \left(\frac{V}{d}\right)^2$$

where $\sigma_{Maxwell}$ is the Maxwell pressure, ε_0 and ε_r denote the absolute and relative dielectric permittivities, respectively, V is the driving voltage, and d the thickness of the polymer film. Readers of this Review are referred to Theory of Dielectric Elastomer authored by Suo for a more comprehensive discussion of the underlying theory

of actuation.[252]

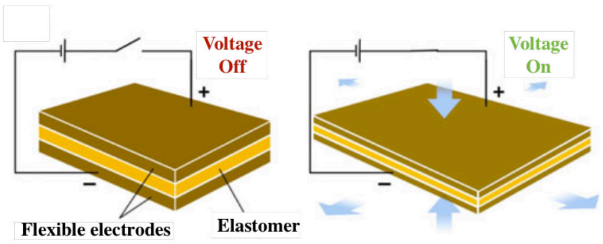

Figure 15: Basic operating principle of a dielectric elastomer actuator. Adapted and reproduced with permission from ref.[251]. Copyright {2013} Springer.

The selection of DE material is paramount to the design of actuators. The material properties of specific DEs control actuation behavior, as the Maxwell strain discussed in the preceding paragraph is dependent upon these parameters. Subsequently, the strains and deformations achievable vary from material to material. Two of the most heavily researched materials for DE technology are acrylic (3M's VHB 4910) and PDMS (CF-19-2186 from NuSil). Acrylate copolymers exhibit a relatively high dielectric constant for neat polymers, and have a high field strength.[254] Maximum Maxwell pressures of acrylics with prestraining, which will be discussed in subsequent paragraphs, can reach 1.2 MPa.[32] The large Maxwell pressure results in similarly large deformations, as these materials are highly elastic due to a combination of soft, branched aliphatic groups, and light cross-linking of the acrylic chains.[252,255] Maximum strains of 380% have been reported with the use of acrylic DE actuators.[32] Further larger strains as high as 17x have also been obtained when programmed mechanical bias is additional applied.[118] Because of these material characteristics, higher overall actuation performance is observed when contrasted to other DE materials such as silicone and polyurethane. Furthermore, because acrylate copolymers can be readily synthesized from common monomers, nanocomposites can be easily developed with enhanced actuation properties. Compared to acrylic materials, silicones are subjected to lower Maxwell pressures, with pressures around 3 MPa reported. Consequently, strains approximately 5x lower than that in acrylics are typically observed.[32] However, though higher actuation performance is observed with acrylic, silicone elastomers are also widely used due to their faster response time, as acrylic elastomers exhibit high viscoelastic losses.[252] Clearly, then, different DE materials are better suited for different applications based on their inherent advantages and limitations. As an example, acrylics, as described previously, are capable of large strains, yet exhibit viscoelasticity. Silicones have fast response time, but limited actuation strains, and as a result, can suitable for energy harvesting.[256] Polyurethanes in general are excessively stiff, while thermal plastic elastomers may lack in stiffness.[256] A deeper discussion of specific materials and their properties, including a relative comparison of forces and strains can be found in a review authored by Brochu *et al*.[32] Careful selection of material based on design requirements is paramount for the fabrication of successful DE actuators.

Most importantly, highly compliant dielectric elastomers typically exhibit electromechanical instability, or pull in failure, due to the long plateau on the stress-strain

response curve as illustrated in **Figure 16**.[32,257,258] As such, stable actuation is limited by the apparent breakdown electric field, which is substantially lower than the breakdown electric field strength of the DE material. The material's intrinsic breakdown occurs when the voltage mobilizes charged species in the DE film, producing electrical conduction in the film when local electric fields exceed the dielectric strength of the film. Electromechanical instability occurs when a constant actuation voltage is applied that results in the thinning of the DE film, increasing the electric field, which in turn leads to larger strain. This positive feedback eventually leads to dielectric breakdown. An effective approach in controlling this pull-in failure and thus obtaining high actuation performance in line with the DE's intrinsic breakdown field strength is prestraining, which brings about the rapid rising stiffness of the DE film approaching the maximum elongation to overcome this positive feedback loop.[225] On the actuator side, prestraining of DE films can improve the actuation strain and energy density of subsequently fabricated actuators.[249,256] Additional benefits of prestraining include being able to 'program' actuation in a certain direction by prestraining in the orthogonal direction of the desired actuation direction, improved mechanical efficiency, and faster response speeds.[32]

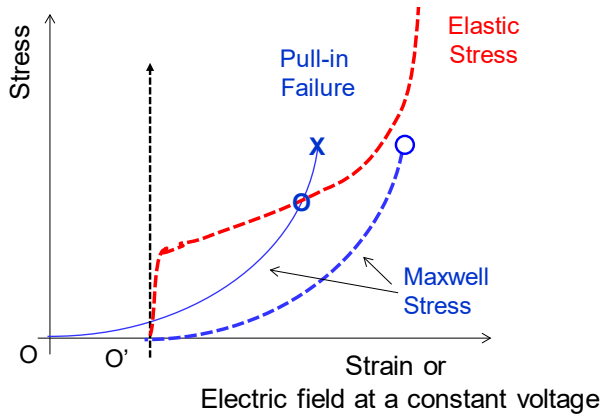

Figure 16. Characteristic stress-strain curve of a dielectric elastomer film as a function of mechanical strain or electric field (under constant voltage actuation). The lines with origin at O are for a non-prestrained film and at O' for the prestrained film. The cross (X) indicates dielectric breakdown. Small o and large O represent the apparent breakdown field and actual breakdown strength, respectively.

However, prestraining films may also bring about deleterious effects. This added processing step brings about new complexities, adding fiscal, time, and performance considerations. In order to maintain the tension in the film, additional rigid, passive structures are required, introducing several copmlications.[32,256] These structures lead to local stress concentrations in the DE film, leading to potential failure of the actuator due to stress relaxation and fatigue.[256] Furthermore, the additional mass of the supporting structure add significantly to the volume and mass, which can reduce the work density and power to mass ratio of the device.[30,256] Due to these limitations, the reduction or elimination of prestrain while still achieving the same performance is desirable.

The development of new DE materials and composites has been show to eliminate the need of prestrain, while

still maintaining high actuation performance. Vargantwar *et al*. demonstrated a thermoplastic elastomer gel (TPEG) comprising acrylic triblock copolymers swollen with a high dielectric to demonstrate pre-strain DE capable of high actuation strain at low electric fields.[259] Suo *et al*. described a model of a dielectric elastomer with interpenetrating networks that did not require pre-straining for actuation.[260] The interpenetrating network comprised two lengths of chains, one long, and one short, with the long chain network filling space to keep the elastomer compliant at small deformations, while the short chain restrains the elastomer from excessive thinning.[260] Niu *et al*. tuned the stress-strain relationship by varying the amount of cross-linker in a UV curable precursor to completely suppress electromechanical instability (EMI) and eliminate the need for prestrain due to the rapid stiffening of the material above a threshold stretch ratio.[253] It was reported that strains of 314% or a maximum breakdown of 236 V μm were achievable while fully suppressing EMI).[253] Ha *et al*. empirically demonstrated high-performance interpenetrating networks based on acrylic elastomers and poly(1,6-hexanediol diacrylate) that retain benefits resulting from pre-strain without utilizing external mechanical prestrain.[261,262] The poly(1,6-hexanediol diacrylate) network formed inside the highly pre-strained elastomer network, supporting the pre-strain of the elastomer. Because this network is under compression, it can balance the elastomer network under tension, preserving the pre-strain of the VHB network. It was observed that a film with 18.3 wt. % of poly(1,6-hexanediol diacrylate) in VHB could preserve pre-strain up to 275%, and electrically induced strains up to 233%.[262]

Bottlebrush elastomers have been recently reported as materials that feature inherently strained polymer networks eliminating this EMI. These elastomers are macromolecules with two or more polymeric side chains grafted to a polymer backbone, allowing for unique properties. The brush architecture allows for the expansion of the diameter of the polymer chain, in turn reducing the entanglement while negating effects of increased stiffness.[263] Daniel *et al*. demonstrated bottlebrush elastomers with extremely low modulus (~100 Pa), 1000% strain at break, and that are solvent free, which eliminate potential phase segregation and porosity that may arise with the use of solvents.[263] The same group expanded on that work by demonstrating the tunability of actuator rigidity and elasticity over broad ranges without changes in chemical composition using bottlebrush elastomers.[264] By varying the side-chain length, grafting density, and crosslink density, they demonstrated the synthesis of DEs based on bottlebrush elasttomers with moduli ranging from 1 MPa down to 100 Pa.[264]

The Pei group demonstrated reversible, large-strain bistable actuation with bistable electroactive polymers (BSEP) without the requirement of pre-straining.[67,225,265] The term bistable in this sense alludes to the ability of the DE film to exist in two geometries: the original form factor, and its actuated shape. As an illustration of the

working principle of BSEP materials, poly(tert-butylacrylate) (PTBA), a rigid, thermoplastic, which acts as a dielectric elastomer above 50 °C was used, with a thin layer of silver nanowires buried at the surfaces. **Figure 17** illustrates the deformation of the PTBA BSEP material. The stiff PTBA at room temperature can be heated to above its glass-elastic temperature of 40 °C.[265] Once softened, the polymer can undergo electrical actuation to any state between its fully relaxed, and fully actuated state. Once the bias voltage is removed, the temperature can be lowered below the glass transition temperature to lock in the desired shape. The utilization of the AgNW electrodes with the BSEP material allowed for repeatable bistable electrically induced actuation, as the electrode supports strains greater than 100% and can be used for Joule heating to soften the material.[67] A followup work was conducted by Ren *et al.*, in which a phase changing polymer comprising stearyl acrylate and a long chain urethane diacrylate was utilized as a BSEP material.[266] The stearyl acrylate was utilized for its phase changing ability due to its sharp transition within 10°C between the crystalline and molten states of its stearyl moieties, while the long-chain urethane diacrylate was used for its high tensile strength in both the rigid and rubbery states, allowing for large-strain electrical actuation. The resulting BSEP material can be actuated at 50 °C up to 70% strain, and has potential for biomedical applications, as the transition temperature occurs at a temperature close to body temperature but below the perceptible pain threshold temperature of 43.2 ± 0.4°C.[266,267]

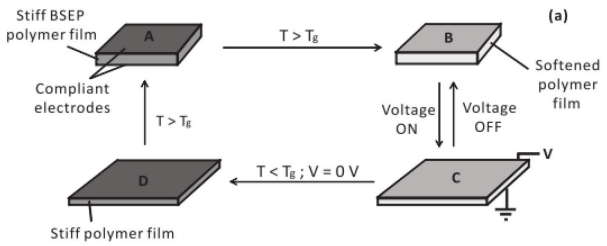

Figure 17: Bistable acruation mechanism of a BSEP material. Reprinted with permission from ref[225]. Copyright {2012} Wiley-VCH.

Though dielectric elastomers are a class of materials that get relatively less attention, new discoveries in recent years may push this technology as an alternative to actuator technology. Due to the low-cost and ease of fabrication of devices utilizing these materials, several applications have been researched in recent years. Some of these applications will be discussed in a later section.

3. Devices

The transistor is the fundamental component behind modern electronic devices. Though in recent years the industry has observed a deceleration in Moore's law, new discoveries and innovation have continued to progress at a rapid pace, with the new generation of flexible and stretchable electronics one prime example. These devices, though trailing behind traditional inorganic devices, offer the potential benefit of low cost, consumer adjustable electronics. However, in contrast to the discrete classes of materials described in the previous sections, intrinsically compliant transistors, and all integrated devices, require not only specific materials' properties tailored for particular use, but also

compatibility between different classes of materials in addition to the various processing steps necessitated for their incorporation. As a result, several processing challenges arise, including mitigating the potential solvent attack of various layers,[268,269] and ensuring the surface energies of various components are aligned[137,270] to prevent delamination during use.

As an example of the challenges required in the fabrication process, Liang *et al.* demonstrated a fully intrinsically stretchable and transparent transistor based on silver nanowires, carbon nanotubes, and an elastomeric dielectric.[46] AgNWs were patterned through spray coating for use as the source/drain electrode, and embedded and transferred within a stretchable PU matrix.[46] Semiconductive SWCNT ink was prepared in solution with fluorosurfactant and propylene glycol to enhance the wetting and levelling control during deposition of the active layer.[46] A stretchable and transparent dielectric layer was selected taking in account its mechanical stretchability, compatibility with the source/drain electrode, viscosity, and ability to be dissolved in a solvent which would not attack the underlying channel or bottom electrodes. The sandwich stack was finally laminated with another AgNW-PU gate electrode, producing a TFT capable of withstanding 50% strain and 500 cycles of stretching to 20% strain without significant degradation in performance.[46] Though fundamentally the structure of these next generation devices remains largely unchanged from their inorganic counterparts, additional measures must be considered to ensure a feasible and practical process flow, in addition to careful selection and tuning of material properties.

3.1. Sensors

Sensing capabilities are paramount to the functionality of electronic skins. Though various sensors have been demonstrated and commercially implemented throughout the years, the advent of flexible and stretchable technology simultaneously brings about more challenges and more exciting possibilities. The following sections go in further detail about these new sensors and some challenges present during design and fabrication of these sensors.

3.1.1. Pressure sensor

As the primary function of human skin is force sensing,[271] several groups have developed their own versions of pressure sensors to emulate this property of human skin.[24,52,158].

The Bao group demonstrated an organic, flexible pressure sensor by incorporating a compressible rubber for use as the dielectric in an organic field effect transistor (OFET).[5] As the output current in these organic devices are directly correlated to the dielectric capacitance, a property dependent on the thickness of the dielectric, this compressible dielectric enables the sensing of applied pressure. As a proof of concept of the viability of the compressible rubber as a suitable dielectric for pressure sensing, capacitors were fabricated using both unstructured and pyramid structured PDMS as the dielectric.[5] Significantly higher pressure sensitivity was

observed with the microstructured dielectric due to lower elastic resistance as a result of the air voids (which has a lower dielectric constant) within the PDMS film), increasing the capacitance in the patterned film from the reduction in the distance between electrodes and increase in effective dielectric constant.[5] The microstructured PDMS was fabricated into an OFET, using a rubrene single crystal as the active materials, gold source-drain electrodes, and ITO on PET as the top gate. The device was grounded on the highly doped Si substrate. The schematic of the low-impedance-output active-matrix design is illustrated in **Figure 18a**. **Figure 18b** shows the output curve as a function of external pressure, and demonstrates the ability to discretely increase the output current in response to greater loads. This pressure sensing ability is directly attributed to the compliant dielectric increasing in capacitance upon compression, subsequently increasing the gate electric field at the interface between dielectric and active layer. A further study conducted by Schwartz *et al*. built on this work and integrated the microstructured PDMS in thin film, flexible polymer transistors with sensitivity 15 times higher than the aforementioned work by operating the transistor in the subthreshold regime, where the output current depends superlinearly on the capacitance change induced by applied pressure.[21] With these new developments, a pixel array of transistors was developed with the capability of comforming to an adult human wrist and recording characteristic pulse pressure shapes, including small features in the diastolic tail of the pulse tradiationally difficult to resolve in a vast majority of sensors used in arterial tonometry.[21] The pulse waves, in addition to a photograph of the sensor attached to an adult wrist illustrating the ability to conform to non-flat form factors are depicted in **Figure 19a/b** and **Figure 19c**, respectively

Koeppe *et al*. demonstrated a flexible device capable of determining the magnitude and position of light and touch points using a silicone elastomer waveguides in conjunction with LEDs and photodiodes.[272] Ramuz *et al*. built off this work and demonstrated a stretchable optical pressure sensor utilizing a PDMS film as the waveguide and substrate, and OLEDs and polymer organic photodiodes (OPDs) as the light source and photodetector, respectively.[7] The selection of organic devices for the light emitting and photodetecting

component of the integrated pressure sensor was to

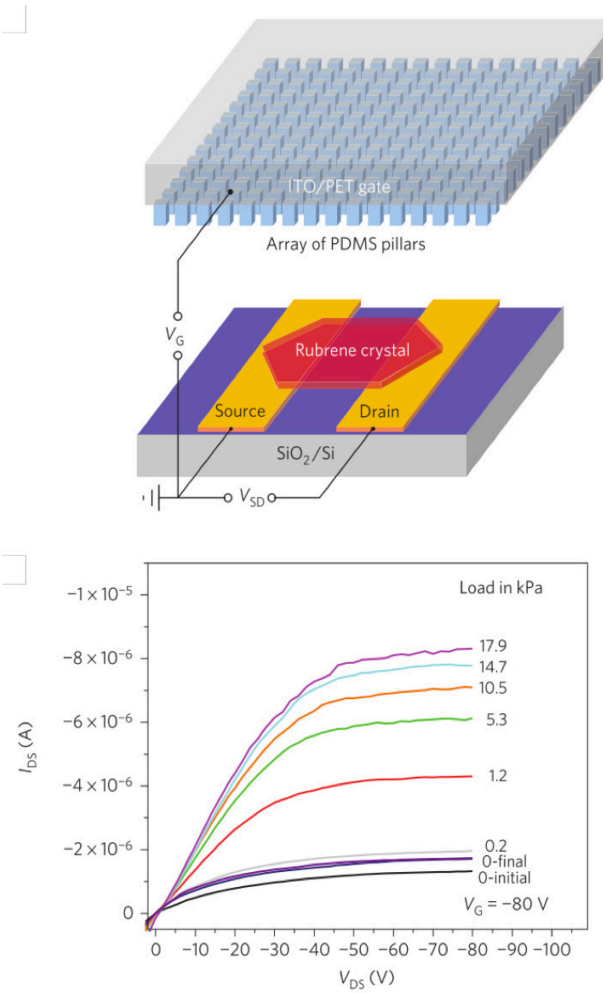

Figure 18: Pressure response of organic transistor with microstructured PDMS dielectric layer (a) schematic of pressure-sensing organic transistors with rubrene single crystals and PDMS dielectric film. (b) Output curve of pressure-sensor with varying applied external pressure. Adapted and reproduced with permission from ref.[5]. Copyright {2010} Nature Publishing Group.

ensure high performance on flexible and stretchable substrates for electronic skin and physiological measurement applications. The PDMS was embossed with two sets of identical gratings, as illustrated in **Figure 20**, to in- and out-couple light generate by the OLED. When compressed, the waveguide formed by the compression of the PDMS supports fewer modes, resulting in a lower intensity of light detected by the photodiode at the out-coupling grating stage.[7] With the device structure as seen in **Figure 20a**, the pressure sensitivity, defined by the slope of the photocurrent variation plot, reached a peak sensitivity as high as 0.2 kPa^{-1}.[7] When stretched to a 50% strain, the sensitivity increased to 0.32 kPa^{-1}, with the increase in sensitivity being attributed to the reduction in thickness of the waveguide.[7]

As an example of materials selection based on specific requirements, the Suo group developed a biocompatible hybrid pressure and strain sensor based on ionic conductors.[273] The use of ionic conductors lead to electrical double layers forming at the interface between electrodes and ionic conductor, in addition to the ionic conductors and dielectric, forming two capacitors in series with each other. Upon deformation in the acrylic elastomer dielectric, the capacitance in the electric double layer increases, allowing the functionality as a strain and pressure sensor. In conjunction with a polyacrylamide hydrogel containing NaCl functioning as the ionic conductor, a sheet of sensors was fabricated which could detect the location of touch, and resolve the pressure of a single finger.[273]

Pressure sensors based on the nanotube and nanowire conductors mentioned previously have also been developed. Lipomi *et al.* fabricated transparent conductors using SWCNT sprayed on PDMS capable of withstanding strains up to 150%, with demonstrated conductivities up to 2,200 S/cm in the stretched state.[8] These nanotube films were subsequently integrated for

use as electrodes for stretchable capacitors utilized for pressure and strain sensors that manifest changes in these parameters through changes in capacitance. The stretchable capacitors were formed through the lamination of two patterned compliant electrodes sandwiching an Ecoflex silicone elastomer, forming an 8 x 8 pixel array of capacitors.[8] Different modes of deformation were able to be distinguished: tensile straining would affect pixels along the axis of strain, while pressure would affect pixels in the vicinity of the applied load. This distinction obtained through the use of stretchable materials helps mitigate the crosstalk inherent in pressure sensors, with the cross talk approximately half that observed for a similar device fabricated on a non-stretchable polymer substrate.[5,8] Yao *et al.* used a similar concept with the Ecoflex dielectric sandwiched between two screen-printed patterned AgNW electrodes.[274] The resulting capacitive sensor can detect strain up to 50%, pressure up to 1.2 MPa, and finger touch with high sensitivity.[274] Furthermore, as proof of concept of the viability of these sensors for practical application, these devices were used to monitor thumb movement, sense strain of the knee in patellar reflex, and various other human motions illustrated in **Figure 21**. AgNW capacitors were also fabricated by embedding the wires within PDMS[275] or a polyurethane substrate[276] and using a highly compliant dielectric spacer, with the resulting sensor arrays capable of sensing stretch, pressure, and touch sensitivities.

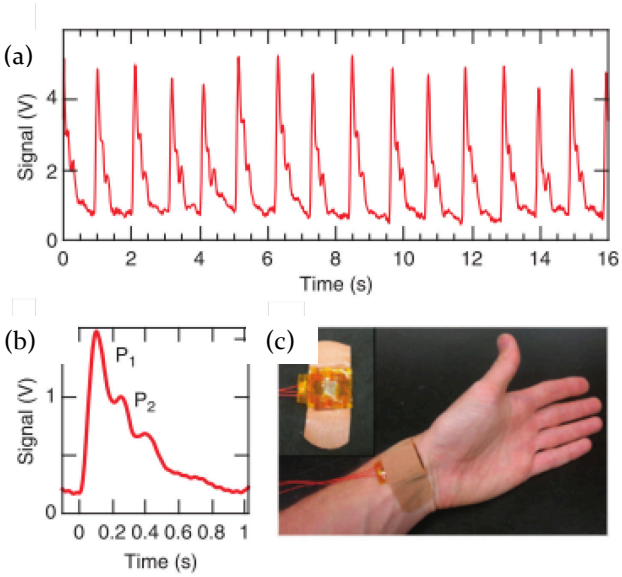

Figure 19: Pulse wave of radial artery measured with pressure sensing flexible polymer transistor (a) Real time transient signal from the radial artery of an adult human wrist. (b) Averaged signal from 16 periods. (c) Flexible pressure sensor attached to an adult human wrist above the radial artery. Reprinted with permission from ref.[21]. Copyright {2013} Nature Publishing Group.

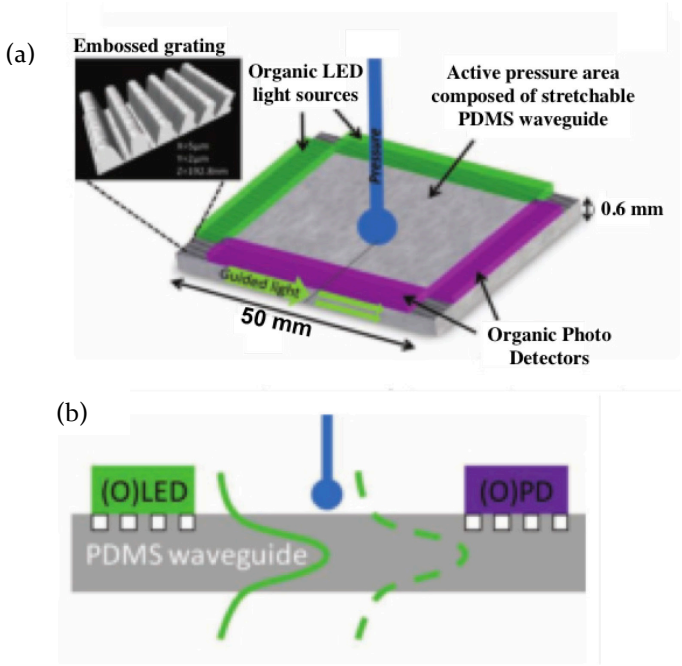

Figure 20: Transparent, optical, pressure-sensitive artificial skin (a) Schematic top-down view of the stretchable pressure sensor. AFM image in the inset illustrates embossed gratings onto the PDMS film. (b) Cross-sectional view of the optical pressure sensor illustrating in- and out-coupled light at the embossed grating stage. Change in photocurrent as a result of the disrupted waveguide process when pressure is applied is measured by the

photodetector. Adapted and reproduced with permission from ref.[7]. Copyright {2012} Wiley-VCH.

Because sensing modalities rely on a change in parameters based on external stimuli of the tested parameter, the use of complaint materials becomes necessary. The deformation induced by the applied load alters material properties in such a way that the resultant output scan discern between various mechanical manipulations of varying force. Though the material properties of commonly used materials in these devices such as AgNWs, PDMS, SWCNT, or PU have been extensively researched, the challenge remains to devise clever methods to amalgamate these discrete components in a concise integrated system to achieve the desired functionality.

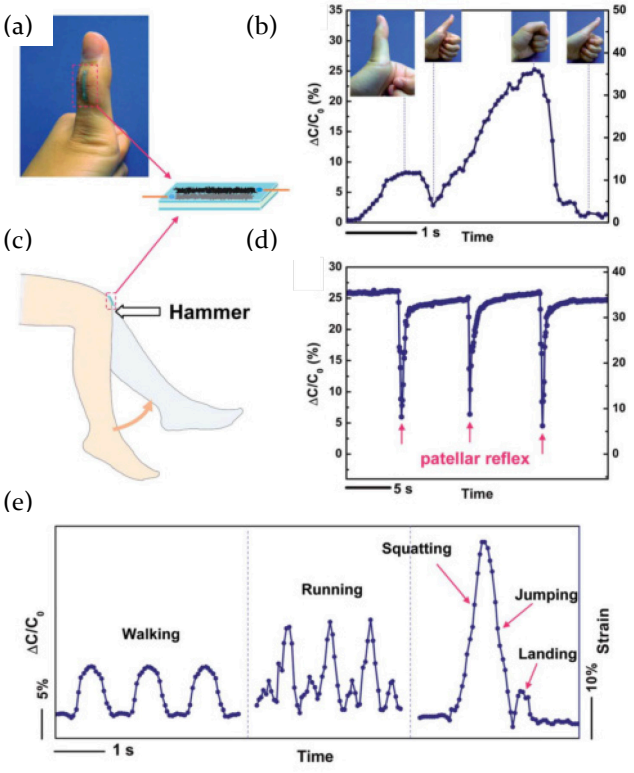

Figure 21: Strain sensing capability of capacitive sensors. (a) One pixel sensor on thumb joint. (b) Capacitve change associated with thumb flexure. (c) Schematic of patellar reflex in the knee. (d) Capacitve change caused by knee motion in patellar reflex. (e) Relative capacitive change for various human motions: walking, running and jumping from squatting. Reprinted with permission from ref. [274]. Copyright [2013] Royal Society of Chemistry.

3.1.2. Temperature sensor

Temperature sensing is another critical functionality of human skin. In the context of electronic skins, temperature sensing can serve multiple purposes: amongst these include being able to mimic the human response mechanism to prevent injury and to garner information about environmental surroundings,[271] in addition to being able to provide continuous, real time thermal characterization of human skin for diagnostic purposes.[277] Whereas the sensing mechanism for pressure sensors was based on the compression of materials inducing a change in materials parameters such as capacitance[4,5,8] or the number of waveguide modes,[7] temperature sensing relies on the resistivity dependence of materials. As a conceptual illustration of the basic working principle of these temperature sensors, a temperature sensor fabricated on a silicon-on-insulator wafer and transferred to a prestrained, buckled PDMS substrate is discussed.[9] The thermal sensor, termed thermistor, consisted of two chromium (Cr) / gold (Au) layers, one serving as the active layer, the other as the electrode.[9] This thermistor was fabricated independently of the buckled PDMS substrate, the two components which were subsequently laminated together with silicon ribbons functioning as an adhesive layer between the two.[9] **Figure 22a** illustrates the resistance at room temperature of the stretchable thermal sensor as a

function of the applied strain. From a range of 0 – 30% strain, the resistance is invariant with strain, verifying the efficacy of the system as a conductor capable of withstanding strain without significant deviation in material property. **Figure 22b** demonstrates the functionality of the temperature sensor over a range of strain, showing a linear relationship between electrical resistance, with no hysteresis for the relationship between resistance and strain. These results highlight the potential of utilizing the temperature dependence of various materials for temperature sensing applications.

More sophisticated systems for temperature sensors have been developed following this principle of temperature dependence of resistivity. Someya *et al.* demonstrated flexible thermal sensors in conjunction with organic transistor active matrices for data readout.[10] Organic diodes were fabricated on and ITO on PET film, with 30 nm of the p-type semiconductor 3,4,9,10-perylene-tetracarboxylic-diimide (PDCDI) deposited, followed by gold cathode electrodes.[10] The thermal sensing diode was laminated on the transistor with silver paste patterned by a microdispenser, and was integrated in a network with pressure sensors to be able to simultaneously obtain distributions of both pressure and temperature.

Thermal sensors have also been fabricated in stretchable systems, with several of these stretchable polyaniline nanofiber temperature sensor sensors utilizing

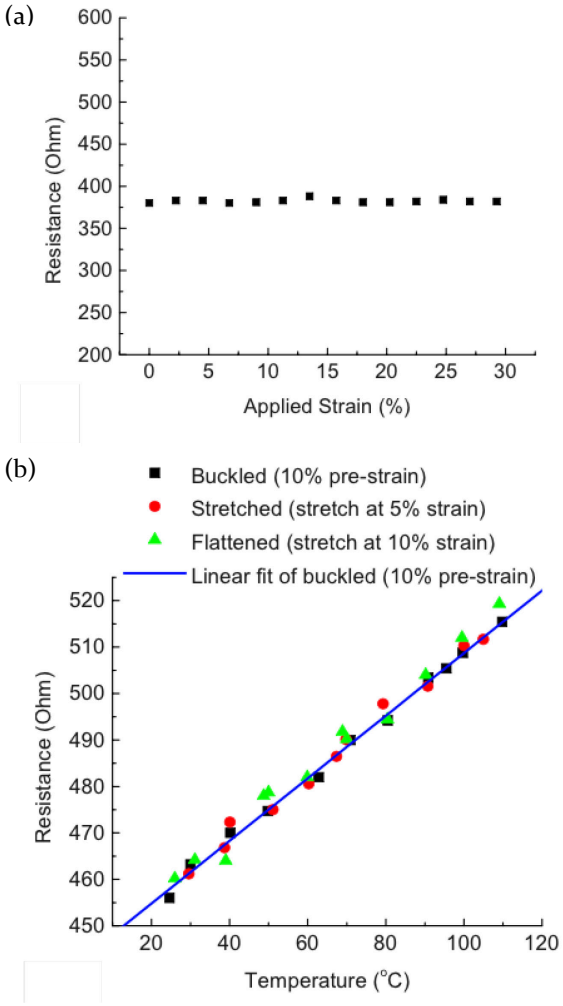

Figure 22: Performance of a stretchable temperature sensor. (a) Resistance of a stretchable temperature sensor under continuous strain at room temperature and a strain step of 2.25% showing high electrical stability in response to strain. (b) Electrical resistance as a function of temperature at a applied strain of 0, 5, ad 10%. Reprinted with permission from ref. [9]. Copyright [2009] American Institute of Physics.

AgNWs for various applications. Hong *et al.* fabricated a array with an active matrix design of SWCNT TFTs, with a detailed schematic of the fabrication process depicted in **Figure 23a** and **Figure 23b**.[12] The integrated device consists of SWCNT TFTs and polyaniline nanofiber temperature sensors fabricated through electrical polymerization on PET films, connected with stretchable interconnections of Galinstan, a eutectic liquid metal alloy.[12] AgNW stickers comprising AgNWs embedded in

PDMS were used as a contact layer between the temperature sensor and liquid metal interconnect, and to protect sensors from external impact due to their robust mechanical properties. The active circuit design is illustrated in **Figure 23c**. With this material, the thermal sensor was able to be thermally stable and accurately measure temperatures between 15 to 45 °C, with no hysteresis observed, and a linear resistance dependence on temperature. In addition, the sensor could be biaxially stretched up 30% without change in performance. The efficacy of the temperature sensor in its stretched and unstretched condition was verified through the fabrication of a 5 x 5 pixel array. Due to the stretchability of the sensor array, and the sticky nature of the Ecoflex substrate, the stretchable sensor easily conformed to the hand, with a heart shaped aluminum container filled with water at 15 °C placed on top of the sensor. Optical images taken before (**Figures 23d – 23e**) and after (**Figures 23h-23i**) stretching illustrate optical images of the sensor, in addition to normalized drain current and temperature in equation:[278,279]

$$R = R_0 \exp\left(\frac{E_a}{2kT}\right) = R_0 \exp\left(\frac{B}{T}\right) \quad (1)$$

where R denotes the resistance at temperature T, R_o the resistance at T = ∞, E_a the activation energy, k the Boltzman constant, and B the thermal index. This equation can be written in linear form as:[278]

$$\ln(R) = \ln(R_0) + \frac{E_a}{2kT} = \ln(R_0) + \frac{B}{T} \quad (2)$$

the unstretched and stretched state, respectively. Due to the ability of the sensor to conform to the palm, in addition to the invariance of performance upon stretching, this stretchable sensor illustrates its potential for attachable electronic skins.

Yan *et al.* embedded AgNWs as electrodes in conjunction with graphene detection channels to develop intrinsically stretchable thermistors capable of stretching up to 50%.[278] These electrodes and detection channels were embedded in PDMS to achieve high intrinsic stretchability without sacrificing thermal sensing properties. Unlike the previously mentioned thermal sensors which were able to sense temperature without a dependence on strain,[9,10,12] the thermistors developed in this study are limited to applications where no variations in strain are present. However, this limitation simultaneously opens up new possibilities. The dependence of temperature on resistivity was found to be non-linear, and described with the following

If the temperature coefficient of resistance (TCR) is defined as:[278,280]

$$TCR = \frac{dR}{dT}\frac{1}{R} \quad (3)$$

then **Equation 2** and **Equation 3** can be combined to yield:[278]

$$TCR = -\frac{B}{T^2} \quad (4)$$

Equation 3 highlights the dependence of TCR on resistance, which, as the resistance changes with strain,

demonstrates the dependence of TCR on the mechanical deformation of the device. **Equation 4** reveals that as the thermal index B is an indicator of thermal sensitivity, this thermistor developed by Yan *et al*. has tunable thermal sensitivity depending on strain. As different values of B can lead to varying importance for different applications, such as low B values being used in circuit temperature compensation at low temperatures and high B values more suitable for high-temperature sensing,[278,281] this stretchable graphene thermistor represents electronic skins that can be mass produced in a 'one size fits all' manufacturing process, but be effectively tuned for various applications depending on different requirements.

Trung *et al.* developed a fabrication process for fully elastomeric and stretchable temperature sensor arrays that could be integrated with a strain sensor for increased functionality.[11] The sensor (shown as a schematic in **Figure 24a**) was fabricated with PEDOT:PU dispersion composite as the source, drain, and gate, PU as the dielectric, reduced graphene oxide (R-GO) / PU as a temperature-responsive channel layer, AgNW/PEDOT:PSS/PU dispersion as a strain sensing layer, and PDMS as the substrate.[11] In addition to being fully transparent and elastic, all materials were deposited through spin-coating, allowing for a potentially low-cost, scalable fabrication method. Compared with the temperature sensors mentioned previously,[12,278] this fully intrinsically transparent and stretchable temperature sensor exhibited the highest strain at 70%, and a high sensitivity of 1.34% resistance change per °C.[11] As an example of the high sensitivity of the device, temperature fluctuations as small as 0.2 °C could be detected, making the easily conformable sensor an ideal candidate for monitoring the temperature of human skin. As a proof of concept of the efficacy of these devices for electronic skin applications, a stretchable strain sensor was vertically integrated with the temperature sensor on the top side (**Figure 24b**), and attached on a human neck and arm to monitor temperature changes and muscle movements during consumption of a warm liquid and working out, respectively. As seen from **Figure 24c** and **Figure 24d**, the device was able to simultaneously resolve both temperature and strain during the consumption of a hot liquid. The temperature measured from the device before and after drinking was 33.2 °C and 34.1 °C, respectively, corroborated by the 33.24 °C and 34.22 °C measured through an IR camera (**Figures 24e, 24f**).[11] When the sensor was applied to a human bicep during dumbbell curls, the device measured an increase in temperature (**Figure 24g**) before workout to after workout from 31.7 °C to 32.6 °C, confirmed by an IR camera (**Figure 24i, 24j**) reading 31.97 °C and 32.79 °C. This increase in temperature is due to the release of heat to control body temperature.[11] The strain induced in the bicep workout can be seen in **Figure 24h**. As illustrated by this proof of concept demonstration, in addition to the high sensitivity, multi-functionality, and high strain the device can be subjected to, fully elastic devices have a great

potential to be used for electronic skin applications.

In the case of temperature sensors, the sensing modality relies on the temperature dependence of resistance for various materials. As in the case of pressure sensing, the amalgamation of various stretchable materials can cumulate in high sensitivity, high performance temperature sensors. In some cases, these temperature sensors can be endowed with additional sensing mechanisms to act as a multifunctional device more closely mimicking real human skin.[10,11] Furthermore, this section highlighted the plurality of uses for silver nanowires, ranging from electrodes,[278] to connection pads,[12] to the sensing layer.[11]

3.1.3. Touch sensor

While touch sensors are most commonly associated with display devices such as cell phones, tablets, and laptops, when integrated with electronic skins, these devices allow for the visualization of the interface between human and machine interaction. Although touch sensors have been touched upon briefly in passing in discussion of multifunctional sensors,[274] an in-depth presentation has not yet been made, and will be elucidated upon in this section of the Review.

Though iterations of touch sensors relied primarily on resistive sensing,[282–284] most widely used commercially today are based on capacitive touch sensing due to their durability, optical clarity, and multi-touch capability.[13] The operating principle of a capacitive touch sensor is based on drawing charge with a conductor, such as a human finger. In an untouched state, a uniform voltage is applied throughout the capacitor, generating a uniform electrostatic field throughout. When touched, the touch point becomes grounded, generating a potential difference between the touch point and the bottom electrode, which induces a current flow from electrode to finger.

In a touch sensor that also supports multifunctional capabilities of strain and pressure sensing, Cotton *et al*. fabricated parallel plate capacitors using 50 nm gold films as the electrodes sandwiching a PDMS membrane. The initial sensor capacitance was measured to be 409 fF, which drops by ~100 fF upon finger touch, demonstrating the ability to, at the very least, register human touch.[285] Due to the capability to measure strain and pressure as well, this touch sensor was able to operate under mechanical strain. Within this last year, Li *et al*. fabricated a multicolor hyperelastic light emitting capacitor for use as a multipixel color display and multipoint touch sensor capable of biaxial stretching up to 200%.[286] The light emitting component was fabricated by premixing ZnS phosphor powders with silicon gels, and using photopatterning and transfer printing techniques to obtain red, green, and blue pixels on a single substrate.[286] The top layer was encapsulated with Ecoflex, and the resulting pixel sheet and sandwiched between rows of ionically conducting hydrogels also encapsulated with Ecoflex to form the

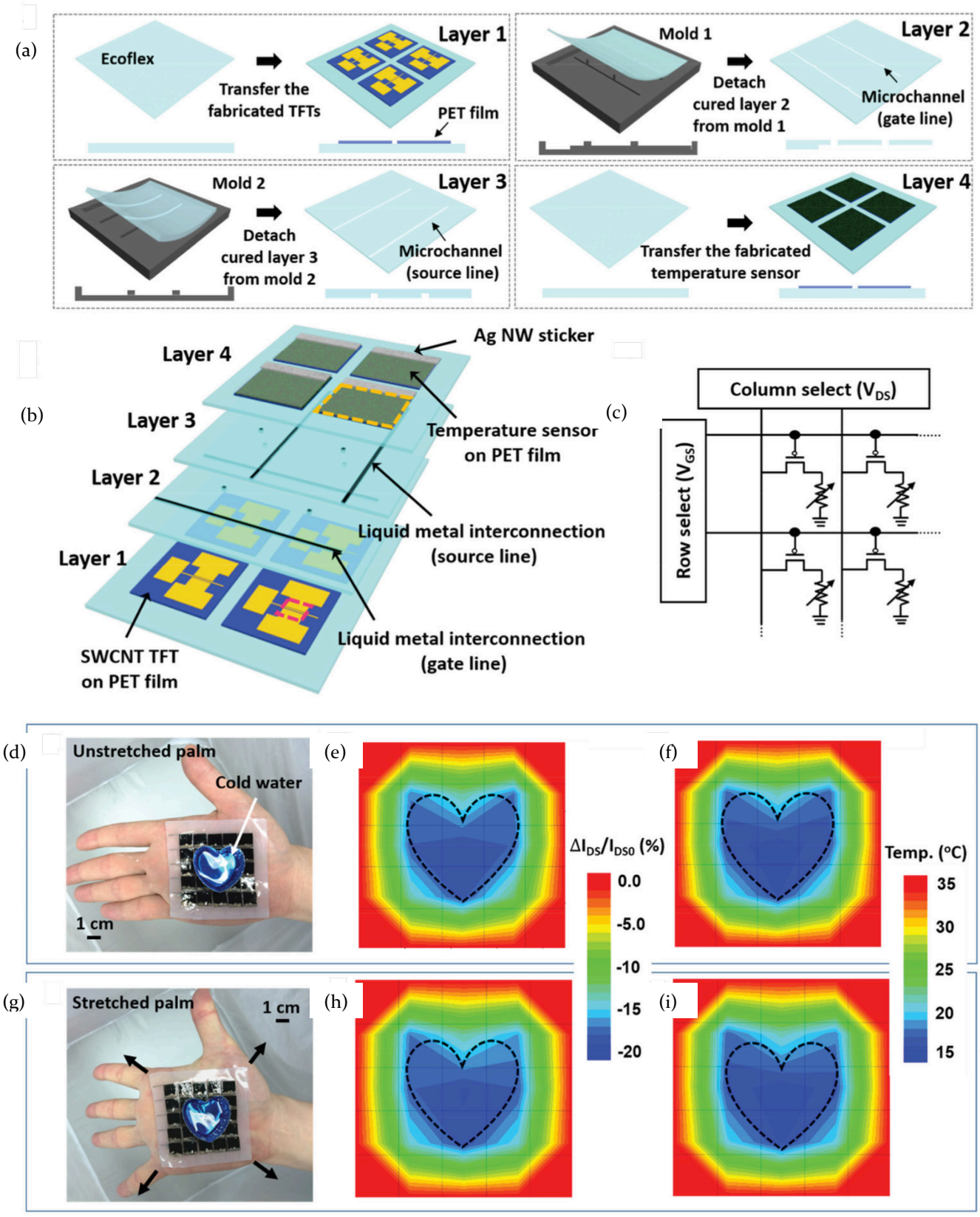

Figure 23: Stretchable active matrix temperature sensor array of polyaniline nanofibers. (a) Fabrication process for the stretchable active matrix temperature sensor array. (b) Assembly of prepared layers for the fabrication process. (c) Circuit diagram of the stretchable active matrix sensor array. (d) Optical image of temperature array on a human palm with a heart shaped cold water container at 15 °C. (e) Normalized drain current. (f) Corresponding mapping of temperature from the normalized drain current. (g), (h), (i) Corresponding images to (d), (e), (f), respectively, under the stretched condition. Adapted and reproduced with permission from ref [12]. Copyright [2015] Wiley-VCH.

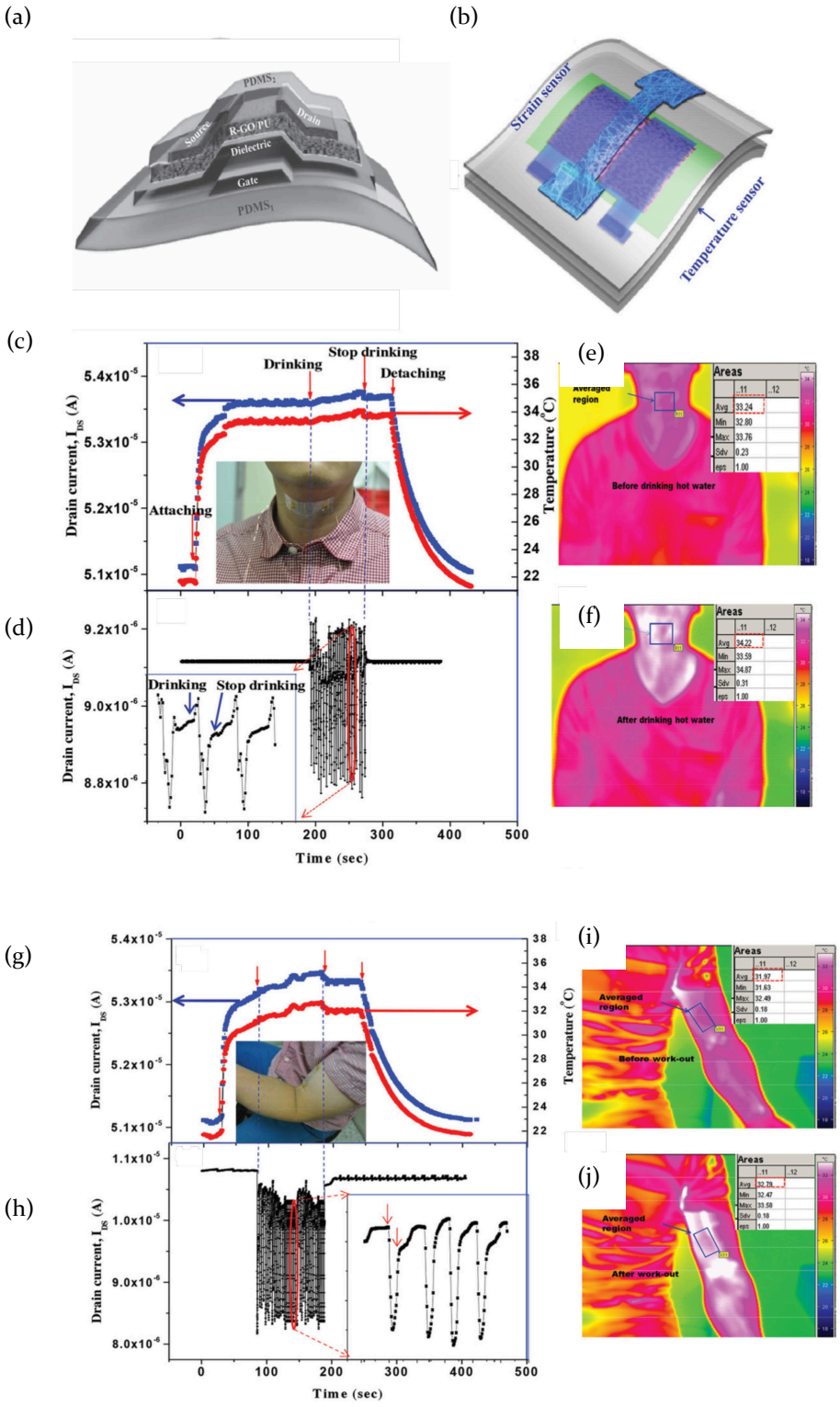

Figure 24: Transparent and stretchable temperature sensor. (a) Schematic of device structure of the transparent and stretchable sensor. (b) Schematic of integrated temperature and strain sensor. (c) Neck skin temperature during consumption of hot beverage. (d) Corresponding strain associated with consumption of hot beverage. (e), (f) IR thermograms of neck before and after consumption of hot beverage. (g) Bicep temperature during working (h) Corresponding strain associated with bicep workout. (i), (j) IR thermograms of bicep before and after workout. Adapted and reproduced with permission from ref [11]. Copyright [2015] Wiley-VCH.

conductor. In addition to being able to form dynamic, multicolored patterns under various deformation, the touch interface was able to also identify the exact locations of both single and multipoint touch inputs at strains of ε = 0, 100, and 200%.[286]

Due to their optoelectronic properties, silver nanowires have also been featured frequently in reports of touch sensors.[13,287] Hu *et al*. demonstrated stretchable pressure sensors using AgNW/PU variable capacitors that could simultaneously sense touch by changes in the capacitance of each pixel capacitor and the fringing capacitance directly above the capacitor. The Pei group demonstrated a healable touch screen sensor based on a furan/maleimide Diels-Alder cycloaddition polymer discussed previously.[14] Though the stretchability of the touch sensor was not analyzed in this work, the polymer was based on a stretchable conductor previously reported by the author.[27] Because details of the self-healing polymer has been previously detailed in this Review, the technical details behind the chemistry involved will not be repeated here. The healable capacitor was fabricated in a capacitive touch sensor by stacking row and column electrodes at a 90° angle to form an array of 8 x 8 sensing points, with each point the intersection of a row and column electrode. As a proof of concept, the healable capacitive array was used in conjunction with a touch screen control system to draw a smiley face on the LED array, as illustrated in **Figure 25**.

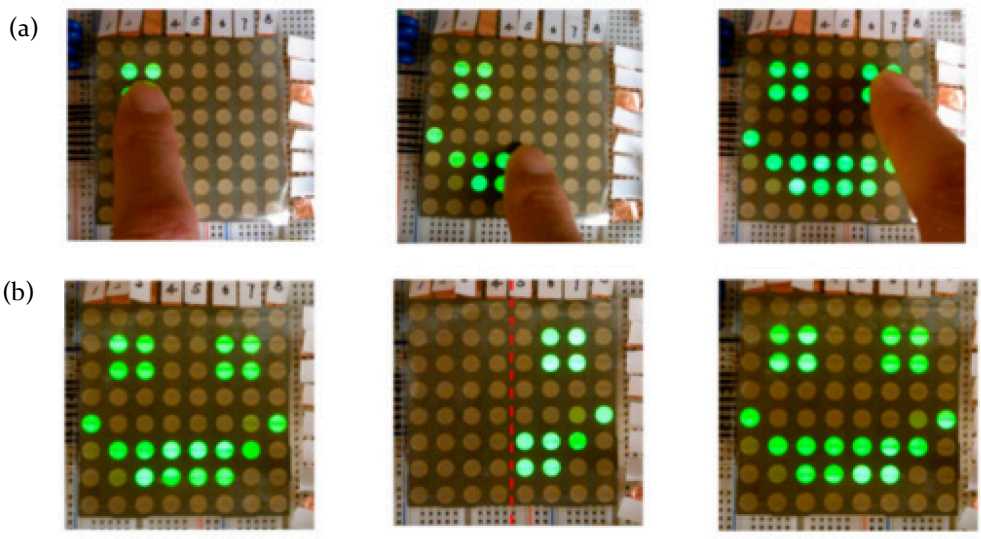

Figure 25: Optical photographs of the healable touch sensor. (a) Photographs of the operation of the healable touch sensor. (b) Photographs of the healing of the touch sensor. (left) before electrical disruption of the touch sensor; (middle) after cutting down the red line; (right) after healing the touch sensor. Reprinted with permission from ref. [14]. Copyright [2014] American Chemical Society

Figure 25a demonstrates the operation of the touch sensor: when in contact with a human finger, the capacitor terminated by the finger is able to draw charge, leading to underlying touch screen control system to light a green LED. In **Figure 25b**, a razor blade is used to cut along the dotted red line in the middle figure. This physical damage done to the touch sensor disrupts the electrical network, preventing half of the smiley face from

lighting up. However, after heating the touch sensor at 80 °C for 30 seconds, following by cooling again, the electrical network is healed, leading to the formation of the smiley face once again.

Touch sensors are an integral component of our modern electronics. Though there is not a completely analogous counterpart for human skin, the reading and visualization of data that touch sensors enable render this sensing mechanism one critical component of electronic skin. Moreover, it provides another dimension of the human-machine interaction that is poised to change in the upcoming years with further development of these elastomeric skins.

3.2. Dielectric elastomer actuators

Though dielectric elastomers have been utilized for several applications, the scope of this Review will be limited to applications related to wearable and electronic skin technology. For a more thorough and comprehensive review on dielectric elastomer materials and dielectric elastomer devices, the reader is referred to reviews authored by Brochu *et al*,[32] Anderson *et al.*,[40] and Carpi *et al.*[250]

Dielectric elastomers have directly been utilized in some of the sensing technologies described previously. A capacitive strain sensor was fabricated using a silicone dielectric elastomer sandwiched between carbon nanotube composite electrodes, with the functionality of the sensor similar to elastomeric capacitors described in aforementioned sections.[288] In addition, the same group demonstrated 'touch screens' for the visually impaired, using a bistable electroactive polymer to fabricate refreshable Braille displays.[225,289,290]

However, due to their inherent nature of actuation, dielectric elastomers may possess a distinct advantage in soft robotics, which may be a more compelling use case for this technology. Shian *et al.* illustrated a number of gripper actions allowed though the incorporation of stiff fibers in voltage actuated dielectric elastomer beams.[39] The use of stiff fibers was found to break the symmetry of the electrically induced deformation to program a direction of shape change to allow a gripping motion. Using a cylindrical actuator comprising an elastomer sleeve attached to a series of stiff rings, an axial actuator was demonstrated as the stiff rings constrain the expansion of the elastomer. This axial actuator can be seen to conform and grip both a cylinder and a grape, as can be seen in **Figure 26a**. Kofod *et al.* also demonstrated a gripper, using a three-clawed structure which opens upon application of a voltage and contracts upon removal of voltage to pick up, deliver, and drop a cylindrical object (**Figure 26b**).[291]

Full-fledged robots have also been developed on the basis of dielectric elastomer technology. Pei *et al.* demonstrated a walking six-legged robot based on multifunctional electroelastomer rolls that combine load bearing, actuation, and sensing functions.[292] This six-legged robot inspired by biological systems was capable of moving at a speed of 7 cm/s.[292] A robotic

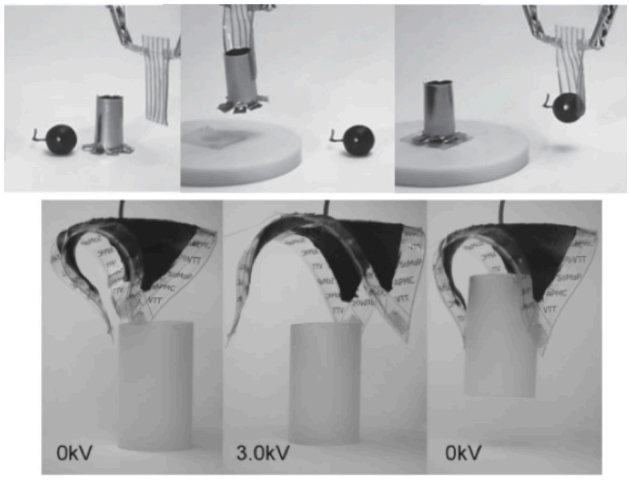

Figure 26: Optical photographs of the actuation of dielectric elastomer grippers. (a) Photographs of an axial actuator relaxed (left); gripping a cylinder (middle); and gripping a grape (right). (b) Photographs of a three clawed gripper under contraction (right); relaxed under application of 3.0 kV voltage (middle), and contracted gripping a cylinder (right). Adapted and reproduced with permission from refs [39,291]. Copyright [2015, 2007] Wiley-VCH and American Institute of Physics.

system designed to arm wrestle a human was also prototyped at the EAPAD conference in 2005.[293] The rotary motion of the arm was actuated with dielectric elastomer actuators, and demonstrates the potential of these materials for both artificial muscles and for robotic applications. In addition to land-based robots, these dielectric elastomer based robots may one day take to the sky as well. Zhao *et al*. developed a prototype of a rotary joint for a flapping wing actuated by dielectric elastomer that may one day enable long distance, robotic flights.[294] Waché *et al*. demonstrated rotary motion with a torsional dielectric elastomer actuator design that could one day be applied for flight.[295]

In addition to robotics, due to the artificial muscle-like nature of dielectric elastomers, their incorporation for biological applications should be expected. McCoul *et al*. demonstrated the use of a biomimetic dielectric elastomer tubular actuator capable of controlling hydraulic flow by pinching a secondary silicone tube shut in the absence of a fluidic bias or voltage.[296]

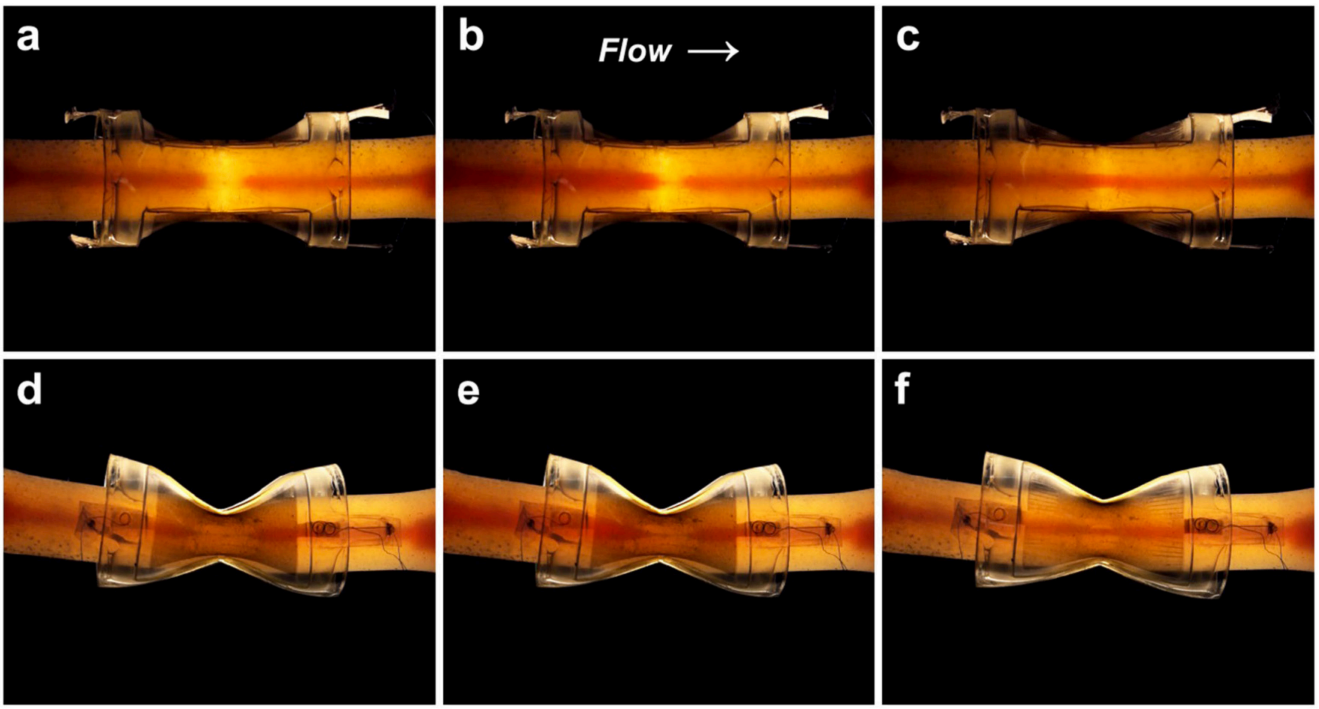

Figure 27: Visual characterization of the dielectric elastomer valve. (a) 0 applied bias, 0 mL h^{-1} flow. (b) 0 applied bias, 400 mL h^{-1} flow. (c) 3.2 kV applied bias, 400 mL h^{-1} flow. (d) – (f): side views of (a) – (c) Adapted with permission from ref [296] Copyright [2015] IOP Publishing.

The operation of this actuator acting as an artificial vein is illustrated in **Figure 27**, where the flow of a red dye was controlled through an applied bias. This capability of controlling fluid flow can be applied for potential bio-inspired applications such as artificial veins or implantable artificial sphincters. These examples of dielectric elastomer actuators highlight the potential of this technology for use in robotic applications. By having properties that mimic the natural properties of muscles, in addition to the ability to actuate in pre-programmed shapes and directions, dielectric elastomers represent a cost effective, lightweight, energy efficient technology.

3.3. Conclusion

The field of stretchable electronics has grown at a spectacular pace with the development of stretchable materials. The development of these new materials has enabled a whole new generation of devices, previously only imagined as futuristic, radical extensions of science fiction, or pie in the sky conceptual ideas. With these soft sensors and actuators, our concept of modern electronics can be expected to make a paradigm shift in several fields and industry, including wearable health and fitness trackers, large-scale, display-based consumer electronics, military and robotics, and energy generation and storage applications. More specific to this Review, with the continued development of electronic skins and soft robotics, we are poised to make a radical shift in the way we view and interface with our electronics. This Review uncovers but just a sliver of the potential that this new generation of electronics may possess. While major challenges still exist, such as materials properties at large-strain deformations, reliability and fatigue after repeated deformation, the future of next generation electronics looks not only bright, but stretchable as well.

AUTHOR INFORMATION

Corresponding Author

Professor Qibing Pei

E-mail: qpei@seas.ucla.edu

Author Contributions

The manuscript was written through contributions of all authors. / All authors have given approval to the final version of the manuscript. /

Notes

The authors declare no competing financial interest.

ACKNOWLEDGMENT

D.C. and Q.P. wish to acknowledge finance support from the Air Force Office of Scientific Research (Program Director: Dr. Charles Lee; Grant no. FA9550-15-1-0340), Advanced Research Projects Agency-Energy (ARPA-E) of the Department of Energy (Award Nos. DE-AR0000532 and DE-AR0000531), and the National Robotic Initiative Program of the National Science Foundation (Grant no. 1638163).

REFERENCES

(1) Wakharia, S. J.; Jitendra, P.; Ms, S. E.; Wakharia, D. J. An Integration of Emotional Attire - the Artificial Intelligence. *Int. J. Eng. Res. Appl.* **2012**, *2* (1), 497–502.

(2) Liverneaux, P. A.; Berner, S. H.; Bednar, M. S.; Parekattil, S. J.; Ruggiero, G. M.; Selber, J. C. *Telemicrosurgery*; 2013.

(3) Someya, T.; Sekitani, T.; Iba, S.; Kato, Y.; Kawaguchi, H.; Sakurai, T. A Large-Area, Flexible Pressure Sensor Matrix with Organic Field-Effect Transistors for Artificial Skin Applications. *Proc. Natl. Acad. Sci. U. S. A.* **2004**, *101* (27), 9966–9970.

(4) Hu, W.; Niu, X.; Zhao, R.; Pei, Q. Elastomeric Transparent Capacitive Sensors Based on an Interpenetrating Composite of Silver Nanowires and Polyurethane. *Appl. Phys. Lett.* **2013**, *102* (8).

(5) Mannsfeld, S. C. B.; Tee, B. C.-K.; Stoltenberg, R. M.; Chen, C. V. H.-H.; Barman, S.; Muir, B. V. O.; Sokolov, A. N.; Reese, C.; Bao, Z. Highly Sensitive Flexible Pressure Sensors with Microstructured Rubber Dielectric Layers. *Nat. Mater.* **2010**, *9* (10), 859–864.

(6) Gong, S.; Schwalb, W.; Wang, Y.; Chen, Y.; Tang, Y.; Si, J.; Shirinzadeh, B.; Cheng, W. A Wearable and Highly Sensitive Pressure Sensor with Ultrathin Gold Nanowires. *Nat. Commun.* **2014**, *5*, 3132.

(7) Ramuz, M.; Tee, B. C. K.; Tok, J. B. H.; Bao, Z. Transparent, Optical, Pressure-Sensitive Artificial Skin for Large-Area Stretchable Electronics. *Adv. Mater.* **2012**, *24* (24), 3223–3227.

(8) Lipomi, D. J.; Vosgueritchian, M.; Tee, B. C.-K.; Hellstrom, S. L.; Lee, J. a; Fox, C. H.; Bao, Z. Skin-like Pressure and Strain Sensors Based on Transparent Elastic Films of Carbon Nanotubes. *Nat. Nanotechnol.* **2011**, *6* (12), 788–792.

(9) Yu, C.; Wang, Z.; Yu, H.; Jiang, H. A Stretchable Temperature Sensor Based on Elastically Buckled Thin Film Devices on Elastomeric Substrates. *Appl. Phys. Lett.* **2009**, *95* (14), 2007–2010.

(10) Someya, T.; Kato, Y.; Sekitani, T.; Iba, S.; Noguchi, Y.; Murase, Y.; Kawaguchi, H.; Sakurai, T. Conformable, Flexible, Large-Area Networks of Pressure and Thermal Sensors with Organic Transistor Active Matrixes. *Proc. Natl. Acad. Sci. U. S. A.* **2005**, *102* (35), 12321–12325.

(11) Trung, T. Q.; Ramasundaram, S.; Hwang, B. U.; Lee, N. E. An All-Elastomeric Transparent and Stretchable Temperature Sensor for Body-Attachable Wearable Electronics. *Adv. Mater.* **2015**, 502–509.

(12) Hong, S. Y.; Lee, Y. H.; Park, H.; Jin, S. W.; Jeong, Y. R.; Yun, J.; You, I.; Zi, G.; Ha, J. S. Stretchable Active Matrix Temperature Sensor Array of Polyaniline Nanofibers for Electronic Skin. *Adv. Mater.* **2015**, *28*, 930–935.

(13) Cui, Z.; Poblete, F. R.; Cheng, G.; Yao, S.; Jiang, X.; Zhu, Y. Design and Operation of Silver Nanowire Based Flexible and Stretchable Touch Sensors. *J. Mater. Res.* **2014**, *30* (1), 79–85.

(14) Li, J.; Liang, J.; Li, L.; Ren, F.; Hu, W.; Li, J.; Qi, S.; Pei, Q. Healable Capacitive Touch Screen Sensors Based on Transparent Composite Electrodes Comprising Silver Nanowires and a Furan / Maleimide Diels-Alder Cycloaddition Polymer. *ACS Nano* **2014**, *8* (12), 12874–12882.

(15) Gong, J.; Li, Y.; Hu, Z.; Zhou, Z.; Deng, Y. Ultrasensitive NH 3 Gas Sensor from Polyaniline Nanograin Enchased TiO 2 Fibers. *J. Phys. Chem. C* **2010**, *114*, 9970–9974.

(16) Yi, J.; Lee, J. M.; Park, W. Il. Vertically Aligned ZnO Nanorods and Graphene Hybrid Architectures for High-Sensitive Flexible Gas Sensors. *Sensors Actuators, B Chem.* **2011**, *155* (1), 264–269.

(17) Liu, H.; Li, M.; Voznyy, O.; Hu, L.; Fu, Q.; Zhou, D.; Xia, Z.; Sargent, E. H.; Tang, J. Physically Flexible, Rapid-Response Gas Sensor Based on Colloidal Quantum Dot Solids. *Adv. Mater.* **2014**, *26* (17), 2718–2724.

(18) Kim, D.-H.; Lu, N.; Ghaffari, R.; Rogers, J. a. Inorganic Semiconductor Nanomaterials for Flexible and Stretchable Bio-Integrated Electronics. *NPG Asia Mater.* **2012**, *4* (4), e15.

(19) Choi, S.; Lee, H.; Ghaffari, R.; Hyeon, T.; Kim, D.-H. Recent

Advances in Flexible and Stretchable Bio-Electronic Devices Integrated with Nanomaterials. *Adv. Mater.* **2016**, n/a-n/a.

(20) Bandodkar, A. J.; Jeerapan, I.; You, J.-M.; Nuñez-Flores, R.; Wang, J. Highly Stretchable Fully-Printed CNT-Based Electrochemical Sensors and Biofuel Cells: Combining Intrinsic and Design-Induced Stretchability. *Nano Lett.* **2015**, acs.nanolett.5b04549.

(21) Schwartz, G.; Tee, B. C.-K.; Mei, J.; Appleton, A. L.; Kim, D. H.; Wang, H.; Bao, Z. Flexible Polymer Transistors with High Pressure Sensitivity for Application in Electronic Skin and Health Monitoring. *Nat. Commun.* **2013**, *4* (May), 1859.

(22) Wang, X.; Gu, Y.; Xiong, Z.; Cui, Z.; Zhang, T. Silk-Molded Flexible, Ultrasensitive, and Highly Stable Electronic Skin for Monitoring Human Physiological Signals. *Adv. Mater.* **2014**, *26* (9), 1336–1342.

(23) Zhao, X.; Hua, Q.; Yu, R.; Zhang, Y.; Pan, C. Flexible, Stretchable and Wearable Multifunctional Sensor Array as Artificial Electronic Skin for Static and Dynamic Strain Mapping. *Adv. Electron. Mater.* **2015**, *1* (7), n/a-n/a.

(24) Chou, H.-H.; Nguyen, A.; Chortos, A.; To, J. W. F.; Lu, C.; Mei, J.; Kurosawa, T.; Bae, W.-G.; Tok, J. B.-H.; Bao, Z. A Chameleon-Inspired Stretchable Electronic Skin with Interactive Colour Changing Controlled by Tactile Sensing. *Nat. Commun.* **2015**, *6*, 8011.

(25) Ge, J.; Sun, L.; Zhang, F. R.; Zhang, Y.; Shi, L. A.; Zhao, H. Y.; Zhu, H. W.; Jiang, H. L.; Yu, S. H. A Stretchable Electronic Fabric Artificial Skin with Pressure-, Lateral Strain-, and Flexion-Sensitive Properties. *Adv. Mater.* **2015**, 722–728.

(26) Ho, D. H.; Sun, Q.; Kim, S. Y.; Han, J. T.; Kim, D. H.; Cho, J. H. Stretchable and Multimodal All Graphene Electronic Skin. *Adv. Mater.* **2016**, n/a-n/a.

(27) Li, J.; Qi, S.; Liang, J.; Li, L.; Xiong, Y.; Hu, W.; Pei, Q. Synthesizing a Healable Stretchable Transparent Conductor. *ACS Appl. Mater. Interfaces* **2015**, *7*, 14140–14149.

(28) Benight, S. J.; Wang, C.; Tok, J. B. H.; Bao, Z. Stretchable and Self-Healing Polymers and Devices for Electronic Skin. *Prog. Polym. Sci.* **2013**, *38* (12), 1961–1977.

(29) Milwich, M.; Selvarayan, S. K.; Gresser, G. T. *Fibrous Materials and Textiles for Soft Robotics*; 2015.

(30) Madden J.D.W, Vandesteeg N.A, A. P. .; Madden, J. D. W.; Vandesteeg, N. a.; Anquetil, P. a.; Madden, P. G. a; Takshi, A.; Pytel, R. Z.; Lafontaine, S. R.; Wieringa, P. a.; Hunter, I. W. Artificial Muscle technology:Physical Principles and Naval Prospects. *IEEE J. Ocean. Eng.* **2004**, *29* (3), 706–728.

(31) Pelrine, R.; Kornbluh, R.; Pei, Q.; Stanford, S.; Oh, S.; Eckerle, J.; Full, R.; Rosenthal, M.; Meijer, K. Dielectric Elastomer Artificial Muscle Actuators : Toward Biomimetic Motion. **2002**, *4695*, 126–137.

(32) Brochu, P.; Pei, Q. Advances in Dielectric Elastomers for Actuators and Artificial Muscles. *Macromol. Rapid Commun.* **2010**, *31* (1), 10–36.

(33) Bar-Cohen, Y. Electroactive Polymers as Artificial Muscles - Capabilities, Potentials, and Challenges. In *Robotics 2000*; 2000; pp 188–196.

(34) Bar-Cohen, Y. Electro-Active Polymers: Current Capabilities and Challenges. *Smart Struct. Mater. 2002 Electroact. Polym. Actuators Devices* **2002**, *4695*, 1–7.

(35) Krishnamoorthy, S. Nanostructured Sensors for Biomedical Applications-a Current Perspective. *Curr. Opin. Biotechnol.* **2015**, *34*, 118–124.

(36) Son, D.; Lee, J.; Qiao, S.; Ghaffari, R.; Kim, J.; Lee, J. E.; Song, C.; Kim, S. J.; Lee, D. J.; Jun, S. W.; et al. Multifunctional Wearable Devices for Diagnosis and Therapy of Movement Disorders. *Nat. Nanotechnol.* **2014**, *9* (5), 397–404.

(37) Zang, Y.; Zhang, F.; Di, C.; Zhu, D. Advances of Flexible Pressure Sensors toward Artificial Intelligence and Health Care Applications. *Mater. Horiz.* **2015**, *2* (2), 140–156.

(38) Bandodkar, A. J.; Wang, J. Non-Invasive Wearable

Electrochemical Sensors: A Review. *Trends Biotechnol.* **2014**, *32* (7), 363–371.

(39) Shian, S.; Bertoldi, K.; Clarke, D. R. Dielectric Elastomer Based "Grippers" for Soft Robotics. *Adv. Mater.* **2015**, *27*, 6814–6819.

(40) Anderson, I. a.; Gisby, T. a.; McKay, T. G.; O'Brien, B. M.; Calius, E. P. Multi-Functional Dielectric Elastomer Artificial Muscles for Soft and Smart Machines. *J. Appl. Phys.* **2012**, *112* (4).

(41) Sun, Y.; Choi, W. M.; Jiang, H.; Huang, Y. Y.; Rogers, J. a. Controlled Buckling of Semiconductor Nanoribbons for Stretchable Electronics. *Nat. Nanotechnol.* **2006**, *1* (3), 201–207.

(42) Feng, X.; Yang, B. D.; Liu, Y.; Wang, Y.; Dagdeviren, C.; Liu, Z.; Carlson, A.; Li, J.; Huang, Y.; Rogers, J. a. Stretchable Ferroelectric Nanoribbons with Wavy Configurations on Elastomeric Substrates. *ACS Nano* **2011**, *5* (4), 3326–3332.

(43) Khang, D.-Y.; Jiang, H.; Huang, Y.; Rogers, J. A. A Stretchable Form of Single-Crystal Silicon for High-Performance Electronics on Rubber Substrates. *Science (80-.).* **2006**, *311* (January), 208–212.

(44) Kim, D.-H.; Ahn, J.-H.; Choi, W. M.; Kim, H.-S.; Kim, T.-H.; Song, J.; Huang, Y.; Liu, Z.; Lu, C.; Rogers, J. A. Stretchable and Foldable Silicon Integrated Circuits. *Science (80-.).* **2008**, *320* (April), 507–511.

(45) Xu, S.; Zhang, Y.; Cho, J.; Lee, J.; Huang, X.; Jia, L.; Fan, J. a; Su, Y.; Su, J.; Zhang, H.; et al. Stretchable Batteries with Self-Similar Serpentine Interconnects and Integrated Wireless Recharging Systems. *Nat. Commun.* **2013**, *4*, 1543.

(46) Liang, J.; Li, L.; Chen, D.; Hajagos, T.; Ren, Z.; Chou, S.-Y.; Hu, W.; Pei, Q. Intrinsically Stretchable and Transparent Thin-Film Transistors Based on Printable Silver Nanowires, Carbon Nanotubes and an Elastomeric Dielectric. *Nat. Commun.* **2015**, *6* (May), 7647.

(47) Yu, Z.; Niu, X.; Liu, Z.; Pei, Q. Intrinsically Stretchable Polymer Light-Emitting Devices Using Carbon Nanotube-Polymer Composite Electrodes. *Adv. Mater.* **2011**, *23* (34), 3989–3994.

(48) Zhao, C.; Wang, C.; Yue, Z.; Shu, K.; Wallace, G. G. Intrinsically Stretchable Supercapacitors Composed of Polypyrrole Electrodes and Highly Stretchable Gel Electrolyte. *ACS Appl. Mater. Interfaces* **2013**, *5* (18), 9008–9014.

(49) Rogers, J. a; Someya, T.; Huang, Y. Materials and Mechanics for Stretchable Electronics. *Science (80-.).* **2010**, *327* (2010), 1603–1607.

(50) Bowden, N.; Brittain, S.; Evans, A. G.; Hutchinson, J. W.; Whitesides, G. M. Spontaneous Formation of Ordered Structures in Thin Films of Metals Supported on an Elastomeric Polymer. *Nature* **1998**, *393* (May), 146–149.

(51) Bauer, S. Flexible Electronics: Sophisticated Skin. *Nat. Mater.* **2013**, *12* (10), 871–872.

(52) Wang, C.; Hwang, D.; Yu, Z.; Takei, K.; Park, J.; Chen, T.; Ma, B.; Javey, a. User-Interactive Electronic Skin for Instantaneous Pressure Visualization. *Nat Mater* **2013**, *12* (10), 899–904.

(53) Lipomi, D. J.; Bao, Z. Stretchable, Elastic Materials and Devices for Solar Energy Conversion. *Energy Environ. Sci.* **2011**, *4* (9), 3314.

(54) Kaltenbrunner, M.; White, M. S.; Głowacki, E. D.; Sekitani, T.; Someya, T.; Sariciftci, N. S.; Bauer, S. Ultrathin and Lightweight Organic Solar Cells with High Flexibility. *Nat. Commun.* **2012**, *3*, 770.

(55) Yu, Z.; Liu, Z.; Wang, M.; Sun, M.; Lei, G.; Pei, Q. Highly Flexible Polymer Light-Emitting Devices Using Carbon Nanotubes as Both Anodes and Cathodes. *J. Photonics Energy* **2011**, *1* (1), 11003.

(56) Yu, Z.; Hu, L.; Liu, Z.; Sun, M.; Wang, M.; Grüner, G.; Pei, Q. Fully Bendable Polymer Light Emitting Devices with Carbon Nanotubes as Cathode and Anode. *Appl. Phys. Lett.* **2009**, *95* (20), 2007–2010.

(57) Kumar, A.; Zhou, C. The Race to Replace Tin-Doped

Indium Oxide: Which Material Will Win? *ACS Nano* **2010**, *4* (1), 11–14.

(58) Chen, D.; Liang, J.; Pei, Q. Flexible and Stretchable Electrodes for next Generation Polymer Electronics: A Review. *Sci. China Chem.* **2016**, 1–13.

(59) Yu, Z.; Li, L.; Zhang, Q.; Hu, W.; Pei, Q. Silver Nanowire-Polymer Composite Electrodes for Efficient Polymer Solar Cells. *Adv. Mater.* **2011**, *23* (38), 4453–4457.

(60) Li, L.; Liang, J.; Chou, S.-Y.; Zhu, X.; Niu, X.; ZhibinYu; Pei, Q. A Solution Processed Flexible Nanocomposite Electrode with Efficient Light Extraction for Organic Light Emitting Diodes. *Sci. Rep.* **2014**, *4*, 4307.

(61) Li, L.; Yu, Z.; Chang, C.; Hu, W.; Niu, X.; Chen, Q.; Pei, Q. Efficient White Polymer Light-Emitting Diodes Employing a Silver Nanowire–polymer Composite Electrode. *Phys. Chem. Chem. Phys.* **2012**, *14* (41), 14249.

(62) Chen, D.; Liang, J.; Liu, C.; Saldanha, G.; Zhao, F.; Tong, K.; Liu, J.; Pei, Q. Thermally Stable Silver Nanowire-Polyimide Transparent Electrode Based on Atomic Layer Deposition of Zinc Oxide on Silver Nanowires. *Adv. Funct. Mater.* **2015**, 7512–7520.

(63) Nam, S.; Song, M.; Kim, D.-H.; Cho, B.; Lee, H. M.; Kwon, J.-D.; Park, S.-G.; Nam, K.-S.; Jeong, Y.; Kwon, S.-H.; et al. Ultrasmooth, Extremely Deformable and Shape Recoverable Ag Nanowire Embedded Transparent Electrode. *Sci. Rep.* **2014**, *4*, 4788.

(64) Li, J.; Liang, J.; Jian, X.; Hu, W.; Li, J.; Pei, Q. A Flexible and Transparent Thin Film Heater Based on a Silver Nanowire/Heat-Resistant Polymer Composite. *Macromol. Mater. Eng.* **2014**, *299* (11), 1403–1409.

(65) Spechler, J. A.; Koh, T. W.; Herb, J. T.; Rand, B. P.; Arnold, C. B. A Transparent, Smooth, Thermally Robust, Conductive Polyimide for Flexible Electronics. *Adv. Funct. Mater.* **2015**, 7428–7434.

(66) Hu, W.; Niu, X.; Li, L.; Yun, S.; Yu, Z.; Pei, Q. Intrinsically Stretchable Transparent Electrodes Based on Silver-Nanowire–crosslinked-Polyacrylate Composites. *Nanotechnology* **2012**, *23* (34), 344002.

(67) Yun, S.; Niu, X.; Yu, Z.; Hu, W.; Brochu, P.; Pei, Q. Compliant Silver Nanowire-Polymer Composite Electrodes for Bistable Large Strain Actuation. *Adv. Mater.* **2012**, *24* (10), 1321–1327.

(68) Gong, C.; Liang, J.; Hu, W.; Niu, X.; Ma, S.; Hahn, H. T.; Pei, Q. A Healable, Semitransparent Silver Nanowire-Polymer Composite Conductor. *Adv. Mater.* **2013**, *25* (30), 4186–4191.

(69) Tee, B. C.-K.; Wang, C.; Allen, R.; Bao, Z. An Electrically and Mechanically Self-Healing Composite with Pressure- and Flexion-Sensitive Properties for Electronic Skin Applications. *Nat. Nanotechnol.* **2012**, *7* (12), 825–832.

(70) Sun, H.; You, X.; Jiang, Y.; Guan, G.; Fang, X.; Deng, J.; Chen, P.; Luo, Y.; Peng, H. Self-Healable Electrically Conducting Wires for Wearable Microelectronics. *Angew. Chemie - Int. Ed.* **2014**, *53* (36), 9526–9531.

(71) Wang, H.; Zhu, B.; Jiang, W.; Yang, Y.; Leow, W. R.; Wang, H.; Chen, X. A Mechanically and Electrically Self-Healing Supercapacitor. *Adv. Mater.* **2014**, *26* (22), 3638–3643.

(72) Zhu, M.; Rong, M. Z.; Zhang, M. Q. Self-Healing Polymeric Materials towards Non-Structural Recovery of Functional Properties. *Polym. Int.* **2014**, *63* (10), 1741–1749.

(73) Imato, K.; Takahara, A.; Otsuka, H. Self-Healing of a Cross-Linked Polymer with Dynamic Covalent Linkages at Mild Temperature and Evaluation at Macroscopic and Molecular Levels. *Macromolecules* **2015**, *48* (16), 5632–5639.

(74) Wojtecki, R. J.; Meador, M. a; Rowan, S. J. Using the Dynamic Bond to Access Macroscopically Responsive Structurally Dynamic Polymers. *Nat. Mater.* **2011**, *10* (1), 14–27.

(75) Wool, R. P. Self-Healing Materials: A Review. *Soft Matter* **2008**, *4* (3), 400.

(76) Williams, K. A; Boydston, A. J.; Bielawski, C. W. Towards Electrically Conductive, Self-Healing Materials. *J. R. Soc.*

Interface **2007**, *4* (13), 359–362.

(77) Cordier, P.; Tournilhac, F.; Soulié-Ziakovic, C.; Leibler, L. Self-Healing and Thermoreversible Rubber from Supramolecular Assembly. *Nature* **2008**, *451* (7181), 977–980.

(78) Montarnal, D.; Tournilhac, F.; Hidalgo, M.; Couturier, J. L.; Leibler, L. Versatile One-Pot Synthesis of Supramolecular Plastics and Self-Healing Rubbers. *J. Am. Chem. Soc.* **2009**, *131* (23), 7966–7967.

(79) Wang, L.; Wang, Z.; Zhang, X.; Shen, J.; Chi, L.; Fuchs, H. A New Approach for the Fabrication of an Alternating Multilayer Film of poly(4-Vinylpyridine) and poly(acryiic Acid) Based on Hydrogen Bonding. *Macromol. Rapid Commun.* **1997**, *514*, 509–514.

(80) Kossmehl, G.; Nagel, H.; Pahl, a. Cross-linking Reactions on Polyamides by Bis-and Tris (Maleimide)s. *Angew. Makromol. Chem.* **1995**, *221*, 139–157.

(81) Chen, X.; Wudl, F.; Mal, A. K.; Shen, H.; Nutt, S. R.; Chen, X.; Wudl, F.; Mal, A. K.; Shen, H.; Nutt, S. R. New Thermally Remendable Highly Cross-Linked Polymeric Materials New Thermally Remendable Highly Cross-Linked Polymeric Materials. *Macromolecules* **2003**, *36* (6), 1802–1807.

(82) Klement, W.; Willens, R. H.; Duwez, P. Non-Crystalline Structure in Solidified Gold–Silicon Alloys. *Nature* **1960**, *187* (4740), 869–870.

(83) Zhu, S.; So, J. H.; Mays, R.; Desai, S.; Barnes, W. R.; Pourdeyhimi, B.; Dickey, M. D. Ultrastretchable Fibers with Metallic Conductivity Using a Liquid Metal Alloy Core. *Adv. Funct. Mater.* **2013**, *23* (18), 2308–2314.

(84) Cheng, S.; Rydberg, A.; Hjort, K.; Wu, Z. Liquid Metal Stretchable Unbalanced Loop Antenna. *Appl. Phys. Lett.* **2009**, *94* (14).

(85) Hayes, G. J.; So, J.-H.; Qusba, A.; Dickey, M. D.; Lazzi, G. Flexible Liquid Metal Alloy (EGaIn) Microstrip Patch Antenna. *TAP_IEEE Trans. Antennas Propag.* **2012**, *60* (5), 2151–2156.

(86) So, J.-H.; Dickey, M. D. Inherently Aligned Microfluidic Electrodes Composed of Liquid Metal. *Lab Chip* **2011**, *11* (5), 905–911.

(87) Palleau, E.; Reece, S.; Desai, S. C.; Smith, M. E.; Dickey, M. D. Self-Healing Stretchable Wires for Reconfigurable Circuit Wiring and 3D Microfluidics. *Adv. Mater.* **2013**, *25* (11), 1589–1592.

(88) Ladd, C.; So, J. H.; Muth, J.; Dickey, M. D. 3D Printing of Free Standing Liquid Metal Microstructures. *Adv. Mater.* **2013**, *25* (36), 5081–5085.

(89) Kim, H. J.; Son, C.; Ziaie, B. A Multiaxial Stretchable Interconnect Using Liquid-Alloy-Filled Elastomeric Microchannels. *Appl. Phys. Lett.* **2008**, *92* (1), 1–4.

(90) Park, J.; Wang, S.; Li, M.; Ahn, C.; Hyun, J. K.; Kim, D. S.; Kim, D. K.; Rogers, J. a; Huang, Y.; Jeon, S. Three-Dimensional Nanonetworks for Giant Stretchability in Dielectrics and Conductors. *Nat. Commun.* **2012**, *3* (May), 916.

(91) Vosgueritchian, M.; Lipomi, D. J.; Bao, Z. Highly Conductive and Transparent PEDOT:PSS Films with a Fluorosurfactant for Stretchable and Flexible Transparent Electrodes. *Adv. Funct. Mater.* **2012**, *22* (2), 421–428.

(92) Lipomi, D. J.; Lee, J. a.; Vosgueritchian, M.; Tee, B. C.-K.; Bolander, J. a.; Bao, Z. Electronic Properties of Transparent Conductive Films of PEDOT:PSS on Stretchable Substrates. *Chem. Mater.* **2012**, *24* (2), 373–382.

(93) Tait, J. G.; Worfolk, B. J.; Maloney, S. a.; Hauger, T. C.; Elias, A. L.; Buriak, J. M.; Harris, K. D. Spray Coated High-Conductivity PEDOT:PSS Transparent Electrodes for Stretchable and Mechanically-Robust Organic Solar Cells. *Sol. Energy Mater. Sol. Cells* **2013**, *110*, 98–106.

(94) Teng, C.; Lu, X. Y.; Zhu, Y.; Wan, M. X.; Jiang, L. Polymer in Situ Embedding for Highly Flexible, Stretchable and Water Stable PEDOT:PSS Composite Conductors. *Rsc Adv.* **2013**, *3* (20), 7219–7223.

(95) Hansen, T. S.; West, K.; Hassager, O.; Larsen, N. B. Highly Stretchable and Conductive Polymer Material Made from poly(3,4-Ethylenedioxythiophene) and Polyurethane Elastomers. *Adv. Funct. Mater.* **2007**, *17* (16), 3069–3073.

(96) Mu, H.; Li, W.; Jones, R.; Steckl, a.; Klotzkin, D. A Comparative Study of Electrode Effects on the Electrical and Luminescent Characteristics of Alq3/TPD OLED: Improvements due to Conductive Polymer (PEDOT) Anode. *J. Lumin.* **2007**, *126* (1), 225–229.

(97) Benor, A.; Takizawa, S. Y.; P??rez-Bol??var, C.; Anzenbacher, P. Efficiency Improvement of Fluorescent OLEDs by Tuning the Working Function of PEDOT:PSS Using UV-Ozone Exposure. *Org. Electron. physics, Mater. Appl.* **2010**, *11* (5), 938–945.

(98) Nguyen, T. P.; Le Rendu, P.; Long, P. D.; De Vos, S. a. Chemical and Thermal Treatment of PEDOT:PSS Thin Films for Use in Organic Light Emitting Diodes. *Surf. Coatings Technol.* **2004**, *180–181*, 646–649.

(99) Lim, F. J.; Ananthanarayanan, K.; Luther, J.; Ho, G. W. Influence of a Novel Fluorosurfactant Modified PEDOT:PSS Hole Transport Layer on the Performance of Inverted Organic Solar Cells. *J. Mater. Chem.* **2012**, No. c, 25057–25064.

(100) Yang, Y.; Lee, K.; Mielczarek, K.; Hu, W.; Zakhidov, a. Nanoimprint of Dehydrated PEDOT:PSS for Organic Photovoltaics. *Nanotechnology* **2011**, *22*, 485301.

(101) Yeo, J. S.; Yun, J. M.; Kim, D. Y.; Kim, S. S.; Na, S. I. Successive Solvent-Treated PEDOT:PSS Electrodes for Flexible ITO-Free Organic Photovoltaics. *Sol. Energy Mater. Sol. Cells* **2013**, *114*, 104–109.

(102) Clevios PH 1000 http://www.heraeus-clevios.com/media/webmedia_local/media/datenblaetter/81076210_Clevios_PH_1000_20101222.pdf (accessed Mar 8, 2016).

(103) Xia, Y.; Ouyang, J. PEDOT:PSS Films with Significantly Enhanced Conductivities Induced by Preferential Solvation with Cosolvents and Their Application in Polymer Photovoltaic Cells. *J. Mater. Chem.* **2011**, *21* (13), 4927.

(104) Yin, H.-E.; Wu, C.-H.; Kuo, K.-S.; Chiu, W.-Y.; Tai, H.-J. Innovative Elastic and Flexible Conductive PEDOT:PSS Composite Films Prepared by Introducing Soft Latexes. *J. Mater. Chem.* **2012**, *22* (9), 3800.

(105) Savagatrup, S.; Chan, E.; Renteria-garcia, S. M.; Printz, A. D.; Zaretski, A. V; Connor, T. F. O.; Rodriquez, D.; Valle, E.; Lipomi, D. J. Plasticization of PEDOT : PSS by Common Additives for Mechanically Robust Organic Solar Cells and Wearable Sensors. *Adv. Funct. Mater.* **2015**, *25* (3), 427–436.

(106) Kim, M.; Lee, Y. S.; Kim, Y. C.; Choi, M. S.; Lee, J. Y. Flexible Organic Light-Emitting Diode with a Conductive Polymer Electrode. *Synth. Met.* **2011**, *161* (21–22), 2318–2322.

(107) Lee, S. K.; Kim, B. J.; Jang, H.; Yoon, S. C.; Lee, C.; Hong, B. H.; Rogers, J. a.; Cho, J. H.; Ahn, J. H. Stretchable Graphene Transistors with Printed Dielectrics and Gate Electrodes. *Nano Lett.* **2011**, *11* (11), 4642–4646.

(108) Lee, M.-S.; Lee, K.; Kim, S.-Y.; Lee, H.; Park, J.; Choi, K.-H.; Kim, H.-K.; Kim, D.-G.; Lee, D.-Y.; Nam, S.; et al. High-Performance, Transparent, and Stretchable Electrodes Using Graphene–Metal Nanowire Hybrid Structures. *Nano Lett.* **2013**, *13* (6), 2814–2821.

(109) Kim, R. H.; Bae, M. H.; Kim, D. G.; Cheng, H.; Kim, B. H.; Kim, D. H.; Li, M.; Wu, J.; Du, F.; Kim, H. S.; et al. Stretchable, Transparent Graphene Interconnects for Arrays of Microscale Inorganic Light Emitting Diodes on Rubber Substrates. *Nano Lett.* **2011**, *11* (9), 3881–3886.

(110) Geim, A. K. Graphene : Status and Prospects. *Science (80-.).* **2014**, *324* (2009), 1530–1534.

(111) Allen, M. J.; Tung, V. C.; Kaner, R. B. Honeycomb Carbon: A Review of Graphene. *Chem. Rev.* **2010**, *110* (1), 132–145.

(112) Kim, K. S.; Zhao, Y.; Jang, H.; Lee, S. Y.; Kim, J. M.; Kim, K. S.; Ahn, J.-H.; Kim, P.; Choi, J.-Y.; Hong, B. H. Large-Scale Pattern Growth of Graphene Films for Stretchable

Transparent Electrodes. *Nature* **2009**, *457* (7230), 706–710.

(113) Chen, J.; Jang, C.; Xiao, S.; Ishigami, M.; Fuhrer, M. S. Intrinsic and Extrinsic Performance Limits of Graphene Devices on SiO2. *Nat. Nanotechnol.* **2008**, *3* (4), 206–209.

(114) Bae, S.; Kim, H.; Lee, Y.; Xu, X.; Park, J.-S.; Zheng, Y.; Balakrishnan, J.; Lei, T.; Kim, H. R.; Song, Y. Il; et al. Roll-to-Roll Production of 30-Inch Graphene Films for Transparent Electrodes. *Nat. Nanotechnol.* **2010**, *5* (8), 574–578.

(115) Gómez-Navarro, C.; Burghard, M.; Kern, K. Elastic Properties of Chemically Derived Single Graphene Sheets. *Nano Lett.* **2008**, *8* (7), 2045–2049.

(116) Xu, Z.; Liu, Z.; Sun, H.; Gao, C. Highly Electrically Conductive Ag-Doped Graphene Fibers as Stretchable Conductors. *Adv. Mater.* **2013**, *25* (23), 3249–3253.

(117) Chen, Z.; Ren, W.; Gao, L.; Liu, B.; Pei, S.; Cheng, H.-M. Three-Dimensional Flexible and Conductive Interconnected Graphene Networks Grown by Chemical Vapour Deposition. *Nat. Mater.* **2011**, *10* (6), 424–428.

(118) Keplinger, C.; Sun, J.-Y. Y.; Foo, C. C.; Rothemund, P.; Whitesides, G. M.; Suo, Z. Stretchable, Transparent, Ionic Conductors. *Science (80-.).* **2013**, *341* (6149), 984–987.

(119) Bardeen, J.; Brattain, W. H. The Transistor, A Semi-Conductor Triode. *Phys. Rev.* **1948**, *74*, 230–231.

(120) Sekitani, T.; Zschieschang, U.; Klauk, H.; Someya, T. Flexible Organic Transistors and Circuits with Extreme Bending Stability. *Nat. Mater.* **2010**, *9* (12), 1015–1022.

(121) Loi, A.; Manunza, I.; Bonfiglio, A. Flexible, Organic, Ion-Sensitive Field-Effect Transistor. *Appl. Phys. Lett.* **2005**, *86* (10), 1–3.

(122) Bonfiglio, A.; Mameli, F.; Sanna, O. A Completely Flexible Organic Transistor Obtained by a One-Mask Photolithographic Process. *Appl. Phys. Lett.* **2003**, *82* (20), 3550–3552.

(123) Katz, H. E.; Lovinger, a. J.; Johnson, J.; Kloc, C.; Siegrist, T.; Li, W.; Lin, Y.-Y.; Dodabalapur, a. A Soluble and Air-Stable Organic Semiconductor with High Electron Mobility. *Nature* **2000**, *404* (6777), 478–481.

(124) Zschieschang, U.; Ante, F.; Yamamoto, T.; Takimiya, K.; Kuwabara, H.; Ikeda, M.; Sekitani, T.; Someya, T.; Kern, K.; Klauk, H. Flexible Low-Voltage Organic Transistors and Circuits Based on a High-Mobility Organic Semiconductor with Good Air Stability. *Adv. Mater.* **2010**, *22* (9), 982–985.

(125) Kaltenbrunner, M.; Sekitani, T.; Reeder, J.; Yokota, T.; Kuribara, K.; Tokuhara, T.; Graz, I.; Bauer-gogonea, S.; Bauer, S.; Someya, T.; et al. An Ultra-Lightweight Design for Imperceptible Plastic Electronics. *Nature* **2013**, *499* (7549), 458–463.

(126) Lee, W.; Kim, D.; Rivnay, J.; Matsuhisa, N.; Lonjaret, T.; Yokota, Tomoyuki; Yawo, H.; Sekino, M.; Malliaras, G. G.; Someya, T. Integration of Organic Electrochemical and Field-Effect Transistors for Ultraflexible , High Temporal Resolution Electrophysiology Arrays. *Adv. Mater.* **2016**, *28*, 9722–9728.

(127) Nawrocki, R. A.; Matsuhisa, N.; Yokota, T.; Someya, T. 300-Nm Imperceptible , Ultraflexible , and Biocompatible E-Skin Fit with Tactile Sensors and Organic Transistors. *Adv. Electron. Mater.* **2016**, *2*, 1500452.

(128) Lipomi, D. J.; Chong, H.; Vosgueritchian, M.; Mei, J.; Bao, Z. Toward Mechanically Robust and Intrinsically Stretchable Organic Solar Cells: Evolution of Photovoltaic Properties with Tensile Strain. *Sol. Energy Mater. Sol. Cells* **2012**, *107*, 355–365.

(129) Savagatrup, S.; Printz, A. D.; Wu, H.; Rajan, K. M.; Sawyer, E. J.; Zaretski, A. V.; Bettinger, C. J.; Lipomi, D. J. Viability of Stretchable poly(3-Heptylthiophene) (P3HpT) for Organic Solar Cells and Field-Effect Transistors. *Synth. Met.* **2015**, *203*, 208–214.

(130) Liang, J.; Li, L.; Niu, X.; Yu, Z.; Pei, Q. Elastomeric Polymer Light-Emitting Devices and Displays. *Nat. Photonics* **2013**, *7* (10), 817–824.

(131) Song, E.; Kang, B.; Choi, H. H.; Sin, D. H.; Lee, H.; Lee, W.

H.; Cho, K. Stretchable and Transparent Organic Semiconducting Thin Film with Conjugated Polymer Nanowires Embedded in an Elastomeric Matrix. *Adv. Electron. Mater.* **2016**, *2*.

(132) Wu, H. C.; Benight, S. J.; Chortos, A.; Lee, W. Y. W. H.; Mei, J.; To, J. W. F.; Lu, C.; He, M.; Tok, J. B. H.; Chen, W. C.; et al. Flexible, Highly Efficient All-Polymer Solar Cells. *Nat. Chem.* **2015**, *4* (June), n/a-n/a.

(133) Muller, C.; Goffri, S.; Breiby, D. W.; Andreasen, J. W.; Chanzy, H. D.; Janssen, R. a J.; Nielsen, M. M.; Radano, C. P.; Sirringhaus, H.; Smith, P.; et al. Tough, Semiconducting Polyethylene-poly(3-Hexylthiophene) Diblock Copolymers. *Adv. Funct. Mater.* **2007**, *17* (15), 2674–2679.

(134) O'Connor, T. F.; Zaretski, A. V.; Shiravi, B. a.; Savagatrup, S.; Printz, A. D.; Diaz, M. I.; Lipomi, D. J. Stretching and Conformal Bonding of Organic Solar Cells to Hemispherical Surfaces. *Energy Environ. Sci.* **2014**, *7* (1), 370.

(135) Liang, L.; Gao, C.; Chen, G.; Guo, C.-Y. Large-Area, Stretchable, Super Flexible and Mechanically Stable Thermoelectric Films of Polymer/carbon Nanotube Composites. *J. Mater. Chem. C* **2016**, *4* (3), 526–532.

(136) Choi, C.; Kim, S. H.; Sim, H. J.; Lee, J. A.; Choi, a Y.; Kim, Y. T.; Lepró, X.; Spinks, G. M.; Baughman, R. H.; Kim, S. J. Stretchable, Weavable Coiled Carbon Nanotube/MnO2/Polymer Fiber Solid-State Supercapacitors. *Sci. Rep.* **2015**, *5*, 9387.

(137) Li, Z.; Ding, J.; Lefebvre, J.; Malenfant, P. R. L. Surface Effects on Network Formation of Conjugated Polymer Wrapped Semiconducting Single Walled Carbon Nanotubes and Thin Film Transistor Performance. *Org. Electron.* **2015**, *26*, 15–19.

(138) Xu, W.; Dou, J.; Zhao, J.; Tan, H.; Ye, J.; Tange, M.; Gao, W.; Xu, W.; Zhang, X.; Guo, W.; et al. Printed Thin Film Transistors and CMOS Inverters Based on Semiconducting Carbon Nanotube Ink Purified by a Nonlinear Conjugated Copolymer. *Nanoscale* **2016**, *8* (8), 4588–4598.

(139) Chae, S. H.; Yu, W. J.; Bae, J. J.; Duong, D. L.; Perello, D.; Jeong, H. Y.; Ta, Q. H.; Ly, T. H.; Vu, Q. A.; Yun, M.; et al. Transferred Wrinkled Al2O3 for Highly Stretchable and Transparent Graphene-Carbon Nanotube Transistors. *Nat. Mater.* **2013**, *12* (5), 403–409.

(140) Wu, M. Y.; Zhao, J.; Xu, F.; Chang, T. H.; Jacobberger, R. M.; Ma, Z.; Arnold, M. S. Highly Stretchable Carbon Nanotube Transistors Enabled by Buckled Ion Gel Gate Dielectrics. *Appl. Phys. Lett.* **2015**, *107* (5), 53301-1-053301–053305.

(141) Takahashi, T.; Takei, K.; Gillies, A. G.; Fearing, R. S.; Javey, A. Carbon Nanotube Active-Matrix Backplanes for Conformal Electronics and Sensors. *Nano Lett.* **2011**, *11*, 5408–5413.

(142) Son, D.; Koo, J. H.; Song, J. K.; Kim, J.; Lee, M.; Shim, H. J.; Park, M.; Lee, M.; Kim, J. H.; Kim, D. H. Stretchable Carbon Nanotube Charge-Trap Floating-Gate Memory and Logic Devices for Wearable Electronics. *ACS Nano* **2015**, *9* (5), 5585–5593.

(143) Zhou, X.; Park, J. J.-Y.; Huang, S.; Liu, J.; McEuen, P. P. L. Band Structure, Phonon Scattering, and the Performance Limit of Single-Walled Carbon Nanotube Transistors. *Phys. Rev. Lett.* **2005**, *95* (14), 146805.

(144) Getty, S. a; Cobas, E.; Fuhrer, M. S. Extraordinary Mobility in Semiconducting Carbon Nanotubes Extraordinary Mobility in Semiconducting Carbon Nanotubes. **2004**, *4* (December 2003), 35–39.

(145) Cai, L.; Wang, C. Carbon Nanotube Flexible and Stretchable Electronics. *Nanoscale Res. Lett.* **2015**, *10* (1), 1013.

(146) Wang, C.; Takei, K.; Takahashi, T.; Javey, A. Carbon Nanotube Electronics -Moving Forward. *Chem. Soc. Rev.* **2013**, *42* (7), 2592–2609.

(147) Cao, Q.; Rogers, J. a. Ultrathin Films of Single-Walled Carbon Nanotubes for Electronics and Sensors: A Review

of Fundamental and Applied Aspects. *Adv. Mater.* **2009**, *21* (1), 29–53.

(148) Chortos, A.; Koleilat, G. I.; Pfattner, R.; Kong, D.; Lin, P.; Nur, R.; Lei, T.; Wang, H.; Liu, N.; Lai, Y.-C.; et al. Mechanically Durable and Highly Stretchable Transistors Employing Carbon Nanotube Semiconductor and Electrodes. *Adv. Mater.* **2015**, 1–8.

(149) Young Oh, J.; Rondeau-Gagné, S.; Chiu, Y.-C.; Chortos, A.; Lissel, F.; Nathan Wang, G.-J.; Schroeder, B. C.; Kurosawa, T.; Lopez, J.; Katsumata, T.; et al. Intrinsically Stretchable and Healable Semiconducting Polymer for Organic Transistors. *Nat. Publ. Gr.* **2016**, *539* (7629), 411–415.

(150) Lee, C.; Ko, J.; Lee, J.; Chung, I. Fabrication and Characterization of a Pentacene Thin Film Transistor with a Polymer Insulator as a Gate Dielectric. *J. Vac. Sci. Technol. A Vacuum, Surfaces, Film.* **2008**, *26* (4), 710.

(151) Choi, W.; Kim, M. H.; Na, Y. J.; Lee, S. D. Complementary Transfer-Assisted Patterning of High-Resolution Heterogeneous Elements on Plastic Substrates for Flexible Electronics. *Org. Electron. physics, Mater. Appl.* **2010**, *11* (12), 2026–2031.

(152) Chen, F.-C.; Chen, T.-D.; Zeng, B.-R.; Chung, Y.-W. Influence of Mechanical Strain on the Electrical Properties of Flexible Organic Thin-Film Transistors. *Semicond. Sci. Technol.* **2011**, *26* (3), 34005.

(153) Chun, J. Y.; Han, J. W.; Han, J. M.; Seo, D. S. Ultraviolet Alignment Effect and Properties of Organic Thin Film Transistors Based on Soluble Triisopropylsilyl-Pentacene with Photoreactive Polymer. *Jpn. J. Appl. Phys.* **2009**, *48* (1), 1–4.

(154) Jang, J.; Kim, S. H.; Nam, S.; Chung, D. S.; Yang, C.; Yun, W. M.; Park, C. E.; Koo, J. B. Hysteresis-Free Organic Field-Effect Transistors and Inverters Using Photocrosslinkable Poly(vinyl Cinnamate) as a Gate Dielectric. *Appl. Phys. Lett.* **2008**, *92* (14), 2006–2009.

(155) Jang, J.; Nam, S.; Hwang, J.; Park, J.-J.; Im, J.; Park, C. E.; Kim, J. M. Photocurable Polymer Gate Dielectrics for Cylindrical Organic Field-Effect Transistors with High Bending Stability. *J. Mater. Chem.* **2012**, *22* (3), 1054.

(156) Bae, J. H.; Kim, W. H.; Kim, H.; Lee, C.; Lee, S. D. Structural Origin of the Mobility Enhancement in a Pentacene Thin-Film Transistor with a Photocrosslinking Insulator. *J. Appl. Phys.* **2007**, *102* (6), 1–7.

(157) Egerton, P. L.; Pitts, E.; Reiser, a. Photocycloaddition in Solid Poly (Vinyl Cinnamate). The Photoreactive Polymer Matrix as an Ensemble of Chromophore Sites. *Macromolecules* **1981**, *14* (1), 95–100.

(158) Sokolov, A. N.; Tee, B. C. K.; Bettinger, C. J.; Tok, J. B. H.; Bao, Z. Chemical and Engineering Approaches to Enable Organic Field-Effect Transistor for Electronic Skin Applications. *Acc. Chem. Res.* **2012**, *45* (3), 361–371.

(159) Orgiu, E.; Manunza, I.; Sanna, M.; Cosseddu, P.; Bonfiglio, a. Transparent Dielectric Films for Organic Thin-Film Transistors: A Perspective for Low Cost, Low Size Technologies. *Thin Solid Films* **2008**, *516* (7), 1533–1537.

(160) Ling, M. M.; Bao, Z.; Li, D. Transistor Performance of Top Rough Surface of Pentacene Measured by Laminated Double Insulated-Gate Supported on a Poly(dimethylsiloxanes) Base Structure. *Appl. Phys. Lett.* **2006**, *88* (3), 1–3.

(161) Reese, C.; Chung, W. J.; Ling, M. M.; Roberts, M.; Bao, Z. High-Performance Microscale Single-Crystal Transistors by Lithography on an Elastomer Dielectric. *Appl. Phys. Lett.* **2006**, *89* (20), 2004–2007.

(162) Cao, Q.; Hur, S. H.; Zhu, Z. T.; Sun, Y.; Wang, C.; Meitl, M. a.; Shim, M.; Rogers, J. a. Highly Bendable, Transparent Thin-Film Transistors That Use Carbon-Nanotube-Based Conductors and Semiconductors with Elastomeric Dielectrics. *Adv. Mater.* **2006**, *18* (3), 304–309.

(163) Madsen, F. B.; Daugaard, a E.; Hvilsted, S.; Benslimane, M. Y.; Skov, a L. Dipolar Cross-Linkers for PDMS Networks with Enhanced Dielectric Permittivity and Low Dielectric

Loss. *Smart Mater. Struct.* **2013**, *22* (10), 11.

(164) Dünki, S. J.; Dascalu, M.; Nüesch, F. A.; Opris, D. M. Silicones with Enhanced Permittivity for Dielectric Elastomer Actuators. *Proc. SPIE 9798, Electroact. Polym. Actuators Devices* **2016**, *9798*, 97982K–1–97982K–12.

(165) Ha, M.; Xia, Y.; Green, A. a.; Zhang, W.; Renn, M. J.; Kim, C. H.; Hersam, M. C.; Frisbie, C. D. Printed, Sub-3V Digital Circuits on Plastic from Aqueous Carbon Nanotube Inks. *ACS Nano* **2010**, *4* (8), 4388–4395.

(166) Xia, Y.; Zhang, W.; Ha, M.; Cho, J. H.; Renn, M. J.; Kim, C. H.; Frisbie, C. D. Printed Sub-2 V Gel-Electrolyte-Gated Polymer Transistors and Circuits. *Adv. Funct. Mater.* **2010**, *20* (4), 587–594.

(167) Cho, J. H.; Lee, J.; Xia, Y.; Kim, B.; He, Y.; Renn, M. J.; Lodge, T. P.; Daniel Frisbie, C. Printable Ion-Gel Gate Dielectrics for Low-Voltage Polymer Thin-Film Transistors on Plastic. *Nat. Mater.* **2008**, *7* (11), 900–906.

(168) Cho, J. H.; Lee, J.; He, Y.; Kim, B.; Lodge, T. P.; Frisbie, C. D. High-Capacitance Ion Gel Gate Dielectrics with Faster Polarization Response Times for Organic Thin Film Transistors. *Adv. Mater.* **2008**, *20* (4), 686–690.

(169) Pu, J.; Zhang, Y.; Wada, Y.; Tse-Wei Wang, J.; Li, L. J.; Iwasa, Y.; Takenobu, T. Fabrication of Stretchable MoS2 Thin-Film Transistors Using Elastic Ion-Gel Gate Dielectrics. *Appl. Phys. Lett.* **2013**, *103* (2).

(170) Lee, S.-K.; Kabir, S. M. H.; Sharma, B. K.; Kim, B. J.; Cho, J. H.; Ahn, J.-H. Photo-Patternable Ion Gel-Gated Graphene Transistors and Inverters on Plastic. *Nanotechnology* **2014**, *25* (1), 14002.

(171) Lee, J.; Panzer, M. J.; He, Y.; Lodge, T. P.; Frisbie, C. D. Ion Gel Gated Polymer Thin-Film Transistors. *J. Am. Chem. Soc.* **2007**, *129* (15), 4532–4533.

(172) Oh, K.; Lee, J. Y.; Lee, S. S.; Park, M.; Kim, D.; Kim, H. Highly Stretchable Dielectric Nanocomposites Based on Single-Walled Carbon Nanotube/ionic Liquid Gels. *Compos. Sci. Technol.* **2013**, *83*, 40–46.

(173) Kohlmeyer, R. R.; Javadi, A.; Pradhan, B.; Pilla, S.; Setyowatt, K.; Chen, J.; Gong, S. Electrical and Dielectric Properties of Hydroxylated Carbon Nanotube-Elastomer Composites. *J. Phys. Chem. C* **2009**, *113* (41), 17626–17629.

(174) Shi, J.; Chan-Park, M. B.; Li, C. M. Adhesive-Free Transfer of Gold Patterns to PDMS-Based Nanocomposite Dielectric for Printed High-Performance Organic Thin-Film Transistors. *ACS Appl. Mater. Interfaces* **2011**, *3* (6), 1880–1886.

(175) Zirkl, M.; Haase, A.; Fian, A.; Schön, H.; Sommer, C.; Jakopic, G.; Leising, G.; Stadlober, B.; Graz, I.; Gaar, N.; et al. Low-Voltage Organic Thin-Film Transistors with High-K Nanocomposite Gate Dielectrics for Flexible Electronics and Optothermal Sensors. *Adv. Mater.* **2007**, *19* (17), 2241–2245.

(176) Tien, N. T.; Trung, T. Q.; Seoul, Y. G.; Kim, D. Il; Lee, N. E. Physically Responsive Field-Effect Transistors with Giant Electromechanical Coupling Induced by Nanocomposite Gate Dielectrics. *ACS Nano* **2011**, *5* (9), 7069–7076.

(177) Xia, Y.; Cho, J. H.; Lee, J.; Ruden, P. P.; Frisbie, C. D. Comparison of the Mobility-Carrier Density Relation in Polymer and Single-Crystal Organic Transistors Employing Vacuum and Liquid Gate Dielectrics. *Adv. Mater.* **2009**, *21* (21), 2174–2179.

(178) Menard, E.; Podzorov, V.; Hur, S. H.; Gaur, A.; Gershenson, M. E.; Rogers, J. a. High-Performance N- And P-Type Single-Crystal Organic Transistors with Free-Space Gate Dielectrics. *Adv. Mater.* **2004**, *16* (23–24), 2097–2101.

(179) Gautam, R.; Saxena, M.; Gupta, R. S.; Gupta, M. Gate All around MOSFET with Vacuum Gate Dielectric for Improved Hot Carrier Reliability and RF Performance. *IEEE Trans. Electron Devices* **2013**, *60* (6), 1820–1827.

(180) Han, J.-W.; Moon, D.-I.; Sub Oh, J.; Choi, Y.-K.; Meyyappan, M. Vacuum Gate Dielectric Gate-All-around Nanowire for Hot Carrier Injection and Bias Temperature Instability Free Transistor. *Appl. Phys. Lett.* **2014**, *104* (25),

253506.

(181) Bar-Cohen, Y. *Electroactive Polymer (EAP) Actuators as Artificial Muscles: Reality, Potential, and Challenges*; Press Monographs; SPIE Press, 2001.

(182) Hollerbach, J. M.; Hunter, I. W.; Ballantyne, J. The Robotics Review; Khatib, O., Craig, J. J., Lozano-Pérez, T., Eds.; MIT Press: Cambridge, MA, USA, 1992; pp 299–342.

(183) BigDog - The Most Advanced Rough-Terrain Robot on Earth http://www.bostondynamics.com/robot_bigdog.html (accessed May 17, 2017).

(184) Chou, C.; Hannaford, B. Measurment and Modeling of McKibben Pneumatic Artificial Muscles. *IEEE Trans. Robot. Autom.* **1996**, *12* (1), 90–102.

(185) Shepherd, R. F.; Ilievski, F.; Choi, W.; Morin, S. A.; Stokes, A. A.; Mazzeo, A. D.; Chen, X.; Wang, M.; Whitesides, G. M. Multigait Soft Robot. *Proc. Natl. Acad. Sci. U. S. A.* **2011**, *108* (51), 20400–20403.

(186) Hunter, I. W.; Lafontaine, S. A Comparison of Muscle with Artificial Actuators.pdf. *IEEE Tech. Dig. Solid-State Sens. Actuator Work.* **1992**, 178–185.

(187) Bar-cohen, Y.; Vidal, F. Front Matter: Volume 9798. *Proc. SPIE 9798, Electroact. Polym. Actuators Devices* **2016**, *9798*, 1–29.

(188) Roentgen, W. C. About the Changes in Shape and Volume of Dielectrics Caused by Electricity. *Sect. III G. Wiedemann (Ed.), Annu. Phys. Chem. Ser.* **1880**, *11*, 771–786.

(189) Bar-cohen, Y. Front Matter: Volume 9056. *Proc. SPIE 9056, Electroact. Polym. Actuators Devices* **2014**, *9056*, 1–22.

(190) Bar-cohen, Y. Front Matter: Volume 9430. *Proc. SPIE 9430, Electroact. Polym. Actuators Devices* **2015**, *9430*, 1–30.

(191) Haines, C. S.; Lima, M. D.; Li, N.; Spinks, G. M.; Foroughi, J.; Madden, J. D. W.; Kim, S. H.; Fang, S.; Andrade, M. J. De; Göktepe, F.; et al. Artificial Muscles from Fishing Line and Sewing Thread. *Science (80-.).* **2014**, *343*, 868–872.

(192) Kornbluh, R.; Peirine, R.; Pei, Q.; Oh, S.; Joseph, J.; International, S. R. I.; Avenue, R.; Ca, M. P. Ultrahigh Strain Response of Field-Actuated Elastomeric Polymers. *Smart Struct. Mater. 2000 Electroact. Polym. Actuators Devices* **2000**, *3987*, 51–64.

(193) Pelrine, R.; Kornbluh, R.; Joseph, J.; Heydt, R.; Pei, Q.; Chiba, S. High-Field Deformation of Elastomeric Dielectrics for Actuators. *Mater. Sci. Eng. C* **2000**, *11*, 89–100.

(194) Xia, F.; Cheng, Z.; Xu, H.; Li, H.; Zhang, Q.; Kavarnos, G. J.; Ting, R. Y.; Abdel-sadek, G.; Belfield, K. D. High Electromechanical Responses in a Poly(vinylidene Fluoride-Trifluoroethylene-Chlorofluoroethylene) Terpolymer. *Adv. Mater.* **2002**, *14* (21), 1574–1577.

(195) Pelrine, R.; Kornbluh, R.; Joseph, J.; Chiba, S.; Park, M. Electrostriction of Polymer Films for Microactuators. *Proc. IEEE Tenth Annu. Int. Work. Micro Electro Mech. Syst.* **1997**, 238–243.

(196) Moulson, A. J.; Herbert, J. M. Piezoelectric Ceramics. In *Electroceramics: Materials, Properties, Applications, Second Edition*; John Wiley & Sons, 2003; pp 339–410.

(197) Huang, C.; Klein, R.; Xia, F.; Li, H.; Zhang, Q. M. Poly (Vinylidene Fluoride-Trifluoroethylene) Based High Performance Electroactive Polymers. *IEEE Trans. Dielectr. Electr. Insul.* **2004**, *11* (2), 299–311.

(198) Hunter, I. W.; Lafontaine, S.; Hollerbach, J. M.; Hunter, P. J. Fast Reversible NiTi Fibers for Use in Microrobotics. *Proc. IEEE Micro Electro Mech. Syst.* **1991**, 166–170.

(199) Tobushi, H.; Hayashi, S.; Kojima, S. Mechanical Properties of Shape Memory Polymer of Polyurethane Series. *JSME Int. J.* **1992**, *35* (3), 296–302.

(200) Spinks, B. G. M.; Mottaghitalab, V.; Bahrami-samani, M.; Whitten, P. G.; Wallace, G. G. Carbon-Nanotube-Reinforced Polyaniline Fibers for High-Strength Artificial Muscles. *Adv. Mater.* **2006**, *18*, 637–640.

(201) Nemat-Nasser, S. Micromechanics of Actuation of Ionic Polymer-Metal Composites. *J. Appl. Phys.* **2013**, *92* (5),

2002.

(202) Shahinpoor, M.; Kim, K. J. Ionic Polymer – Metal Composites : IV. Industrial and Medical Applications. *Smart Mater. Struct.* **2005**, *14*, 197–214.

(203) ETREMA Products Terfenol-D Magnetostrictive Smart Material (Tb0.3Dy0.7Fe1.92) http://www.matweb.com/search/datasheettext.aspx?matguid=aa68cad05c7c4d39932834d68e669a5d.

(204) Meijer, K.; Rosenthal, M.; Full, R. J. Muscle-like Actuators? A Comparison between Three Electroactive Polymers. *Smart Struct. Mater. 2001 Electroact. Polym. Actuators Devices* **2001**, *4329*, 7–15.

(205) Baughman, R. H. Conducting Polymers in Redox Devices and Intelligent Materials Systems. *Makromol. Chemie. Macromol. Symp.* **1991**, *51* (1), 193–215.

(206) Pei, Q.; Inganas, O. Conjugated Polymers and the Bending Cantilever Method: Electrical Muscles and Smart Devices. *Adv. Mater.* **1992**, *4* (4), 227–278.

(207) Pei, Q.; Inganas, O. Electrochemical Applications of the Bending Beam Method. 1. Mass Transport and Volume Changes in Polypyrrole during Redox. *J. Phys. Chem.* **1992**, *96* (25), 10507–10514.

(208) Pei, Q.; Inganas, O. Electrochemical Applications of the Bending Beam Method .2. Electroshrinking and Slow Relaxation in Polypyrrole. *J. Phys. Chem.* **1993**, *97* (22), 6034–6041.

(209) Otero, T. F.; Angulo, E.; Rodríguez, J.; Santamaría, C. Electrochemomechanical Properties from a Bilayer: Polypyrrole / Non-Conducting and Flexible Material - Artificial Muscle. *J. Electroanal. Chem.* **1992**, *341*, 369–375.

(210) Otero, T. F.; Martínez, J. G. Conducting Polymers as EAPs: Fundamentals and Materials. In *Electromechanically Active Polymers: A Concise Reference*; Carpi, F., Ed.; Springer International Publishing: Cham, 2016; pp 237–255.

(211) Pei, Q.; Inganäs, O. Electrochemical Applications of the Bending Beam Method; a Novel Way to Study Ion Transport in Electroactive Polymers. *Solid State Ionics* **1993**, *60*, 161–166.

(212) Smela, E. Conjugated Polymer Actuators for Biomedical Applications. *Adv. Mater.* **2003**, *15* (6), 481–494.

(213) Pei, Q.; Inganas, O.; Lundstrom, I. Bending Bilayer Strips Built from Polyaniline for Artificial Electrochemical Muscles. *Smart Mater. Struct.* **1993**, *2* (1), 1–6.

(214) Kaneto, K.; Kaneko, M.; Min, Y.; MacDiarmid, A. G. "Artificial Muscle": Electromechanical Actuators Using Polyaniline Films. *Synth. Met.* **1995**, *71*, 2211–2212.

(215) Zainudeen, U. L.; Careem, M. A.; Skaarup, S. PEDOT and PPy Conducting Polymer Bilayer and Trilayer Actuators. *Sensors Actuators, B Chem.* **2008**, *134* (2), 467–470.

(216) Lu, W. Use of Ionic Liquids for Pi -Conjugated Polymer Electrochemical Devices. *Science (80-.).* **2002**, *297* (5583), 983–987.

(217) Baughman, R. H. Conducting Polymer Artificial Muscles. *Synth. Met.* **1996**, *78* (3), 339–353.

(218) Hara, S.; Zama, T.; Takashima, W.; Kaneto, K. Tris(trifluoromethylsulfonyl)methide-Doped Polypyrrole as a Conducting Polymer Actuator with Large Electrochemical Strain. *Synth. Met.* **2006**, *156* (2–4), 351–355.

(219) Smela, E.; Gadegaard, N. Surprising Volume Change in PPy(DBS): An Atomic Force Microscopy Study. *Adv. Mater.* **1999**, *11* (11), 953–957.

(220) Pons, J. L. *Emerging Actuator Technologies: A Micromechatronic Approach*; John Wiley & Sons, 2005.

(221) Liu, Y.; Flood, A. H.; Bonvallet, P. A.; Vignon, S. A.; Northrop, B. H.; Tseng, H. R.; Jeppesen, J. O.; Huang, T. J.; Brough, B.; Baller, M.; et al. Linear Artificial Molecular Muscles. *J. Am. Chem. Soc.* **2005**, *127* (27), 9745–9759.

(222) Anquetil, P. A.; Yu, H.; Madden, J. D.; Madden, P. G.; Swager, T. M.; Hunter, I. W. Thiophene-Based Conducting Polymer Molecular Actuators. *Smart Struct. Mater. 2002 Electroact. Polym. Actuators Devices* **2002**, *4695*, 424–434.

(223) Scherlis, D. A.; Marzari, N. π-Stacking in Thiophene Oligomers As the Driving Force for Electroactive Materials and Devices. *J. Am. Chem. Soc.* **2005**, *127* (9), 3207–3212.

(224) Erbas-Cakmak, S.; Leigh, D. A.; McTernan, C. T.; Nussbaumer, A. L. Artificial Molecular Machines. *Chem. Rev.* **2015**, *115* (18), 10081–10206.

(225) Niu, X.; Yang, X.; Brochu, P.; Stoyanov, H.; Yun, S.; Yu, Z.; Pei, Q. Bistable Large-Strain Actuation of Interpenetrating Polymer Networks. *Adv. Mater.* **2012**, *24* (48), 6513–6519.

(226) Shahinpoor, M.; Kim, K. J. Ionic Polymer – Metal Composites : I. Fundamentals. *Smart Mater. Struct.* **2001**, *10*, 819–833.

(227) Asaka, K.; Takagi, K.; Kamamichi, N.; Cha, Y.; Porfiri, M. IPMCs as EAPs: Applications. In *Electromechanically Active Polymers: A Concise Reference*; Carpi, F., Ed.; Springer International Publishing: Cham, 2016; pp 1–24.

(228) Shahinpoor, M. Mechanoelectrical Phenomena In Ionic Polymers. *Math. Mech. Solids* **2003**, *8*, 281–288.

(229) Nemat-Nasser, S. Micromechanics of Actuation of Ionic Polymer-Metal Composites. *J. Appl. Phys.* **2002**, *92* (5), 2899–2915.

(230) Bahramzadeh, Y.; Shahinpoor, M. A Review of Ionic Polymeric Soft Actuators and Sensors. *Soft Robot.* **2014**, *1* (1), 38–52.

(231) Baughman, R. H.; Zakhidov, A. a; de Heer, W. a. Carbon Nanotubes --- the Route toward Applications. *Science (80-.).* **2002**, *297* (5582), 787–792.

(232) Baughman, R. H. Carbon Nanotube Actuators. *Science (80-.).* **1999**, *284* (5418), 1340–1344.

(233) Shankar, R.; Ghosh, T. K.; Spontak, R. J. Dielectric Elastomers as next-Generation Polymeric Actuators. *Soft Matter* **2007**, *3* (9), 1116–1129.

(234) Madden, J. D. W.; Barisci, J. N.; Anquetil, P. A.; Spinks, G. M.; Wallace, G. G.; Baughman, R. H.; Hunter, I. W. Fast Carbon Nanotube Charging and Actuation. *Adv. Mater.* **2006**, *18* (7), 870–873.

(235) Aliev, A. E.; Oh, J.; Kozlov, M. E.; Kuznetsov, A. A.; Fang, S.; Fonseca, A. F.; Ovalle, R.; Lima, M. D.; Haque, M. H.; Gartstein, Y. N.; et al. Giant-Stroke, Superelastic Carbon Nanotube Aerogel Muscles. *Science (80-.).* **2009**, *323* (5921), 1575–1578.

(236) Foroughi, J.; Spinks, G. M.; Wallace, G. G.; Oh, J.; Kozlov, M. E.; Fang, S.; Mirfakhrai, T.; Madden, J. D. W.; Shin, M. K.; Kim, S. J.; et al. Torsional Carbon Nanotube Artificial Muscles. *Science (80-.).* **2011**, *334*, 494–498.

(237) Cheng, Z.; Zhang, Q. Field-Activated Electroactive Polymers. *MRS Bull.* **2008**, *33*, 183–187.

(238) Zhang, Q. M.; Bharti, V.; Zhao, X. Giant Electrostriction and Relaxor Ferroelectric Behavior in Electron-Irradiated Poly(vinylidene Fluoride-Trifluoroethylene) Copolymer. *Science (80-.).* **1998**, *280* (5372), 2101–2104.

(239) Bauer, F.; Fousson, E.; Zhang, Q. M. Recent Advances in Highly Electrostrictive P(VDF-TrFE-CFE) Terpolymers. *IEEE Trans. Dielectr. Electr. Insul.* **2006**, *13* (5), 1149–1153.

(240) Bauer, F. Review on the Properties of the Ferrorelaxor Polymers and Some New Recent Developments. *Appl. Phys. A Mater. Sci. Process.* **2012**, *107* (3), 567–573.

(241) Su, J.; Hales, K.; Xu, T.-B. Composition and Annealing Effects on the Response of Electrostrictive Graft Elastomers. *SPIE Proc.* **2003**, *5051*, 191–197.

(242) Warner, M.; Terentjev, E. M. *Liquid Crystal Elastomers*; OUP Oxford, 2003; Vol. 120.

(243) de Gennes, P.-G. A Semi-Fast Artificial Muscle. *Comptes Rendus l'Academie des Sci. Ser. IIB Mech. Phys. Chem. Astron.* **1997**, *5* (324), 343–348.

(244) de Gennes, P.-G.; Hébert, M.; Kant, R. Artificial Muscles Based on Nematic Gels. In *Macromolecular Symposia*; 1997; Vol. 113, pp 39–49.

(245) Naciri, J.; Srinivasan, A.; Jeon, H.; Nikolov, N.; Keller, P.; Ratna, B. R. Nematic Elastomer Fiber Actuator. *Macromolecules* **2003**, *36* (22), 8499–8505.

(246) Lehmann, W.; Skupin, H.; Tolksdorf, C.; Gebhard, E.;

Zentel, R.; Krüger, P.; Lösche, M.; Kremer, F. Giant Lateral Electrostriction in Ferroelectric Liquid-Crystalline Elastomers. *Nature* **2001**, *410*, 447–450.

(247) Huang, C.; Zhang, Q.; Jákli, A. Nematic Anisotropic Liquid-Crystal Gels-Self-Assembled Nanocomposites with High Electromechanical Response. *Adv. Funct. Mater.* **2003**, *13* (7), 525–529.

(248) Fuchigami, Y.; Takigawa, T.; Urayama, K. Electrical Actuation of Cholesteric Liquid Crystal Gels. *ACS Macro Lett.* **2014**, *3* (8), 813–818.

(249) Pelrine, R.; Kornbluh, R.; Pei, Q.; Joseph, J.; Park, S.; Shrout, T.; Baughman, R. H.; Zhang, Q. M.; Bharti, V.; Zhao, X.; et al. High-Speed Electrically Actuated Elastomers with Strain Greater than 100%. *Science (80-.).* **2000**, *287* (5454), 836–839.

(250) Carpi, F.; Anderson, I.; Bauer, S.; Frediani, G.; Gallone, G.; Gei, M.; Graaf, C.; Jean-Mistral, C.; Kaal, W.; Kofod, G.; et al. Standards for Dielectric Elastomer Transducers. *Smart Mater. Struct.* **2015**, *24* (10), 105025.

(251) Murray, C.; McCoul, D.; Sollier, E.; Ruggiero, T.; Niu, X.; Pei, Q.; Carlo, D. Di. Electro-Adaptive Microfluidics for Active tunin(1) Murray, C.; McCoul, D.; Sollier, E.; Ruggiero, T.; Niu, X.; Pei, Q.; Carlo, D. Di. Electro-Adaptive Microfluidics for Active Tuning of Channel Geometry Using Polymer Actuators. Microfluid. Nanofluidics 20. *Microfluid. Nanofluidics* **2013**, *14* (1–2), 345–358.

(252) Suo, Z. Theory of Dielectric Elastomers. *Acta Mech. Solida Sin.* **2010**, *23* (6), 549–578.

(253) Niu, X.; Stoyanov, H.; Hu, W.; Leo, R.; Brochu, P.; Pei, Q. Synthesizing a New Dielectric Elastomer Exhibiting Large Actuation Strain and Suppressed Electromechanical Instability without Prestretching. *J. Polym. Sci. Part B Polym. Phys.* **2013**, *51* (3), 197–206.

(254) Hu, W.; Zhang, S. N.; Niu, X.; Liu, C.; Pei, Q. An Aluminum Nanoparticle–acrylate Copolymer Nanocomposite as a Dielectric Elastomer with a High Dielectric Constant. *J. Mater. Chem. C* **2014**, *2* (9), 1658.

(255) Pelrine, R.; Kornbluh, R.; Kofod, G. High-Strain Actuator Materials Based on Dielectric Elastomers. *Adv. Mater.* **2000**, *12* (16), 1223–1225.

(256) Niu, X.; Leo, R.; Chen, D.; Hu, W.; Pei, Q. Multilayer Stack Actuator Made from New Prestrain-Free Dielectric Elastomers. In *Electroactive Polymer Actuators and Devices (EAPAD) 2013*; Bar-Cohen, Y., Ed.; 2013; Vol. 8687, p 86871M–86871M–8.

(257) Plante, J. S.; Dubowsky, S. Large-Scale Failure Modes of Dielectric Elastomer Actuators. *Int. J. Solids Struct.* **2006**, *43* (25–26), 7727–7751.

(258) Kofod, G.; Sommer-Larsen, P.; Kornbluh, R.; Pelrine, R. Actuation Response of Polyacrylate Dielectric Elastomers. *J. Intell. Mater. Syst. Struct.* **2003**, *14* (12), 787–793.

(259) Vargantwar, P. H.; Ozcam, A. E.; Ghosh, T. K.; Spontak, R. J. Prestrain-Free Dielectric Elastomers Based on Acrylic Thermoplastic Elastomer Gels: A Morphological and (Electro)mechanical Property Study. *Adv. Funct. Mater.* **2012**, *22* (10), 2100–2113.

(260) Suo, Z.; Zhu, J. Dielectric Elastomers of Interpenetrating Networks. *Appl. Phys. Lett.* **2009**, *95* (23), 17–20.

(261) Ha, S. M.; Yuan, W.; Pei, Q.; Pelrine, R.; Stanford, S. Interpenetrating Networks of Elastomers Exhibiting 300% Electrically-Induced Area Strain. *Smart Mater. Struct.* **2007**, *16* (2), S280–S287.

(262) Ha, S. M.; Yuan, W.; Pei, Q.; Pelrine, R.; Stanford, S. Interpenetrating Polymer Networks for High-Performance Electroelastomer Artificial Muscles. *Adv. Mater.* **2006**, *18* (7), 887–891.

(263) Daniel, W. F. M.; Burdyńska, J.; Vatankhah-Varnoosfaderani, M.; Matyjaszewski, K.; Paturej, J.; Rubinstein, M.; Dobrynin, A. V.; Sheiko, S. S. Solvent-Free, Supersoft and Superelastic Bottlebrush Melts and Networks. *Nat. Mater.* **2016**, *15* (November 2015), 183–189.

(264) Vatankhah-Varnoosfaderani, M.; Daniel, W. F. M.;

Zhushma, A. P.; Li, Q.; Morgan, B. J.; Matyjaszewski, K.; Armstrong, D. P.; Spontak, R. J.; Dobrynin, A. V.; Sheiko, S. S. Bottlebrush Elastomers: A New Platform for Freestanding Electroactuation. *Adv. Mater.* **2016**.

(265) Yu, Z.; Niu, X.; Brochu, P.; Yuan, W.; Li, H.; Chen, B.; Pei, Q. Bistable Electroactive Polymers (BSEP): Large-Strain Actuation of Rigid Polymers. *Proc. SPIE* **2010**, *8340*, 76420C–76420C–9.

(266) Ren, Z.; Hu, W.; Liu, C.; Li, S.; Niu, X.; Pei, Q. Phase-Changing Bistable Electroactive Polymer Exhibiting Sharp Rigid-to-Rubbery Transition. *Macromolecules* **2016**, *49* (1), 134–140.

(267) Stoll, A. M.; Greene, L. C. Relationship between Pain and Tissue Damage due to Thermal Radiation. *J. Appl. Physiol.* **1959**, *14* (3), 373–382.

(268) Forrest, S. R. The Path to Ubiquitous and Low-Cost Organic Electronic Appliances on Plastic. *Nature* **2004**, *428* (6986), 911–918.

(269) Li, J.; Zhao, Y.; Tan, H. S.; Guo, Y.; Di, C.-A.; Yu, G.; Liu, Y.; Lin, M.; Lim, S. H.; Zhou, Y.; et al. A Stable Solution-Processed Polymer Semiconductor with Record High-Mobility for Printed Transistors. *Sci. Rep.* **2012**, *2*, 754.

(270) Liu, Y.; Zhang, X.; Song, C.; Zhang, Y.; Fang, Y.; Yang, B.; Wang, X. An Effective Surface Modification of Carbon Fiber for Improving the Interfacial Adhesion of Polypropylene Composites. *Mater. Des.* **2015**, *88*, 810–819.

(271) Hammock, M. L.; Chortos, A.; Tee, B. C. K.; Tok, J. B. H.; Bao, Z. 25th Anniversary Article: The Evolution of Electronic Skin (E-Skin): A Brief History, Design Considerations, and Recent Progress. *Adv. Mater.* **2013**, *25* (42), 5997–6038.

(272) Koeppe, R.; Bartu, P.; Bauer, S.; Sariciftci, N. S. Light- and Touch-Point Localization Using Flexible Large Area Organic Photodiodes and Elastomer Waveguides. *Adv. Mater.* **2009**, *21*, 3510–3514.

(273) Sun, J. Y.; Keplinger, C.; Whitesides, G. M.; Suo, Z. Ionic Skin. *Adv. Mater.* **2014**, *26* (45), 7608–7614.

(274) Yao, S.; Zhu, Y. Wearable Multifunctional Sensors Using Printed Stretchable Conductors Made of Silver Nanowires. *Nanoscale* **2014**, *6* (4), 2345.

(275) Joo, Y.; Byun, J.; Seong, N.; Ha, J.; Kim, H.; Kim, S.; Kim, T.; Im, H.; Kim, D.; Hong, Y. Silver Nanowire-Embedded PDMS with a Multiscale Structure for a Highly Sensitive and Robust Flexible Pressure Sensor. *Nanoscale* **2015**, *7* (14), 6208–6215.

(276) Hu, W.; Niu, X.; Zhao, R.; Pei, Q. Elastomeric Transparent Capacitive Sensors Based on an Interpenetrating Composite of Silver Nanowires and Polyurethane. *Appl. Phys. Lett.* **2013**, *102* (8), 83303-1-083305–5.

(277) Webb, R. C.; Bonifas, A. P.; Behnaz, A.; Zhang, Y.; Yu, K. J.; Cheng, H.; Shi, M.; Bian, Z.; Liu, Z.; Kim, Y.-S.; et al. Ultrathin Conformal Devices for Precise and Continuous Thermal Characterization of Human Skin. *Nat. Mater.* **2013**, *12* (10), 938–944.

(278) Yan, C.; Wang, J.; Lee, P. S. Stretchable Graphene Thermistor with Tunable Thermal Index. *ACS Nano* **2015**, *9* (2), 2130–2137.

(279) Shahil, K. M. F.; Balandin, A. a. Thermal Properties of Graphene and Multilayer Graphene: Applications in Thermal Interface Materials. *Solid State Commun.* **2012**, *152* (15), 1331–1340.

(280) Kong, D.; Le, L. T.; Li, Y.; Zunino, J. L.; Lee, W. Temperature-Dependent Electrical Properties of Graphene Inkjet-Printed on Flexible Materials. *Langmuir* **2012**, *28* (37), 13467–13472.

(281) Feteira, A. Negative Temperature Coefficient Resistance (NTCR) Ceramic Thermistors: An Industrial Perspective. *J. Am. Ceram. Soc.* **2009**, *92* (5), 967–983.

(282) Zhang, H.; So, E. Hybrid Resistive Tactile Sensing. *IEEE Trans. Syst. Man, Cybern. Part B Cybern.* **2002**, *32* (1), 57–65.

(283) Bertetto, A. M.; Ruggiu, M. Low Cost Resistive Based

Touch Sensor. *Mech. Res. Commun.* **2003**, *30* (2), 101–107.

(284) Bai, Y.; Chen, C. Using Serial Resistors to Reduce the Power Consumption of Resistive Touch Panels. *IEEE Int. Symp. Consum. Electron.* **2007**, 1–6.

(285) Cotton, D. P. J.; Graz, I. M.; Lacour, S. P. A Multifunctional Capacitive Sensor for Stretchable Electronic Skins. *IEEE Sens. J.* **2009**, *9* (12), 2008–2009.

(286) Li, S.; Peele, B. N.; Larson, C. M.; Zhao, H.; Shepherd, R. F. A Stretchable Multicolor Display and Touch Interface Using Photopatterning and Transfer Printing. *Adv. Mater.* **2016**, 1–6.

(287) Mayousse, C.; Celle, C.; Moreau, E.; Mainguet, J.-F.; Carella, A.; Simonato, J.-P. Improvements in Purification of Silver Nanowires by Decantation and Fabrication of Flexible Transparent Electrodes. Application to Capacitive Touch Sensors. *Nanotechnology* **2013**, *24* (21), 215501.

(288) Brochu, P.; Stoyanov, H.; Chang, R.; Niu, X.; Hu, W.; Pei, Q. Capacitive Energy Harvesting Using Highly Stretchable Silicone-Carbon Nanotube Composite Electrodes. *Adv. Energy Mater.* **2014**, *4* (3), 1–9.

(289) Niu, X.; Brochu, P.; Salazar, B.; Pei, Q. Refreshable Tactile Displays Based on Bistable Electroactive Polymer. *Proceeding SPIE* **2011**, *7976*, 797610-1-797610–797616.

(290) Ren, Z.; Niu, X.; Chen, D.; Hu, W.; Pei, Q. A New Bistable Electroactive Polymer for Prolonged Cycle Lifetime of Refreshable Braille Displays. *Proc. SPIE* **2014**, *9056*, 905621-1–9.

(291) Kofod, G.; Wirges, W.; Paajanen, M.; Bauer, S. Energy Minimization for Self-Organized Structure Formation and Actuation. *Appl. Phys. Lett.* **2007**, *90* (8), 1–4.

(292) Pei, Q.; Rosenthal, M. a.; Pelrine, R.; Stanford, S.; Kornbluh, R. D. Multifunctional Electroelastomer Roll Actuators and Their Application for Biomimetic Walking Robots. *SPIE Smart Struct. Mater.* **2003**, *5051*, 281–290.

(293) Kovacs, G.; Lochmatter, P.; Wissler, M.; S, A.; Pelrine R, K. R. P. Q. S. S. O. S. and E. J.; Y, B.-C.; Pelrine R E, K. R. D. and J. J. P.; Pelrine R, K. R. P. Q. B. and J. J.; Heydt R, K. R. P. R. and M. V; Carpi F, C. P. M. a and D. R. D.; et al. An Arm Wrestling Robot Driven by Dielectric Elastomer Actuators. *Smart Mater. Struct.* **2007**, *16* (2), S306–S317.

(294) Zhao, J.; Niu, J.; McCoul, D.; Leng, J.; Pei, Q. A Rotary Joint for a Flapping Wing Actuated by Dielectric Elastomers: Design and Experiment. *Meccanica* **2015**, *50* (11), 2815–2824.

(295) Wache, R.; McCarthy, D. N.; Risse, S.; Kofod, G. Rotary Motion Achieved by New Torsional Dielectric Elastomer Actuators Design. *IEEE/ASME Trans. Mechatronics* **2015**, *20* (2), 975–977.

(296) McCoul, D.; Pei, Q. Tubular Dielectric Elastomer Actuator for Active Fluidic Control. *Smart Mater. Struct.* **2015**, *24* (10), 105016.

Biography

Dustin Chen received his bachelor's degree in materials science and engineering from University of California Berkeley in 2012. In 2017, he received his Ph.D. in materials science and engineering from University of California Los Angeles under the supervision of Professor Qibing Pei studying the use of silver nanowires for optoelectronic applications.

Qibing Pei is Professor of Materials Science and Engineering at the University of California, Los Angeles, and directs the UCLA Soft Materials Research Laboratory studying electronic and electromechanically responsive polymers and nanostructured composites, stretchable polymer electronics, and dielectric elastomers for muscle-like actuation and sensing. He received a B.S. from Nanjing University, China, and a PhD from the Institute of Chemistry, Chinese Academy of Science.

TOC graphic